MANCHESTER 1824
The University of Manchester

Investigations of Bioaerosol Emission and Dispersion Patterns

A thesis submitted to the University of Manchester for the degree of
Doctor of Philosophy
in the Faculty of Science and Engineering

2021

Douglas Morrison
Department of Earth and Environmental Sciences

Contents

Word Count: 27,605

List of publications

Morrison, D., Crawford, I., Marsden, N., Flynn, M., Read, K., Neves, L., Foot, V., Kaye, P., Stanley, W., Coe, H., Topping, D. and Gallagher, M., 2020. "Quantifying bioaerosol concentrations in dust clouds through online UV-LIF and mass spectrometry measurements at the Cape Verde Atmospheric Observatory". *Atmospheric Chemistry and Physics*, 20 (22), pp.14473-14490.

Morrison, D., Li, J., Crawford, I., Che, W., Flynn, M., Chan, M., Lau, A., Fung, J., Topping, D., Yu, J. and Gallagher, M., 2020. "The Observation and Characterisation of Fluorescent Bioaerosols Using Real-Time UV-LIF Spectrometry in Hong Kong from June to November 2018". *Atmosphere*, 11 (9), p.944.

Abstract

Bioaerosols are airborne particles of biological origin. They include viruses, bacteria, fungal spores, pollen, plant fibres, metabolites, toxins, and more. Despite often accounting for less than 1% of the particles within an aerosol mixture, bioaerosols are increasingly recognised for the effects they can have on air quality, human health, ecosystems, climate and atmosphere–ocean biogeochemical cycles. This broad range of effects has attracted newfound interest from a number of disciplines, ranging from climate modelling to epidemiology.

Until recently, observations of bioaerosols were limited to offline techniques. Whether it was using filter samples, cascade impactors or a volumetric spore trap, subsequent microscopical analysis was often labour intensive and slow. However, technological developments have given rise to emerging online methods such as ultra-violet light induced fluorescence (UV-LIF) spectrometry. By utilising the intrinsic fluorescent properties of specific biological compounds, bioaerosols can be rapidly observed. Since the advent of the first UV-LIF spectrometers, a number of advancements have been made to the instruments. This has increased their sensitivity to specific wavelengths and improved the user's capacity to discriminate between distinct particle types. Although early versions of UV-LIF spectrometers have already been employed in a number of environments, including rainforests, city centres and even Antarctica, new opportunities have arisen to conduct experiments with greater levels of data output. As such, it is useful to re-visit old sampling sites with more modern instruments, as well as sample in novel environments.

The research discussed throughout this document involves some of the longest sampling campaigns to use UV-LIF spectrometry to date, and has taken place in a number of locations. These include Cape Verde, Hong Kong, Barbados and the UK. A number of instrument models have been used, with subsequent analysis aided by machine learning technqiues such as hierarchical agglomerative cluster analysis.

Declaration of originality

I hereby confirm that no portion of the work referred to in the thesis has been submitted in support of an application for another degree or qualification of this or any other university or other institute of learning.

Copyright statement

i The author of this thesis (including any appendices and/or schedules to this thesis) owns certain copyright or related rights in it (the "Copyright") and s/he has given The University of Manchester certain rights to use such Copyright, including for administrative purposes.

ii Copies of this thesis, either in full or in extracts and whether in hard or electronic copy, may be made *only* in accordance with the Copyright, Designs and Patents Act 1988 (as amended) and regulations issued under it or, where appropriate, in accordance with licensing agreements which the University has from time to time. This page must form part of any such copies made.

iii The ownership of certain Copyright, patents, designs, trademarks and other intellectual property (the "Intellectual Property") and any reproductions of copyright works in the thesis, for example graphs and tables ("Reproductions"), which may be described in this thesis, may not be owned by the author and may be owned by third parties. Such Intellectual Property and Reproductions cannot and must not be made available for use without the prior written permission of the owner(s) of the relevant Intellectual Property and/or Reproductions.

iv Further information on the conditions under which disclosure, publication and commercialisation of this thesis, the Copyright and any Intellectual Property and/or Reproductions described in it may take place is available in the University IP Policy (see `http://documents.manchester.ac.uk/DocuInfo.aspx?DocID=24420`), in any relevant Thesis restriction declarations deposited in the University Library, The University Library's regulations (see `http://www.library.manchester.ac.uk/about/regulations/`) and in The University's policy on Presentation of Theses.

Acknowledgements

I would like to thank Martin Gallagher, Ian Crawford and David Topping for their supervision. I would also like to thank Julie Samson for her dedication towards the Doctoral Training Partnership and Mike Flynn for making the fieldwork possible.

Chapter 1

Introduction

1.1 Aerosols in the Atmosphere

Aerosols are solid or liquid particles suspended within a gas. Many atmospheric processes depend on the physical and chemical properties of such particles present at high altitudes [1]. The aerosol mixture often has a high degree of heterogeneity, with particles released from a number of natural and anthropogenic sources [2]. When released directly into the atmosphere, aerosols are referred to as 'primary aerosols'. When formed in the atmosphere from precursor gases, they are referred to as 'secondary aerosols'. The time these particles spend in suspension is mostly a function of their size, with larger particles depositing more quickly [3]. Compared to gaseous molecules, the lifetime of almost all aerosols is considerably shorter and is often just a few days.

Aerosols can directly alter the energy balance of the planet by scattering solar radiation [4]. By reflecting sunlight back into space it prevents the sun's shortwave radiation from reaching the planet and consequently leads to a cooling effect. However, certain aerosols are also capable of absorbing outgoing longwave radiation, with strongly absorbing aerosols creating a warming effect. This creates challenges for climate modellers, who must accurately determine the net effect of specific aerosols in the atmosphere. Although it is rarer for aerosols to absorb solar radiation than scatter it [5], dominant examples such as black carbon (BC) are increasingly common [6]. Often released as a by-product of anthropogenic activity, airborne concentrations of BC over urban areas are of growing concern [7].

The inter-play between aerosols and solar radiation is just one way in which aerosols can impact the climate. Many aerosols are also important ice and cloud condensation nucleators [8]. Heterogeneous ice nucleation in the atmosphere occurs when an aerosol catalyses the formation of ice crystals onto their surface by lowering the energy required for crystallisation to begin. This occurs at warmer temperatures than homogeneous ice nucleation [9], which is defined as the formation of ice crystals in the absence of any nucleation site. In either case, the formation of ice leads to an increase in cloud albedo, thereby reflecting more sunlight into space [10]. Cloud condensation nucleation (CCN) is similar in principle to ice nucleation (IN). As water requires a non-gaseous surface to transition from vapour to a liquid, CCN act by offering a surface for water vapour to condense onto [11]. This promotes cloud formation, reducing the amount of sunlight reaching the ground and increasing pre-

cipitation.

The overwhelming majority of suspended particles are contained within the planetary boundary layer (PBL), which is the lowest portion of the troposphere [12]. Thermodynamic perturbations, for example from reduced solar radiation during the night, create shifts in the boundary layer height (BLH) [13]. The BLH describes the vertical limit that most aerosols can be elevated to, and is a significant factor when evaluating the horizontal distances aerosols can travel. It carries implications for the dilution of particulate matter (PM) in the atmosphere, with a generally negative correlation often seen between the BLH and PM concentrations [14]. The BLH has regional variation, changing as a function of topography and land use. Urban areas, typically associated with warmer temperatures due to the Urban Heat Island Effect, often have a higher BLH as a result [15]. This helps to mitigate the concentrations of pollutants, but does enable them to be transported to further regions.

1.2 Bioaerosols

Biological particles (hereafter referred to as bioaerosols) encompass a broad range of particle types, including viruses, bacteria, fungal spores, pollen, plant fibres and more. They are readily emitted from many natural environments, such as plant surfaces or sea spray[16], [17]. Once released, they can be lifted by convective forces or carried by Aeolian processes and travel significant distances [18]. Bioaerosols are increasingly recognised for the effects they can have on air quality, human health, ecosystems and climate [19]. Research indicates that bioaerosols act as some of the most efficient CCN and IN, initiating ice formation at warmer temperatures and cloud formation at lower supersaturations than many other aerosols [20]. Consequently, bioaerosols have attracted attention from climate modellers, who can improve the accuracy of their models by accounting for bioaerosol concentrations and their subsequent effects.

Despite the importance of bioaerosols, they often suffer from poor representation in climate models [21]. This is partially because concentrations are predominantly made from ground-level sampling sites. There are relatively few examples of high altitude measurements, creating uncertainties in their concentrations at cloud-level. These issues are amplified by the lack of observations regarding their removal rate and complex interactions with meteorological conditions. For example, rainfall simultaneously contributes to the wet deposition of suspended particles and also drives the ejection of fungal spores and provides a mechanistic release of bacteria from plant surfaces [22]. Furthermore, air dispersion models that predict the movement of bioaerosols from an emission source have inherent biases [23]. They may not accurately capture the full complement of factors affecting bioaerosol release, and may also miss the transformation such particles undergo when exposed to hostile atmospheric conditions.

The relationship living organisms have with their environment means bioaerosol emissions are in a constant state of flux. Life-cycle stages of plants often coincide with seasonal changes,

for example increased pollen concentrations during summer. Meteorological events are also influential, with precipitation or high relative humidity creating optimal conditions for fungal spore release. Strong winds not only affect the concentrations and distances bioaerosols are transported, but can also enhance their rates of emission. Strong winds can create significant levels of sea spray, while continental trade winds can can elevate dust particles that bacteria use as transport vectors. The interactions bioaerosols have with their environment are too numerous to exhaustively list, but their relationships with diurnal, seasonal, and meteorological cycles all create challenges for modellers.

Given their diversity, bioaerosols encompass a range of sizes, with some examples outlined below in Table 1. The proportion of bioaerosols in an aerosol mixture is usually small, often accounting for than 1% of all suspended particles. However, their larger relative size means they can account for approximately 25% of total aerosol mass [24]. This is amplified in pristine environments, with Graham et al. [25] observing that $\sim$70% of aerosol volume over the Amazon consisted of organic matter.

Table 1.1: Examples of bioaerosols and their respective sizes [26].

Bioaerosol	**Size** (μm)
Pollen	10 - 100
Fungal Spores	0.5 - 30
Bacteria	0.3 - 10
Virus	0.02 - 0.3

1.3 Monitoring Techniques – UV-LIF Spectrometry

Many techniques have historically been used for sampling bioaerosols, including impingers, cyclones, impactors, filters, spore traps, thermal precipitators, gravitational samplers and electrostatic precipitators. These all require off-line analysis techniques which are manually intensive. More recently, ultraviolet light-induced fluorescence (UV-LIF) spectrometers such as the Wideband Integrated Bioaerosol Sensor (WIBS) and Multiparameter Bioaerosol Spectrometer (MBS) have allowed real-time detection and collection of specific bioaerosol characteristics. This technology utilises the intrinsic fluorescent properties found within specific organic molecules, including proteins, co-enzymes, cell wall compounds and certain pigments to differentiate between biological and non-biological particles. Each organic molecule has its own fluorescent signature, with the wavelength of the fluorescent emissions being dependent on the incoming wavelength of the laser that excites it. As such, it is possible for UV-LIF technology to discriminate between organic molecules, and help to identify the particles being observed. An example of some key fluorophores and their excitation/emission bands are outlined in Figure 1.1, alongside the excitation capabilities of certain UV-LIF spectrometers.

The WIBS is a single particle, on-line spectrometer that can provide measurements for the size, asymmetry and fluorescence of bioaerosols between 0.5-30 μm. As single file par-

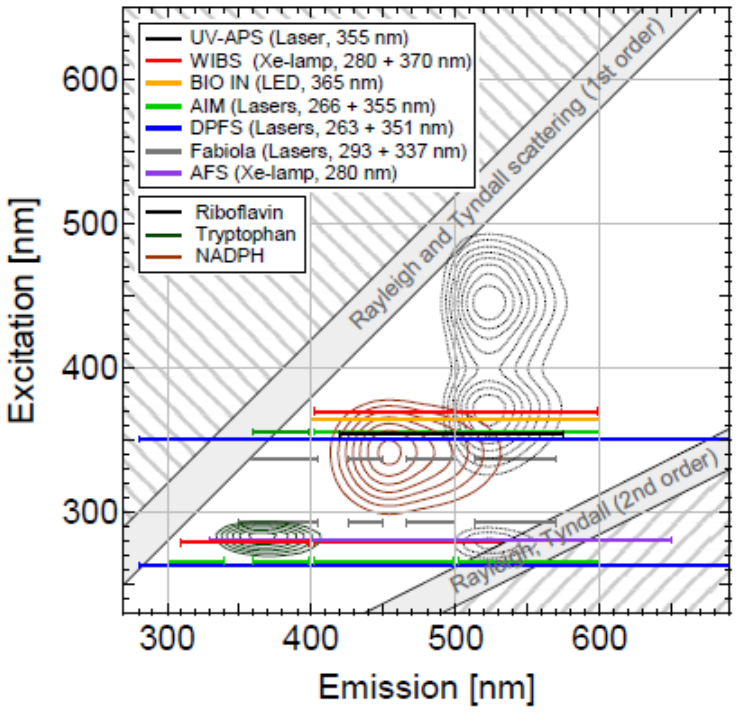

Figure 1.1: Excitation/Emission Bands for Key Fluorophores and the Excitation Capabilities of Certain UV-LIF Technologies [27]

ticles pass through the instrument, they cross the path of a 635 nm diode laser. Light is scattered forward, where it hits a detector so that the particle's size and shape can be determined. Side scattering light is converted into electrical impulses, where they trigger two Xenon flash lamps. These lamps excite the particle at 280 and 370 nm respectively, initiating fluorescent emissions. This fluorescence is then captured on two detector plates sensitive to specific wavelengths, creating a 2x2 excitation-emission matrix. However, with one detector becoming supersaturated with elastically scattered UV light from the 370 nm flash lamp, there are effectively only three channels. The first detector is sensitive to 310-400 nm UV light, while the second covers a broader range from 420-650 nm. Common fluorophores considered in particle analysis include the amino acid Tryptophan, the co-enzyme Nicotinamide adenine dinucleotide phosphate (NAD(P)H) and the vitamin Riboflavin. Each fluorophore excites at 280 nm, 270-400 nm and 450 nm respectively; and fluoresces from 300-400, 400-600 and 520-565 nm [28], [29].

The Multiparameter Bioaerosol Spectrometer (MBS) is in many ways a development from the WIBS models. Although it works in much the same way as the WIBS, and provides similar information (shape, size and fluorescence); it does so with just one Xenon flash lamp, using eight equal wavebands from 310-640 nm that it excites at 280 nm. As such, the MBS produces a 1x8 excitation/emission matrix and is capable of providing greater discrimination between bioaerosols and 'interferent' non-biological particles that exhibit similar fluorescence. Furthermore, the MBS uses two 512-pixel CMOS detector arrays that provide high resolution details of the particle's spatial light scattering pattern.

The Plair Real-Time Airborne Particle Identifier (Rapid-E) offers yet another option for bioaerosol monitoring. Working in a similar way to the equipment discussed above, an ad-

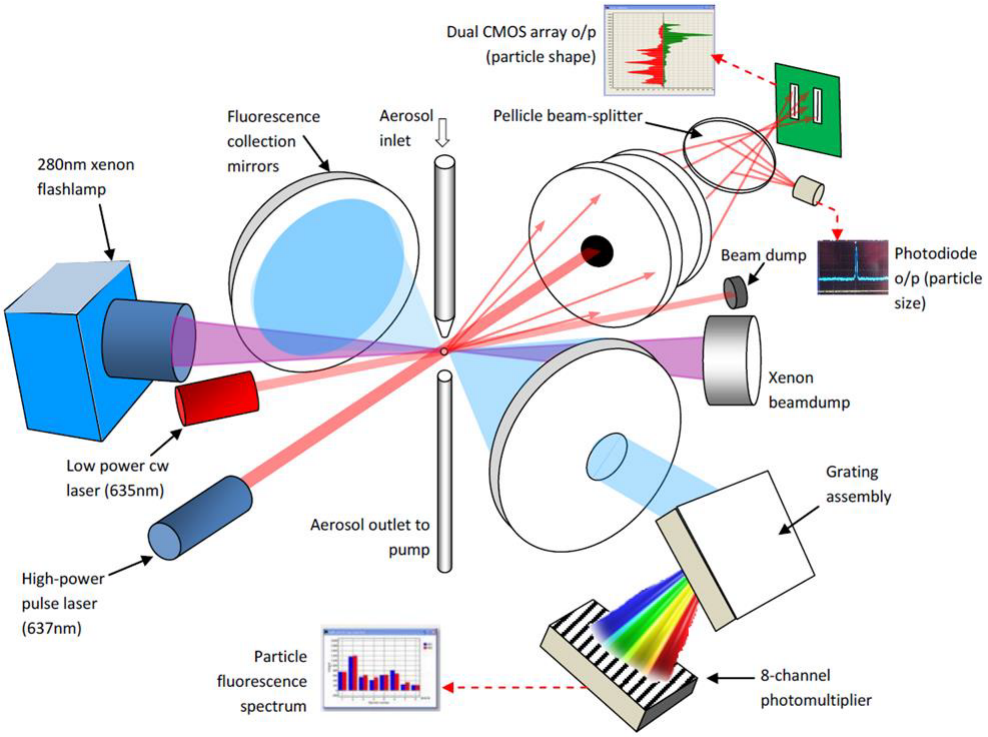

Figure 1.2: Internal Schematic of the MBS (MBS Manual, 2013)

vantage of the Rapid-E is that through toggling between different modes and laser intensities, it can measure particles from 0.5-100 μm. Consequently, particles such as pollen grains, which would often be too large to be measured by the WIBS, can be accurately quantified. Furthermore, the Rapid-E has replaced the Xenon flash lamps with an ultraviolet (UV) pulsed laser. The laser's higher intensity causes a greater number of photons to be emitted, allowing for a greater number of detector channels to be implemented. As such, the Rapid-E offers 32 distinct resolution channels, within a fluorescence range of 320-770 nm. This allows significantly improved particle discrimination. Another advantage of the Rapid-E is the high spectral resolution it provides. Through measuring the light coming off a particle from 24 different angles in real time, it can provide a 2D image based on relative intensities. This allows for some provisional attempts to capture the shape of the particle, and has been proposed as a means of further allowing greater discrimination. However, the technology is relatively new, and has so far not been well characterised. Further lab and field experiments will be needed to determine the usefulness of such a feature. Regardless, one other important feature of the Rapid-E is that it offers a much larger sample volume as it samples air at a higher flow rate. This improves the counting efficiency at lower concentrations, thereby improving the detection limit at higher time resolutions.

Regardless of the UV-LIF equipment deployed, further analysis is required to try and identify the nature of the sampled particles. This is because the optical UV-LIF methodologies only provide data on the shape, size and fluorescent spectral patterns. Using this, alongside known meteorological conditions, the particle type must be inferred. For the last few years the most common technique for further analysis is a form of unsupervised learning – hierarchial agglomerative cluster (HAC) analysis [30]. Through computing the relative inter/intra variance between particles systematically grouped together, a Calinski-Harabasz score

can be calculated that estimates the number of different clusters that measured particles can be assorted into. The Calinski – Harabasz score is defined as the ratio between the within-cluster dispersion of data points and the between-cluster dispersion. In bioaerosol research, HAC analysis is a method of estimating how many distinct particle types are present in a dataset. Such a technique has been proven to successfully discriminate between polystyrene latex spheres (PSL's) of different sizes, and has often been applied to ambient data for which correct classification is unknown. However, there are some issues regarding the technique's accuracy. Laboratory experiments using known bioaerosol and non-bioaerosol datasets have demonstrated range of accuracies depending on the bioaerosol type and age, typically 67.6 to 91.1% accuracy [31], [32]. Consequently, there has been interest in developing 'supervised' methods, whereby accuracy can be improved through the use of training datasets. Machine learning techniques have also been applied to the UV-LIF fluorescence spectra of pollen with discrimination levels reported ranging from 70-91% [33].

Relying on fluorescence alone for the detection of bioaerosols can also be problematic. There are known non-biological particles that also exhibit fluorescence, and can consequently skew the concentrations thought to be observed. Examples of such interferences include secondary organic aerosols (SOA's), mineral dusts, and humic-like substances [34]. Furthermore, some bioaerosols may fluoresce too weakly to be detected, and therefore go uncounted. However, in pristine environments interferences are effectively minimised, which is where most ambient measurements using these methods have been taken. Regarding weakly fluorescent micro-organisms, the result is that most measurements of biological particles are thought to be lower estimates.

1.4 Monitoring Techniques – Alternatives to UV-LIF Spectrometry

Liquid impingers were first introduced in 1914, and are an effective tool for collecting submicron aerosols [35]. During impinger sampling, a known volume of air is bubbled through the impinger containing a specified liquid, which will react or physically dissolve the chemical of interest. Where bioaerosol sampling is considered, certain difficulties can arise. For example, after an extended period of sampling, collection fluid evaporation may impact on either a microorganism's viability or collection efficiency [36], through influencing particle re-aerosolisation, particle bounce or particle penetration. Experiments using alternative collection fluids have had some success in maintaining microorganism viability [37], while other designs utilising centrifugal motion [38] or submersed impingement [39] have maintained collection efficiency through reduced evaporation rates.

Cyclone technologies work through creating an air vortex inside. The mass of bioaerosols causes the particles to have inertia and collide with the outer wall, where they can be collected in a liquid. Consequently, the bioaerosols are turned from an aerosol into a hydrosol. The advantage of this is that cyclones can offer greater microbial viability in the samples collected than those in filter samples, impingers or impactors.

Impactors seek to separate particles from a gas stream, for which there are many different variants. Cascade impactors consist of 'stacked' impaction stages, whereby each stage has a target area for the bioaerosols to be collected. This can consist of growth mediums such as agar, or they can be a filter material or greased plate. Through the use of differently spaced stages, particles can be filtered from a stream based on their inertia, which is a function of their size and velocity. This can provide useful information, as the sizing of bioaersols is an important factor in the hazards they can pose, since it is predominantly size that will dictate how deep into the lungs they are inhaled.

Filter samples are one of the oldest techniques still employed, and are often used to sample airborne viruses [40]. Compared to alternatives, filters are able to most efficiently collect submicron particles over the long-term. They can be made from a host of materials, including cellulose, gelatin and polycarbonate. Depending on the material used, certain problems may be more or less prevalent. For example, gelatin filters are susceptible to environmental conditions. In low humidity, they are known to dry out and break, while higher humidities can cause the gelatin to begin to dissolve [40]. More generally, problems can also be found depending on the particles of interest. For example, viruses are often out-competed by fungal spores and bacteria, that are both ubiquitous in most environments and can overload agar. Virus sampling efficiency has also been noted to decline over time, suggesting their possible desiccation and/or degradation [41]. Post-sampling analysis is usually required to better determine the presence of certain microorganisms. This is typically done using Polymerase Chain Reaction (PCR) technology to look for specific genetic indicators. Though this technique can help show the presence of unique bioaerosols, it is not useful for determining their relative concentrations, simply due to the different affinities that microorganisms may have for their collection media, alongside varying timespans for replication, biasing the presence of certain microbes.

Spore traps are a labour intensive method, first introduced in the 1950's. There are various designs, but the most commonly used is the slit-type volumetric spore sampler, also known as the Hirst trap. A vacuum draws in surrounding air, while a slowly rotating drum with an adhesive tape on the inside causes the airborne particles to attach. This tape can then be removed for analysis. The advantages of such a sampling method is that Hirst traps offer a means of continuous sampling, whereby the volume of air can be regulated. It is also has a highly efficient collection efficiency. However, it is not always clear how representative samples are of the ambient background concentrations. The traps are sensitive to both particle size and wind speed, and some spores can be adhesive-sensitive. It is also an incredibly time consuming process, where qualified personnel are needed to identify specific spores. Furthermore, while it offers continuous sampling, battery units failing, or lack of sunlight in solar powered models, as well as limited use during rain events can have consequences for the dataset. The 'Biowatch Program' was an ambitious attempt to use real-time spore trap techniques, coupled with automated PCR analysis to provide information on bioaerosol concentrations in major U.S Metropolitan areas. This was devised as a protection measure against possible bioterrorism attacks, but ultimately was cancelled. This was

in part due to concern over the accuracy of the bioaerosols being recorded, further highlighting the challenging task of identification.

1.5 Thesis Overview

Chapter 1 provides a general overview of atmospheric aerosols, including their role in the climate system. It also provides a focus on bioaerosols and competing field measurement techniques for their observation. Understanding the principles of UV-LIF spectrometry is essential for the research projects discussed further on.

Chapter 2 provides a literature review of the current state of research regarding bioaerosols. This touches on a number of disciplines for which bioaerosols are consequential.

Four research projects are presented in Chapter 3, of which two have recently been published in peer-reviewed journals. The first paper quantifies bioaerosol concentrations in dust clouds associated with African outflow. The second paper discusses the monsoon-influenced climate of Hong Kong, and how a seasonal shift in wind patterns has consequences for bioaerosol concentrations. The third paper continues the work discussed in the first, with instruments capturing the bioaerosol concentrations received on the other side of the Atlantic, in Barbados. Finally, the fourth paper looks at bioaerosol concentrations recorded at Chilbolton, UK. It discusses a provisional attempt at using the supervised machine learning method 'Gradient Boosting' to create a training dataset for automated pollen recognition.

Chapters 4 and 5 draw together the aforementioned research projects with a summary of their key findings and a discussion of their potential impacts. A general discussion of UV-LIF spectrometry is provided, alongside recommendations for future research projects.

References

[1] I. George and J. Abbatt, "Heterogeneous oxidation of atmospheric aerosol particles by gas-phase radicals," *Nature Chemistry*, vol. 2, no. 9, p. 713, 2010.

[2] A. Calvo, C. Alves, A. Castro, V. Pont, A. Vicente, and R. Fraile, "Research on aerosol sources and chemical composition: Past, current and emerging issues," *Atmospheric Research*, vol. 120, pp. 1–28, 2013.

[3] A. Tsuda, F. S. Henry, and J. P. Butler, "Particle transport and deposition: Basic physics of particle kinetics," *Comprehensive Physiology*, vol. 3, no. 4, pp. 1437–1471, 2011.

[4] H. Levy, L. W. Horowitz, M. D. Schwarzkopf, Y. Ming, J.-C. Golaz, V. Naik, and V. Ramaswamy, "The roles of aerosol direct and indirect effects in past and future climate change," *Journal of Geophysical Research: Atmospheres*, vol. 118, no. 10, pp. 4521–4532, 2013.

[5] N. Braslau and J. Dave, "Effect of aerosols on the transfer of solar energy through realistic model atmospheres. part i: Non-absorbing aerosols," *Journal of Applied Meteorology and Climatology*, vol. 12, no. 4, pp. 601–615, 1973.

[6] L. Fierce, T. B. Onasch, C. D. Cappa, C. Mazzoleni, S. China, J. Bhandari, P. Davidovits, D. Al Fischer, T. Helgestad, A. T. Lambe, *et al.*, "Radiative absorption enhancements by black carbon controlled by particle-to-particle heterogeneity in composition," *Proceedings of the National Academy of Sciences*, vol. 117, no. 10, pp. 5196–5203, 2020.

[7] L. Tang, S. Niu, M. Yan, X. Li, X. Zhang, Y. Zhu, H. Shen, M. Xu, and L. Tang, "Observational study of black carbon in the north suburb of nanjing, china," in *Advanced Air Pollution*, IntechOpen, 2011.

[8] P. DeMott, Y. Chen, S. Kreidenweis, D. Rogers, and D. E. Sherman, "Ice formation by black carbon particles," *Geophysical Research Letters*, vol. 26, no. 16, pp. 2429–2432, 1999.

[9] L. Wang, W. Kong, F. Wang, and H. Liu, "Temperature-gradient effects on heterogeneous ice nucleation from supercooled water," *AIP Advances*, vol. 9, no. 12, p. 125 122, 2019.

[10] S. Park and X. Wu, "Effects of surface albedo on cloud and radiation processes in cloud-resolving model simulations," *Journal of Atmospheric Sciences*, vol. 67, no. 5, pp. 1474–1491, 2010.

[11] K. A. Koehler, P. J. DeMott, S. M. Kreidenweis, O. B. Popovicheva, M. D. Petters, C. M. Carrico, E. D. Kireeva, T. D. Khokhlova, and N. K. Shonija, "Cloud condensation nuclei and ice nucleation activity of hydrophobic and hydrophilic soot particles," *Physical Chemistry Chemical Physics*, vol. 11, no. 36, pp. 7906–7920, 2009.

[12] J. Hovorka, C. Leoni, V. Dočekalová, J. Ondráček, and N. Zíková, "Aerosol distribution in the planetary boundary layer aloft a residential area," in *IOP Conference Series: Earth and Environmental Science*, IOP Publishing, vol. 44, 2016, p. 052 017.

[13] S. Kode and A. Kumar, "Literature review of nighttime boundary layer and concentration models under calm conditions," in *A AND WMA ANNUAL MEETING*, vol. 10, 1995, 95–WP139P.

[14] T. Su, Z. Li, and R. Kahn, "Relationships between the planetary boundary layer height and surface pollutants derived from lidar observations over china: Regional pattern and influencing factors," *Atmospheric Chemistry and Physics*, vol. 18, no. 21, pp. 15 921–15 935, 2018.

[15] L. Menut, C. Flamant, J. Pelon, and P. H. Flamant, "Urban boundary-layer height determination from lidar measurements over the paris area," *Applied Optics*, vol. 38, no. 6, pp. 945–954, 1999.

[16] K. E. Graham, A. J. Prussin, L. C. Marr, L. M. Sassoubre, and A. B. Boehm, "Microbial community structure of sea spray aerosols at three california beaches," *FEMS microbiology ecology*, vol. 94, no. 3, fiy005, 2018.

[17] N. Wéry, A. Galès, and Y. Brunet, "Bioaerosol sources," *Microbiology of aerosols*, pp. 115–135, 2017.

[18] T. Maki, K. C. Lee, K. Kawai, K. Onishi, C. S. Hong, Y. Kurosaki, M. Shinoda, K. Kai, Y. Iwasaka, S. D. Archer, *et al.*, "Aeolian dispersal of bacteria associated with desert dust and anthropogenic particles over continental and oceanic surfaces," *Journal of Geophysical Research: Atmospheres*, vol. 124, no. 10, pp. 5579–5588, 2019.

[19] K.-H. Kim, E. Kabir, and S. A. Jahan, "Airborne bioaerosols and their impact on human health," *Journal of Environmental Sciences*, vol. 67, pp. 23–35, 2018.

[20] S. Huang, W. Hu, J. Chen, Z. Wu, D. Zhang, and P. Fu, "Overview of biological ice nucleating particles in the atmosphere," *Environment International*, vol. 146, p. 106 197, 2021.

[21] J. Fröhlich-Nowoisky, C. J. Kampf, B. Weber, J. A. Huffman, C. Pöhlker, M. O. Andreae, N. Lang-Yona, S. M. Burrows, S. S. Gunthe, W. Elbert, *et al.*, "Bioaerosols in the earth system: Climate, health, and ecosystem interactions," *Atmospheric Research*, vol. 182, pp. 346–376, 2016.

[22] C. M. Rathnayake, N. Metwali, T. Jayarathne, J. Kettler, Y. Huang, P. S. Thorne, P. T. O'Shaughnessy, and E. A. Stone, "Influence of rain on the abundance of bioaerosols in fine and coarse particles," *Atmospheric Chemistry and Physics*, vol. 17, no. 3, pp. 2459–2475, 2017.

[23] M. Tanarhte, S. Bacer, S. M. Burrows, J. A. Huffman, K. M. Pierce, A. Pozzer, R. Sarda-Estève, N. J. Savage, and J. Lelieveld, "Global modeling of primary biological particle concentrations with the emac chemistry-climate model," *Atmospheric Chemistry and Physics Discussions*, pp. 1–33, 2018.

[24] S. Matthias-Maser and R. Jaenicke, "The size distribution of primary biological aerosol particles with radii> 0.2 μm in an urban/rural influenced region," *Atmospheric Research*, vol. 39, no. 4, pp. 279–286, 1995.

[25] B. Graham, P. Guyon, W. Maenhaut, P. E. Taylor, M. Ebert, S. Matthias-Maser, O. L. Mayol-Bracero, R. H. Godoi, P. Artaxo, F. X. Meixner, *et al.*, "Composition and diurnal variability of the natural amazonian aerosol," *Journal of Geophysical Research: Atmospheres*, vol. 108, no. D24, 2003.

[26] W. C. Hinds, *Aerosol technology: properties, behavior, and measurement of airborne particles*. John Wiley & Sons, 1999.

[27] C. Pöhlker, J. Huffman, and U. Pöschl, "Autofluorescence of atmospheric bioaerosols–fluorescent biomolecules and potential interferences," *Atmos. Meas. Tech*, vol. 5, no. 1, pp. 37–71, 2012.

[28] S. C. Hill, M. W. Mayo, and R. K. Chang, "Fluorescence of bacteria, pollens, and naturally occurring airborne particles: Excitation/emission spectra," ARMY RESEARCH LAB ADELPHI MD COMPUTATIONAL and INFORMATION SCIENCES DIRECTORATE, Tech. Rep., 2009.

[29] J. R. Lakowicz, *Principles of fluorescence spectroscopy*. Springer science & business media, 2013.

[30] I. Crawford, S. Ruske, D. Topping, and M. Gallagher, "Evaluation of hierarchical agglomerative cluster analysis methods for discrimination of primary biological aerosol," *Atmospheric Measurement Techniques*, vol. 8, no. 11, p. 4979, 2015.

[31] S. Ruske, D. O. Topping, V. E. Foot, A. P. Morse, and M. W. Gallagher, "Machine learning for improved data analysis of biological aerosol using the wibs," *Atmospheric Measurement Techniques*, vol. 11, no. 11, pp. 6203–6230, 2018.

[32] S. Ruske, D. O. Topping, V. E. Foot, P. Kaye, W. Stanley, I. Crawford, A. Morse, and M. W. Gallagher, "Evaluation of machine learning algorithms for classification of primary biological aerosol using a new uv-lif spectrometer," *Atmospheric Measurement Techniques*, 2017.

[33] B. Crouzy, M. Stella, T. Konzelmann, B. Calpini, and B. Clot, "All-optical automatic pollen identification: Towards an operational system," *Atmospheric Environment*, vol. 140, pp. 202–212, 2016.

[34] J. A. Huffman, A. E. Perring, N. J. Savage, B. Clot, B. Crouzy, F. Tummon, O. Shoshanim, B. Damit, J. Schneider, V. Sivaprakasam, *et al.*, "Real-time sensing of bioaerosols: Review and current perspectives," *Aerosol Science and Technology*, vol. 54, no. 5, pp. 465–495, 2020.

[35] J. B. Harstad, "Sampling submicron t1 bacteriophage aerosols," *Applied microbiology*, vol. 13, no. 6, pp. 899–908, 1965.

[36] E. W. Henningson, I. Fängmark, E. Larsson, and L.-E. Wikström, "Collection efficiency of liquid samplers for microbiological aerosols," *Journal of Aerosol Science*, vol. 19, no. 7, pp. 911–914, 1988.

[37] X. Lin, T. A. Reponen, K. Willeke, S. A. Grinshpun, K. K. Foarde, and D. S. Ensor, "Long-term sampling of airborne bacteria and fungi into a non-evaporating liquid," *Atmospheric Environment*, vol. 33, no. 26, pp. 4291–4298, 1999.

[38] K. Willeke, X. Lin, and S. A. Grinshpun, "Improved aerosol collection by combined impaction and centrifugal motion," *Aerosol Science and Technology*, vol. 28, no. 5, pp. 439–456, 1998.

[39] S. A. Grinshpun, K. Willeke, V. Ulevicius, A. Juozaitis, S. Terzieva, J. Donnelly, G. N. Stelma, and K. P. Brenner, "Effect of impaction, bounce and reaerosolization on the collection efficiency of impingers," *Aerosol Science and Technology*, vol. 26, no. 4, pp. 326–342, 1997.

[40] D. Verreault, S. Moineau, and C. Duchaine, "Methods for sampling of airborne viruses," *Microbiology and molecular biology reviews*, vol. 72, no. 3, pp. 413–444, 2008.

[41] G. Cao, J. Noti, F. Blachere, W. Lindsley, and D. Beezhold, "Development of an improved methodology to detect infectious airborne influenza virus using the niosh bioaerosol sampler," *Journal of Environmental Monitoring*, vol. 13, no. 12, pp. 3321–3328, 2011.

Chapter 2

Literature review

2.1 Human Health

Ever since research into bioaerosols started in the 1800's, they have been implicated in affecting human health. When trying to mitigate some of their deleterious impacts, for example the spread of certain diseases, it is important to understand the pathways to exposure that we each face. This encompasses not only a number of indoor and outdoor environments, but also community factors in which people's interactions with one another can contribute to further risk.

For many people, their occupation is the most important pathway to exposure. Those involved in the waste recycling and composting industry offer one such example. Windrows are long rows of heaped biodegradable waste. In many composting sites these are contained within heavy-duty windrow turners that disturb the waste to improve porosity and oxygen content. This invariably leads to high levels of organic dust (bioaerosols) in the surrounding area, comprised of fungi, bacteria and endotoxins [1]. Operational activities are estimated to increase micro-organism concentrations in the air by several orders of magnitude [2]. This has been closely correlated with occurrence rates of inflammatory and allergic respiratory outcomes among compost workers [3].

Farmers offer another example. Intensive farming involves rearing livestock in densely packed holdings, where bioaerosol levels can be elevated from faecal matter, feather fragments, feed, bedding, and more [4]. Widespread use of antibiotics in such conditions has also seen a rise in resistant strains of zoonotic infectious diseases [5], while organic matter attached to soil particles can be released via tilling activities. The consequences of this have been well documented, and conditions such as 'Farmer's Lung' are increasingly recognised. This is an allergic reaction, triggered from repeated exposure to biological dust that can cause chronic coughing, shortness of breath, pain and physical weakness. It is estimated to affect approximately 2% of all farmers [6]. The only viable preventions includes better ventilation, or the use of face masks to filter out antigens. The health burdens associated with such activities can also be experienced further than the farm perimeter. Some studies have found a close correlation in asthma rates amongst school children, and either their home or school's proximity to an intensive farm [4]. There are many different environments and job roles that increase exposure to bioaerosols, and it is impossible to list them all. Some other

key ones however, include health workers and their risk of catching infectious diseases, veterinarians, abattoir workers and those in the forestry sector.

Indoor bioaerosol research is increasingly understood to be critical in understanding the degree to which we are exposed to certain bioaerosols. People spend more time indoors than previous generations, with the average person in the UK now estimated to spend 90% of their time indoors [7]. Whether in a home, office or leisure facility, such a significant amount of time indoors all but guarantees exposure to the bioaerosols that can thrive in such conditions. Among these, bacteria and fungi are particularly prevalent. Studies have suggested such concentrations are significantly higher than outside, and that children are on average exposed to higher concentrations than adults [8]; emphasising the need for special attention to be paid towards schools.

It is also important to note that bioaerosols occur naturally, in variable concentrations. It is impossible to completely prevent exposure. Instead, acceptable background concentrations must be decided, so that limits and suitable mitigation strategies can be implemented. It is because of this that the Environment Agency has published provisional guidance to composting operators. As discussed by Pearson et al. [9], operators must ensure acceptable levels in residential areas or the nearest 'sensitive receptor' (i.e. workplace) are found no further than 250 m away. The acceptable levels in colony-forming units per cubic meter (cfu/m^3) are:

• 1000 cfu/m^3 for total bacteria

• 300 cfu/m^3 for gram-negative bacteria

• 500 cfu/m^3 for *Aspergillus fumigatus*

However, there are some problems with such limits. First, they are not based upon dose-response relationships. The quantities that pose a danger to an immuno-compromised individual (such as the elderly, sick or children) are not equivalent to healthy adults. Secondly, some hazardous bioaerosols are not included. High levels of endotoxins can contribute to elevated inflammatory responses [10], but no guidelines outlining acceptable levels currently exist. Third, due to the diversity of bioaerosols emitted from certain practices, it is not always easy to see what has occurred naturally in the wider environment, and what has been blown downwind. That being said, thermophilic bacteria or thermotolerant microfungi have been suggested as good indicators for anthropogenic amplification because they are rare in natural environments due to their necessary thermophilic characteristics. The health impacts of bioaerosol exposure are broad, with some dangers having been outlined above. In general, they have been implicated in infectious and respiratory diseases, allergies and cancer. Respiratory diseases are the most commonly reported, in particular rhinitis, asthma, bronchitis and sinusitis. Other effects can include fatigue, weakness and headaches [11].

Once inhaled, the size of the particle can determine its effect. For example, asthma is a condition concerning the upper airways. Particles of 4-10 μm are too large to penetrate deeper

into the lungs, and are consequently the relevant size here. Bioaerosols exist across a spectrum of sizes, but at 4-10 μm it is more typical of pollen, fungal spores and larger bacteria. This means that regions or job roles associated with high concentrations of pollen or fungal spores are more likely to affect asthma sufferers. Due to the seasonality of pollen in the UK, it also means that asthma sufferers can expect their condition to be exacerbated during peak months.

2.2 Ecosystems and Climate

Climate change is anticipated to have significant consequences for bioaerosol concentrations. Gange et al. [12] recorded fruiting periods for 315 autumnal fruiting fungal species over a period of 20 years, and found that the fungi now fruited for twice as long as they did in the 1950's. This can potentially be attributed to climate change, as mean temperatures have increased in August, alongside precipitation in October. This finding is supported by a study of fungal phenology in Norway [13], who found a similar lengthening of the fruiting period. It is thought that climate change may also drive morphological differences in spores. Kauserud et al. [14] found that spores produced at the beginning of autumn were larger than those at the end. This has important health implications, since smaller particles more easily penetrate the lungs, where they can contribute to respiratory problems. As these sizes are correlated with changing meteorological conditions, there are a few plausible scenarios for the future, as the effects of climate change become more pronounced. One is that asthma exacerbations may shift from autumn to the winter. Another is that regions for which a reduction in precipitation is anticipated, may also find a reduction in health compromises resulting from fungal spore exposure. Finally, a third scenario is that regions such as Europe may find an increase in respiratory problems. There is still discussion in discerning what will happen however, as Damialis et al. [15] have found contrasting results. They found in laboratory experiments that although fungal growth increased in line with the projected meteorological changes, that overall spore production decreased.

Where other pathogens exist, such as bacteria and viruses, climate change can also influence their concentrations and dispersion. Wind speed, wind direction, temperature, humidity and atmospheric stability can all influence the dispersal of pathogens, and are themselves subject to climate change. With most projections highlighting an increase in global radiation, temperature and wind speeds, this increases atmospheric mixing, effectively reducing concentrations at point sources while increasing the potential distance that any one particle can travel. This would likely be beneficial for human health, with particles becoming more evenly dispersed. However, the impacts of climate change are complex, and a more complete discussion is needed to determine what its effects may be. Where agriculture is considered, Beggs and Bambrick. [16] have investigated how climate change may affect the timing, distribution, quantity and quality of aeroallergens. Furthermore, Slingo et al. [17] have suggested that food crops may contribute to greater exposure of mycotoxins. Higher temperatures may facilitate the introduction of new pathogens, vectors, or hosts

[18]. Given that many bioaerosols are also positively correlated with precipitation [19], regional concentrations could be affected depending on whether precipitation rates rise or fall. For the United Kingdom, it is more likely that concentrations will increase. In the case of pollen, similarities can be drawn with fungal spore production. Rising temperatures and rainfall may lengthen the pollen season, while higher CO_2 levels are correlated with increased concentrations [20].

Although most of the concern regarding climate change's influence on bioaerosols primarily consider human health, there is also risk for the health of forests [21]. Forest pathogens are diverse, including fungi, bacteria, virsuses, oomycetes, parasitic higher plants, and nematodes. Native pathogens play an important role in the forest ecosystem, shaping the composition of species present. They also affect animal populations, nutrient and water cycling, and overall ecosystem function. However, non-native pathogens have proven problematic for many forests in recent decades, where they can rapidly drive down population numbers for species that have not had time to co-evolve defensive mechanisms. Where climate change expands or contracts a species' range, there may be overlap between forests and novel pathogens. The consequences of this may be sudden, or take decades to truly manifest. Instances where pathogens rapidly kill their host are the most obvious, and resulting epidemics are strongly projected to increase in frequency [22], but it could be the longer-term, cumulative effects of new diseases that prove the most significant. Some examples are already being found of pathogens that are closely connected to climate change. Phytophtora root rot is a destructive genus of pathogen present in many temperate and subtropical regions of the world, and can trigger disease in more than 1000 species. Temperature, moisture and pH are all influential in its reproductive rates, with warmer winter temperatures and a seasonal shift of precipitation from the summer to winter accelerating infection rates in central Europe. As this trend continues, susceptible species including oak, alder, maple, fir and pine will face increased stresses [23]. Furthermore, there will be ever increasing consequences for human society's food security. It has been estimated that low-level persistent crop diseases already destroy enough crops to feed 8.5% of 2011's human population [24]. As the destructive potential increases, it may be compounded by reduced yields in many of the world's major crops [25].

2.3 Contribution to Geochemical Cycles

Aerosol's can play a key role in the global climate. Their suspension in the air can scatter incoming solar radiation, reducing the warming effect of the sun. This is known as the albedo effect and is an important factor when 'balancing' the global energy budget. Furthermore, aerosols can serve as nuclei for cloud droplets, ice crystals and precipitation. Cloud cover further influences the albedo effect, and can have important impacts on local environments. Cloud condensation nuclei (CCN) are particles that in the presence of supersaturated water vapour can activate to become cloud and fog droplets. It was originally thought that only inorganic particles such as mineral dust contained nucleating abilities, but

over the years more evidence has been collected that suggests biological particles may play an important role too. *Pseudomonas syringae* are thought to induce rain [26], while strains such as *Erwinia carotovora carotocora* and *Ewinia carotovora atroseptica* have been shown to be CCN active, with 25-30% activatable at supersaturations larger than 1% [27]. Interestingly, precipitation samples collected in Japan have found the bacteria contained within are largely associated with minerals [28]. This has led some to believe that mineral dust may act as carriers that take bacteria into cloud droplets.

For CCN's to activate, they are dependent on factors such as particle solubility and hygroscopicity, which are themselves subject to the chemical composition of the aerosol [29]. Research has indicated not only that biological particles can act as CCN's, but that they may also be more effective at certain supersaturations than alternatives. Bauer et al. [30] collected cultivable bacteria from cloud water samples in Austria and tested them for their CCN activity at supersaturations between 0.07 and 0.11%. They found all samples to be activatable, whereas insoluble wettable particles of comparable size would not have been.

Ice formation in mixed-phase clouds (at temperatures between 0 and -38$^{\circ}C$) depends on ice nuclei (IN). Without them any suspended droplets within this range would remain in a metastable liquid state. Once crystallisation has begun, they can grow rapidly and stimulate precipitation. IN's encompass a broad range of particles, including mineral dust, metals, soot, biological particles and more. Among these, biological particles are some of the most efficient, with strains such as *Pseudomonas syringae* initiating freezing at temperatures as high as -2 $^{\circ}C$ [31]. This has important implications for frost damage to plants, and therefore can carry significant economic consequences for farmers. Bacterial ice nucleation on leaves can be detected at about -2 $^{\circ}C$, whereas leaves without ice nucleation-active (INA) bacteria contain nuclei that are only active at much lower temperatures. As such, the INA bacteria in the atmosphere that can attach/develop on crops lower the threshold at which frost damage can occur.

There has been ample discussion to the role bioaerosols may play in influencing the global climate. Hoose, Kristjánsson and Burrows. [32] created a model in which bacteria, fungal spores and pollen emissions were parameterised based on recent literature, alongside immersion freezing based on nucleation theory and laboratory measurements. Their simulation found that primary biological aerosol particles (PBAP's) accounted for an average global nucleation rate of just 10-5%, with a highest estimate of 0.6%. On the other hand, Christner et al. [33] observed that ice nucleation active bacteria are ubiquitous in precipitation on different continents; Pratt et al. [34] identified 33% of the ice crystal residual particles sampled in a wave cloud over Wyoming as biogenic; and Prenni et al. [35] found that chamber-measured INs in the Amazon basin were composed to a significant fraction of biological carbonaceous particles. The main argument against biological particle's importance as ice nucleators is their low concentrations at high altitude. However, Murray et al. [36] investigated the role that secondary biogenic particles may play. They hypothesise that biological, nano-meter scaled IN's which are bound to other atmospheric particulates could play a more significant role in cloud glaciation. An example would be birch pollen, which

contains tens of thousands of particulates, each capable of acting as an ice-nucleating site. They propose that similar nano-scale particulates are unlikely to be emitted directly into the atmosphere, but could indirectly be transported on aerosolised soil or dust particles.

Fungi are also a potential source of IN. This is demonstrated by Huffman et al. [37] and Crawford et al. [38], who found that concentrations of bioaerosols increased during rain events, and were closely correlated with concentrations of atmospheric ice nuclei. This correlation was greatest in particles with a size range of 2-6 μm, which are indicative of either bacterial aggregates or fungal spores. Further DNA analysis found "high diversities of airborne bacteria and fungi".

2.4 Dust

As has been alluded to earlier, there is growing evidence that dust and soil particles may play a key role in transporting biological matter. As such, it is useful to look at what factors can drive the uplifting and transportation of dust itself. Dust events are global phenomena in which significant quantities of dust become suspended in the air for prolonged periods of time, and are consequently often transported great distances. They are capable of continent-wide, transoceanic, and global dispersion [39]. Some occur on a seasonal basis, such as the Harmattan wind in Africa, while others occur more irregularly, as a consequence of strong winds. Often covering large areas for months at a time, they have been implicated in compromising human health, particularly through pulmonary disease.

Large deserts such as the Saharan and Sahelian regions of Africa or the Gobi in Asia, are the primary sources of desert top soils, driving dust events on a global scale. Perkins et al. [40] estimates annual quantities of 0.5 – 5 billion tons are uplifted into the atmosphere. Dust clouds may also contain significant concentrations of micro-organisms [41], and pick up other bioaerosols as the clouds move downwind over terrestrial environments. Many studies have looked at the bacterial diversity found within desert topsoils [42], [43]. Concentrations of prokaryotes can vary from $\sim 10^7$ to 10^9 in forest or arid soil types, respectively [44]. Once airborne, the stresses posed to micro-organisms are similar to those found in the soil. They can become dessicated, exposed to UV damage, or made vulnerable to atmospheric chemistry and nutrient deprivation. Their viability is likely enhanced when passing over aquatic environments, due to tolerable humidity levels and attenuation of UV by the particle load of dust clouds [45]. By comparison, fungal spores are typically adapted to be much more resilient to environmental stresses. The spores are coated in hydrophobic proteins that can prevent desiccation and offer UV protection. Viable spores have been recovered from extreme altitudes in the atmosphere [46]. Concentrations are also much lower than for bacteria, especially when sampled above desert regions. In such instances concentrations are as low as 400 spores m^{-3}, but can be as high as 10^6 spores m^{-3} in tropical or temperate regions [47]. Regardless of their relative concentrations however, they are frequently positively correlated with concentrations of desert dust in the atmosphere.

Where biological particles are concerned, it is not necessarily the concentration that is the most important for human health, but instead what the species or genera that are present. There is little research into the movement of prokaryotes and their link to the occurrence rates of certain diseases. However, there is a known association between dust storms and meningitis. Outbreaks typically occur in the Sahel region of North Africa between February and May, affecting as many as 200,000 individuals annually [48]. It is during this period that conditions are usually dry, with frequent dust storms. Once the wet season begins, outbreaks begin to cease [49]. Interestingly, it is not believed that an increased concentration of pathogens present in dust storms is the primary driver of infection rates, but rather the consequences of inhaling dust. It is thought dust particles can cause abrasions of the nasopharyngeal mucosa, which provides an opportunity for the Neisseria meningitides cells residing in the mucosa to access the underlying tissue and blood [50]. That being said, it is also true that the dust can serve as a carrier for pathogens, as demonstrated by Yamaguchi et al. [51]. Many infectious pathogens have been identified during dust events, including *Staphylococcus aureus, Bacillus circulans, Bacillus licheniformis, Pantoea agglomerans, Ralstonia paucula*, and *Cryptococcus albidus* [52]–[57].

Dust events can also act as a major source of nutrient deposition for oceans on a global scale. Although the exact chemical content of what is deposited depends on the source of the dust, most dust particles originate from arid or semi-arid regions. In particular, the continental crust contains large amounts of biogeochemically significant elements [58]. Increased bioavailability of elements such as Phosphorus or Iron can promote biological growth. Although this is often considered a net benefit effect, due in part to ocean life acting as an important carbon sink, it can also have detrimental, localised impacts. For example, the decline in Caribbean coral reefs has been partially attributed to transatlantic dust events. *Aspergillus sydowii* is a fungal spore implicated in a Caribbean-wide seafan disease, that has been cultured from Caribbean air samples [59]. It is believed that dust is acting as a substrate for said spores.

Rather than being freely suspended in the air, bacteria can utilise mineral dust to act as a vector for their transport. Yamaguchi et al. [51] analysed the bacterial community structure for Asian dust particles, and compared them to samples from other regions. It was found that more than 20 bacterial classes were present, with *Actinobacteria, Bacilli* and *Sphingobacteria* dominating in particular. These findings are similar to previous studies on African dust [45], suggesting that the diversity of such communities is largely similar across arid regions. Furthermore, Yamaguchi et al. [51] investigated the bacteria's ability to grow and reproduce when attached to dust, and found many to remain physiologically active. However, they also conclude that the implications this may have for human health are limited. *Actinobacteria* are known to inhabit extreme environments such as hypersaline lakes, *Bacilli* are a spore-forming bacterial genera and *Sphingobacteria* are commonly found in soil and aquatic environments. None of these have been identified as hazardous to humans, although their potential to act as allergens or a source of opportunistic infection does still exist. What is more consequential is their effect on ecosystems. When introduced to new ecosystems, a

bacterium may introduce new genes to the indigenous population. In this way, genetic diversity can be increased within bacterial communities, or community structures themselves can change to either accommodate or be out-competed by new species.

2.5 Transport

Bacteria can be emitted into the atmosphere from almost any surface, including plants, soil, and water [60]. They can be actively released, such as through their host sneezing, or passively released, for example through wind causing sea spray or uplifting soil particles. Fungal spores can be ejected into the air as a response to particular humidity levels. Given that meteorological factors often drive passive emissions, it is useful to identify what effect each specific factor can have on bioaerosol concentrations. Temperature affects the rate of bacterial metabolism and reproduction, as well as culturability. It also impacts atmospheric factors such as boundary layer turbulence. Consequently, Lighthart et al. [61] and Harrison et al. [62] found temperature was positively correlated with bacterial concentrations. Furthermore, drying can reduce the bonding forces between surface particles, and contribute to their susceptibility of being uplifted.

Two studies address the effects of both rain and soil wetness on bacterial flux [63], [64]. They found rain events dramatically increased bacterial concentrations in the air above crops, while also finding a strong net deposition flux. There is also evidence that rain can remove bacteria from leaf surfaces, with concentrations increasing as the rain passed through a canopy.

Deposition rates of viruses from above the atmospheric boundary layer were 9-461 times greater than for bacteria, even in pristine environments [65]. The highest rates for viruses were associated with atmospheric transport from marine rather than terrestrial environments, likely released through sea spray in aggregates. Environmental drivers of deposition were also not equal between types of aerosol. For example, rainfall events and Saharan dust intrusions were positively correlated with bacterial deposition, but not for viral. Meanwhile, viruses were positively correlated with organic aerosols <0.7 μm, while bacteria were positively correlated with organic aerosols >0.7 μm. The paper states that this could be an indication of longer residence time for viruses, and consequently a greater potential to be transported further. This is supported by the identification of similar genetic sequences in viruses across disparate regions. The residence time of bacteria may be shorter for bacteria emitted from the ocean than for bacteria emitted from land surfaces, because of more rapid removal by precipitation [66].

2.6 Aircraft Measurements

The first attempt to take high altitude samples of bioaerosols was in the Arctic [67], using a collection device designed by Colonel Lindbergh. For this, oiled glass slides were ex-

posed during flight, and acted as a trap upon impaction. These slides could then be sealed into cartridges to prevent contamination. Pollen and fungal spores were found, alongside unicellular algae and fragments of insect wings. These micro-organisms are the first of their kind to provide concrete evidence of the role played by air currents in the distribution of fungi across the Northern Hemisphere. This experiment was followed years later by Hirst [68]. He was interested in investigating the potential spores have for long-range transport. This was measured using suction impactors, whereby the spores are retained on an adhesive surface. More modern attempts have utilised UV-LIF technology, with any required off-line analysis acting as a secondary and complementary approach to the real-time measurements made during the flight.

A WIBS-4A has been used to make measurements from the boundary layer to the upper troposphere over the United States Great Plains region [69]. Flights were carried out over undeveloped grassland / cropland, with one flight also occurring over a forested region, and temperatures ranged from 220 to 280K. These are thought to be some of the first flights demonstrating the vertical profile of bioaerosol concentrations over a wide range of temperatures including where ice is known to form. The concentrations of ice-nucleating particles estimated from the WIBS-4A were compared to typical concentrations of ice crystals at mixed-phase cloud temperatures. The authors do note however that there were some uncertainties with such a method. For example, only fluorescent particles were counted, but it may be that non-fluorescent biological particles existed that can also act as ice-nucleators. Furthermore, the equipment can only record particles from 0.8 to 12 μm, meaning larger particles such as intact pollen grains will go unrecorded. The authors claim this should not be significant however, since pollen occurrence is orders of magnitude less than bacteria at the surface [70]. What they concluded from their results is that primary fluorescent biological particles are likely important for ice formation in mixed-phase clouds under certain conditions. This is particularly true when there is a strong lifting effect, that both exposes the particles to sub-zero temperatures, and counteracts the natural loss of such particles through sedimentation. They propose that this could be an important feature where deep convection is present, since vertical velocities are strong. In areas impacted by long-range transport [34] or orographic and front uplift, it may be more sporadic. Only two of five flights targeting orographic flights over the Rocky Mountains found any bioaerosols [71].

The flights clearly demonstrated a changing vertical profile for biological particles, if only for the US Great Plains. Concentrations were 10-100 L^{-1} at temperatures warmer than 270K in the atmospheric boundary layer, while in the mid to upper free troposphere, where temperatures were less than 255K, concentrations were just 0-1 L^{-1}. Concentrations were considerably more variable in the 2-5 km altitudinal range. Interestingly, this is the range in which dust and mineral particles are less active INP's, suggesting that bioaerosols may play a significant role in forming mixed-phase clouds.

Bioaerosol measurements in the free and upper troposphere are scarce. Four recent studies used an aircraft to measure in altitudes greater than 4000 m [69], [72]–[74]. Two of these

used a WIBS [69], [72], while the other two collected aerosols on filters and analysed them off-line. Twohy et al. [69] found no clear trend between bioaerosol concentrations and altitude.

Zawadowicz et al. [75] have proposed using single-particle mass spectrometry (SPMS) to measure bioaerosols. The technique has been used successfully to characterise the chemical composition of aerosol particles in situ and in real time [76]. They argue that because the method can characterise both volatile and refractory aerosol components, that it is an attractive tool for looking at cloud formation [77]. SPMS works through the use of a pulsed UV laser for the ablation and ionisation of single aerosol particles. Ions are then accelerated into a time of flight mass spectrometer. Previous studies have used the SPMS to investigate bioaerosols [78]. A property of bioaerosol spectra that has been exploited for their detection is the presence of phosphate (PO−, PO−2, PO−3) and organic nitrogen ions (CN−, CNO−) [78]. However, such ions have also previously been associated with certain nonbiological particles, for example those present in vehicular exhausts [79].

2.7 Molecular Analysis

Using molecular and isotopic markers to distinguish between specific types of bioaerosols is a technique that has developed rapidly over the last decade. Many micro-organisms are not culturable, and this can contribute to underestimates in the diversity found in samples. By using quantifiable markers, this problem can be mitigated. These techniques also have high specificity, rapidity, and sensitivity. The exact method used can depend on the bioaerosols being investigated. Bacteria can be quantified using the conserved 16S rRNA prokaryotic gene, utilising PCR. Moulds are not so simple. They cannot be efficiently recovered from liquid air samples that used centrifugation techniques similar to what is done for bacteria, and it is difficult to determine what, if any, genomic region should be targeted that will appropriately establish bioaerosol content. There are three organic molecules that have been established as suitable tracers for fungal spores: ergosterol, mannitol and arabitol. Most fungal spores are actively released via wet discharge processes, often during times of high relative humidity [80]. This process involves the secretion of fluid containing hygroscopic compounds, including arabitol and mannitol [81]. Some of this fluid attaches to the spores and becomes aerosolised. Viruses do not possess universal markers, making blinded molecular approaches unsuitable. They also cannot be filtered from air samples very effectively.

It is criticised by some because although the detection of certain markers can attest to the presence of a particular particle, it says nothing of its viability. Not all micro-organisms have known unique and identifiable regions either, meaning not all can be detected in the same way. This makes most protocols unique to a given project and different between studies. However, some recent studies have attempted to address the first issue. Bonifait et al. [82] used Propidium monoazide staining so that only genes from intact cells could be extracted.

References

[1] M. Taha, G. H. Drew, A. Tamer, G. Hewings, G. Jordinson, P. Longhurst, and S. J. Pollard, "Improving bioaerosol exposure assessments of composting facilities—comparative modelling of emissions from different compost ages and processing activities," *Atmospheric environment*, vol. 41, no. 21, pp. 4504–4519, 2007.

[2] R. Persoons, S. Parat, M. Stoklov, A. Perdrix, and A. Maitre, "Critical working tasks and determinants of exposure to bioaerosols and mvoc at composting facilities," *International Journal of Hygiene and Environmental Health*, vol. 213, no. 5, pp. 338–347, 2010.

[3] C. Herr, A. Zur Nieden, M. Jankofsky, N. Stilianakis, R. Boedeker, and T. Eikmann, "Effects of bioaerosol polluted outdoor air on airways of residents: A cross sectional study," *Occupational and Environmental Medicine*, vol. 60, no. 5, pp. 336–342, 2003.

[4] P. Douglas, S. Robertson, R. Gay, A. L. Hansell, and T. W. Gant, "A systematic review of the public health risks of bioaerosols from intensive farming," *International journal of hygiene and environmental health*, vol. 221, no. 2, pp. 134–173, 2018.

[5] Q. Chang, W. Wang, G. Regev-Yochay, M. Lipsitch, and W. P. Hanage, "Antibiotics in agriculture and the risk to human health: How worried should we be?" *Evolutionary applications*, vol. 8, no. 3, pp. 240–247, 2015.

[6] J. A. Hoppin, D. M. Umbach, G. J. Kullman, P. K. Henneberger, S. J. London, M. C. Alavanja, and D. P. Sandler, "Pesticides and other agricultural factors associated with self-reported farmer's lung among farm residents in the agricultural health study," *Occupational and environmental medicine*, vol. 64, no. 5, pp. 334–341, 2007.

[7] B. L. Diffey, "An overview analysis of the time people spend outdoors," *British Journal of Dermatology*, vol. 164, no. 4, pp. 848–854, 2011.

[8] J. Madureira, L. Aguiar, C. Pereira, A. Mendes, M. M. Querido, P. Neves, and J. P. Teixeira, "Indoor exposure to bioaerosol particles: Levels and implications for inhalation dose rates in schoolchildren," *Air Quality, Atmosphere & Health*, vol. 11, no. 8, pp. 955–964, 2018.

[9] C. Pearson, E. Littlewood, P. Douglas, S. Robertson, T. W. Gant, and A. L. Hansell, "Exposures and health outcomes in relation to bioaerosol emissions from composting facilities: A systematic review of occupational and community studies," *Journal of Toxicology and Environmental Health, Part B*, vol. 18, no. 1, pp. 43–69, 2015.

[10] S. May, D. J. Romberger, and J. A. Poole, "Respiratory health effects of large animal farming environments," *Journal of Toxicology and Environmental Health, Part B*, vol. 15, no. 8, pp. 524–541, 2012.

[11] J. Douwes, P. Thorne, N. Pearce, and D. Heederik, "Bioaerosol health effects and exposure assessment: Progress and prospects," *The Annals of occupational hygiene*, vol. 47, no. 3, pp. 187–200, 2003.

[12] A. Gange, E. Gange, T. Sparks, and L. Boddy, "Rapid and recent changes in fungal fruiting patterns," *Science*, vol. 316, no. 5821, pp. 71–71, 2007.

[13] H. Kauserud, L. C. Stige, J. O. Vik, R. H. Økland, K. Høiland, and N. C. Stenseth, "Mushroom fruiting and climate change," *Proceedings of the National Academy of Sciences*, vol. 105, no. 10, pp. 3811–3814, 2008.

[14] H. Kauserud, E. Heegaard, R. Halvorsen, L. Boddy, K. Høiland, and N. C. Stenseth, "Mushroom's spore size and time of fruiting are strongly related: Is moisture important?" *Biology Letters*, vol. 7, no. 2, pp. 273–276, 2011.

[15] A. Damialis, A. B. Mohammad, J. M. Halley, and A. C. Gange, "Fungi in a changing world: Growth rates will be elevated, but spore production may decrease in future climates," *International Journal of Biometeorology*, vol. 59, no. 9, pp. 1157–1167, 2015.

[16] P. J. Beggs and H. J. Bambrick, "Is the global rise of asthma an early impact of anthropogenic climate change?" *Environmental health perspectives*, vol. 113, no. 8, pp. 915–919, 2005.

[17] J. M. Slingo, A. J. Challinor, B. J. Hoskins, and T. R. Wheeler, "Introduction: Food crops in a changing climate," *Philosophical Transactions of the Royal Society B: Biological Sciences*, vol. 360, no. 1463, pp. 1983–1989, 2005.

[18] S. Harrus and G. Baneth, "Drivers for the emergence and re-emergence of vector-borne protozoal and bacterial diseases," *International journal for parasitology*, vol. 35, no. 11-12, pp. 1309–1318, 2005.

[19] S. Yue, H. Ren, S. Fan, Y. Sun, Z. Wang, and P. Fu, "Springtime precipitation effects on the abundance of fluorescent biological aerosol particles and hulis in beijing," *Scientific reports*, vol. 6, p. 29 618, 2016.

[20] A. Brown, "Suffering pollen," *Nature Climate Change*, vol. 4, no. 12, pp. 1050–1050, 2014.

[21] J. Stenlid, J. Oliva, J. B. Boberg, and A. J. Hopkins, "Emerging diseases in european forest ecosystems and responses in society," *Forests*, vol. 2, no. 2, pp. 486–504, 2011.

[22] M. P. Ayres and M. J. Lombardero, "Assessing the consequences of global change for forest disturbance from herbivores and pathogens," *Science of the Total Environment*, vol. 262, no. 3, pp. 263–286, 2000.

[23] T. Jung, "Beech decline in central europe driven by the interaction between phytophthora infections and climatic extremes," *Forest pathology*, vol. 39, no. 2, pp. 73–94, 2009.

[24] M. C. Fisher, D. A. Henk, C. J. Briggs, J. S. Brownstein, L. C. Madoff, S. L. McCraw, and S. J. Gurr, "Emerging fungal threats to animal, plant and ecosystem health," *Nature*, vol. 484, no. 7393, pp. 186–194, 2012.

[25] S. Ali, Y. Liu, M. Ishaq, T. Shah, A. Ilyas, I. U. Din, *et al.*, "Climate change and its impact on the yield of major food crops: Evidence from pakistan," *Foods*, vol. 6, no. 6, p. 39, 2017.

[26] D. Sands, S. DC, S. AL, and D. SMET, "The association between bacteria and rain and possible resultant meteorological implications," 1982.

[27] G. D. Franc and P. J. DeMott, "Cloud activation characteristics of airborne erwinia carotovora cells," *Journal of Applied Meteorology*, vol. 37, no. 10, pp. 1293–1300, 1998.

[28] B. Sattler, H. Puxbaum, and R. Psenner, "Bacterial growth in supercooled cloud droplets," *Geophysical Research Letters*, vol. 28, no. 2, pp. 239–242, 2001.

[29] H. Che, X. Zhang, Y. Wang, L. Zhang, X. Shen, Y. Zhang, Q. Ma, J. Sun, Y. Zhang, and T. Wang, "Characterization and parameterization of aerosol cloud condensation nuclei activation under different pollution conditions," *Scientific reports*, vol. 6, no. 1, pp. 1–14, 2016.

[30] H. Bauer, H. Giebl, R. Hitzenberger, A. Kasper-Giebl, G. Reischl, F. Zibuschka, and H. Puxbaum, "Airborne bacteria as cloud condensation nuclei," *Journal of Geophysical Research: Atmospheres*, vol. 108, no. D21, 2003.

[31] S. Yankofsky, Z. Levin, T. Bertold, and N. Sandlerman, "Some basic characteristics of bacterial freezing nuclei," *Journal of applied meteorology*, vol. 20, no. 9, pp. 1013–1019, 1981.

[32] C. Hoose, J. Kristjánsson, and S. Burrows, "How important is biological ice nucleation in clouds on a global scale?" *Environmental Research Letters*, vol. 5, no. 2, p. 024 009, 2010.

[33] B. C. Christner, C. E. Morris, C. M. Foreman, R. Cai, and D. C. Sands, "Ubiquity of biological ice nucleators in snowfall," *Science*, vol. 319, no. 5867, pp. 1214–1214, 2008.

[34] K. A. Pratt, P. J. DeMott, J. R. French, Z. Wang, D. L. Westphal, A. J. Heymsfield, C. H. Twohy, A. J. Prenni, and K. A. Prather, "In situ detection of biological particles in cloud ice-crystals," *Nature Geoscience*, vol. 2, no. 6, pp. 398–401, 2009.

[35] A. J. Prenni, M. D. Petters, S. M. Kreidenweis, C. L. Heald, S. T. Martin, P. Artaxo, R. M. Garland, A. G. Wollny, and U. Pöschl, "Relative roles of biogenic emissions and saharan dust as ice nuclei in the amazon basin," *Nature Geoscience*, vol. 2, no. 6, pp. 402–405, 2009.

[36] B. Murray, J. Ross, T. Whale, H. Price, J. Atkinson, N. Umo, M. Webb, *et al.*, "The relevance of nanoscale biological fragments for ice nucleation in clouds," *Scientific reports*, vol. 5, p. 8082, 2015.

[37] J. A. Huffman, A. Prenni, P. DeMott, C. Pöhlker, R. Mason, N. Robinson, J. Fröhlich-Nowoisky, Y. Tobo, V. Després, E. Garcia, *et al.*, "High concentrations of biological aerosol particles and ice nuclei during and after rain," *Atmospheric Chemistry and Physics*, vol. 13, no. 13, p. 6151, 2013.

[38] I. Crawford, N. Robinson, M. Flynn, V. Foot, M. Gallagher, J. Huffman, W. Stanley, and P. H. Kaye, "Characterisation of bioaerosol emissions from a colorado pine forest: Results from the beachon-rombas experiment," *Atmospheric Chemistry and Physics*, 2014.

[39] J. Gillies, W. Nickling, and G. McTainsh, "Dust concentrations and particle-size characteristics of an intense dust haze event: Inland delta region, mali, west africa," *Atmospheric Environment*, vol. 30, no. 7, pp. 1081–1090, 1996.

[40] S. Perkins, "Dust, the thermostat how tiny airborne particles manipulate global climate," *Science News*, vol. 160, no. 13, pp. 200–2002, 2001.

[41] D. W. Griffin, C. A. Kellogg, V. H. Garrison, and E. A. Shinn, "The global transport of dust: An intercontinental river of dust, microorganisms and toxic chemicals flows through the earth's atmosphere," *American Scientist*, vol. 90, no. 3, pp. 228–235, 2002.

[42] K. Dose, A. Bieger-Dose, B. Ernst, U. Feister, B. Gómez-Silva, A. Klein, S. Risi, and C. Stridde, "Survival of microorganisms under the extreme conditions of the atacama desert," *Origins of Life and Evolution of the Biosphere*, vol. 31, no. 3, pp. 287–303, 2001.

[43] C. R. Kuske, S. M. Barns, and J. D. Busch, "Diverse uncultivated bacterial groups from soils of the arid southwestern united states that are present in many geographic regions.," *Applied and Environmental Microbiology*, vol. 63, no. 9, pp. 3614–3621, 1997.

[44] W. B. Whitman, D. C. Coleman, and W. J. Wiebe, "Prokaryotes: The unseen majority," *Proceedings of the National Academy of Sciences*, vol. 95, no. 12, pp. 6578–6583, 1998.

[45] D. W. Griffin, V. H. Garrison, J. R. Herman, and E. A. Shinn, "African desert dust in the caribbean atmosphere: Microbiology and public health," *Aerobiologia*, vol. 17, no. 3, pp. 203–213, 2001.

[46] C. A. Kellogg, D. W. Griffin, V. H. Garrison, K. K. Peak, N. Royall, R. R. Smith, and E. A. Shinn, "Characterization of aerosolized bacteria and fungi from desert dust events in mali, west africa," *Aerobiologia*, vol. 20, no. 2, pp. 99–110, 2004.

[47] J. Lacey, "The aerobiology of conidial fungi," *Biology of conidial fungi*, vol. 1, pp. 373–416, 1981.

[48] B. Sultan, K. Labadi, J.-F. Guégan, and S. Janicot, "Climate drives the meningitis epidemics onset in west africa," *PLoS Med*, vol. 2, no. 1, e6, 2005.

[49] A. M. Molesworth, L. E. Cuevas, S. J. Connor, A. P. Morse, and M. C. Thomson, "Environmental risk and meningitis epidemics in africa," *Emerging infectious diseases*, vol. 9, no. 10, p. 1287, 2003.

[50] A. M. Molesworth, L. E. Cuevas, A. P. Morse, J. R. Herman, and M. C. Thomson, "Dust clouds and spread of infection," *The Lancet*, vol. 359, no. 9300, pp. 81–82, 2002.

[51] N. Yamaguchi, T. Ichijo, A. Sakotani, T. Baba, and M. Nasu, "Global dispersion of bacterial cells on asian dust," *Scientific Reports*, vol. 2, p. 525, 2012.

[52] G. L. Archer, "Staphylococcus aureus: A well-armed pathogen," *Reviews of Infectious Diseases*, vol. 26, no. 5, pp. 1179–1181, 1998.

[53] A. Krause, F. Gould, and J. Forty, "Prosthetic heart valve endocarditis caused by bacillus circulans," *Journal of Infection*, vol. 39, no. 2, pp. 160–162, 1999.

[54] Y. A. Lee, H. J. Kim, T. W. Lee, M. J. Kim, M. H. Lee, J. H. Lee, and C. G. Ihm, "First report of cryptococcus albidus-induced disseminated cryptococcosis in a renal transplant recipient," *The Korean journal of internal medicine*, vol. 19, no. 1, p. 53, 2004.

[55] P.-S. LIM, S.-L. CHEN, C.-Y. TSAI, and M.-A. PAI, "Pantoea peritonitis in a patient receiving chronic ambulatory peritoneal dialysis (case report)," *Nephrology*, vol. 11, no. 2, pp. 97–99, 2006.

[56] D. Moissenet, P. Bidet, A. Garbarg-Chenon, G. Arlet, and H. Vu-Thien, "Ralstonia paucula (formerly cdc group iv c-2): Unsuccessful strain differentiation with pcr-based methods, study of the 16s-23s spacer of the rrna operon, and comparison with otherralstonia species (r. eutropha, r. pickettii, r. gilardii, and r. solanacearum)," *Journal of clinical microbiology*, vol. 39, no. 1, pp. 381–384, 2001.

[57] D. J. Park, J. C. Yun, J. E. Baek, E. Y. Jung, D. W. Lee, M.-A. KIM, and S.-H. CHANG, "Relapsing bacillus licheniformis peritonitis in a continuous ambulatory peritoneal dialysis patient (case report)," *Nephrology*, vol. 11, no. 1, pp. 21–22, 2006.

[58] K. H. Wedepohl, "The composition of the continental crust," *Geochimica et cosmochimica Acta*, vol. 59, no. 7, pp. 1217–1232, 1995.

[59] K. L. Rypien, "African dust is an unlikely source of aspergillus sydowii, the causative agent of sea fan disease," *Marine Ecology Progress Series*, vol. 367, pp. 125–131, 2008.

[60] A. M. Jones and R. M. Harrison, "The effects of meteorological factors on atmospheric bioaerosol concentrations—a review," *Science of the total environment*, vol. 326, no. 1-3, pp. 151–180, 2004.

[61] B. Lighthart, B. Shaffer, A. Frisch, and D. Paterno, "Meteorological variables associated with population density of culturable atmospheric bacteria at a summer site in the mid-willamette river valley, oregon," MICROBIAL AEROSOL RESEARCH LAB LLC MONMOUTH OR, Tech. Rep., 2004.

[62] R. M. Harrison, A. M. Jones, P. D. Biggins, N. Pomeroy, C. S. Cox, S. P. Kidd, J. L. Hobman, N. L. Brown, and A. Beswick, "Climate factors influencing bacterial count in background air samples," *International journal of biometeorology*, vol. 49, no. 3, pp. 167–178, 2005.

[63] H. Constantinidou, S. Hirano, L. Baker, C. Upper, *et al.*, "Atmospheric dispersal of ice nucleation-active bacteria: The role of rain.," *Phytopathology*, vol. 80, no. 10, pp. 934–937, 1990.

[64] J. Lindemann and C. Upper, "Aerial dispersal of epiphytic bacteria over bean plants," *Applied and Environmental Microbiology*, vol. 50, no. 5, pp. 1229–1232, 1985.

[65] I. Reche, G. D'Orta, N. Mladenov, D. M. Winget, and C. A. Suttle, "Deposition rates of viruses and bacteria above the atmospheric boundary layer," *The ISME journal*, vol. 12, no. 4, pp. 1154–1162, 2018.

[66] S. M. Burrows, W. Elbert, M. Lawrence, and U. Pöschl, "Bacteria in the global atmosphere-part 1: Review and synthesis of literature data for different ecosystems.," *Atmospheric Chemistry & Physics*, vol. 9, no. 23, 2009.

[67] F. C. Meier and C. A. Lindbergh, "Collecting micro-organisms from the arctic atmosphere: With field notes and material," *The Scientific Monthly*, vol. 40, no. 1, pp. 5–20, 1935.

[68] J. Hirst, O. Stedman, and G. Hurst, "Long-distance spore transport: Vertical sections of spore clouds over the sea," *Microbiology*, vol. 48, no. 3, pp. 357–377, 1967.

[69] C. H. Twohy, G. R. McMeeking, P. J. DeMott, C. S. McCluskey, T. C. Hill, S. M. Burrows, G. R. Kulkarni, M. Tanarhte, D. N. Kafle, and D. W. Toohey, "Abundance of fluorescent biological aerosol particles at temperatures conducive to the formation of mixed-phase and cirrus clouds," *Atmospheric Chemistry and Physics*, vol. 16, no. 13, p. 8205, 2016.

[70] V. Després, J. A. Huffman, S. M. Burrows, C. Hoose, A. Safatov, G. Buryak, J. Fröhlich-Nowoisky, W. Elbert, M. Andreae, U. Pöschl, *et al.*, "Primary biological aerosol particles in the atmosphere: A review," *Tellus B: Chemical and Physical Meteorology*, vol. 64, no. 1, p. 15 598, 2012.

[71] V. T. Phillips, P. J. Demott, C. Andronache, K. A. Pratt, K. A. Prather, R. Subramanian, and C. Twohy, "Improvements to an empirical parameterization of heterogeneous ice nucleation and its comparison with observations," *Journal of the Atmospheric Sciences*, vol. 70, no. 2, pp. 378–409, 2013.

[72] L. D. Ziemba, A. J. Beyersdorf, G. Chen, C. A. Corr, S. N. Crumeyrolle, G. Diskin, C. Hudgins, R. Martin, T. Mikoviny, R. Moore, *et al.*, "Airborne observations of bioaerosol over the southeast united states using a wideband integrated bioaerosol sensor," *Journal of Geophysical Research: Atmospheres*, vol. 121, no. 14, pp. 8506–8524, 2016.

[73] N. DeLeon-Rodriguez, T. L. Lathem, L. M. Rodriguez-R, J. M. Barazesh, B. E. Anderson, A. J. Beyersdorf, L. D. Ziemba, M. Bergin, A. Nenes, and K. T. Konstantinidis, "Microbiome of the upper troposphere: Species composition and prevalence, effects of tropical storms, and atmospheric implications," *Proceedings of the National Academy of Sciences*, vol. 110, no. 7, pp. 2575–2580, 2013.

[74] M. Pósfai, J. Li, J. R. Anderson, and P. R. Buseck, "Aerosol bacteria over the southern ocean during ace-1," *Atmospheric Research*, vol. 66, no. 4, pp. 231–240, 2003.

[75] M. A. Zawadowicz, K. D. Froyd, D. M. Murphy, and D. J. Cziczo, "Improved identification of primary biological aerosol particles using single-particle mass spectrometry," *Atmospheric Chemistry and Physics*, vol. 17, no. 11, pp. 7193–7212, 2017.

[76] D. M. Murphy, "The design of single particle laser mass spectrometers," *Mass Spectrometry Reviews*, vol. 26, no. 2, pp. 150–165, 2007.

[77] D. J. Cziczo, K. D. Froyd, C. Hoose, E. J. Jensen, M. Diao, M. A. Zondlo, J. B. Smith, C. H. Twohy, and D. M. Murphy, "Clarifying the dominant sources and mechanisms of cirrus cloud formation," *Science*, vol. 340, no. 6138, pp. 1320–1324, 2013.

[78] J. F. Cahill, T. K. Darlington, C. Fitzgerald, N. G. Schoepp, J. Beld, M. D. Burkart, and K. A. Prather, "Online analysis of single cyanobacteria and algae cells under nitrogen-limited conditions using aerosol time-of-flight mass spectrometry," *Analytical chemistry*, vol. 87, no. 16, pp. 8039–8046, 2015.

[79] D. A. Sodeman, S. M. Toner, and K. A. Prather, "Determination of single particle mass spectral signatures from light-duty vehicle emissions," *Environmental Science & Technology*, vol. 39, no. 12, pp. 4569–4580, 2005.

[80] C. Ingold *et al.*, "T fungal spores. their libération and dispersal.," *T Fungal spores. Their liberation and dispersal.*, vol. 4, 1971.

[81] W. Elbert, P. Taylor, M. Andreae, and U. Pöschl, "Contribution of fungi to primary biogenic aerosols in the atmosphere: Wet and dry discharged spores, carbohydrates, and inorganic ions," 2007.

[82] L. Bonifait, R. Charlebois, A. Vimont, N. Turgeon, M. Veillette, Y. Longtin, J. Jean, and C. Duchaine, "Detection and quantification of airborne norovirus during outbreaks in healthcare facilities," *Clinical infectious diseases*, vol. 61, no. 3, pp. 299–304, 2015.

Chapter 3

Research

3.1 Quantifying Bioaerosol Concentrations in Dust Clouds through Online UV-LIF and Mass Spectrometry Measurements at the Cape Verde Atmospheric Observatory

Based at the Cape Verde Atmospheric Observatory (CVAO), the aim of this project was to quantify the concentrations of bioaerosols associated with outflow from the African continent. Dust events are a common occurrence within this region and particles are often transported significant distances across the Atlantic Ocean. Climate Modellers should benefit from this quantification as it allows for fluctuations relative to dust and other inorganic particles to be observed. This is important as bioaerosols are excellent ice nucleating particles and their presence has implications for the local climate. Our observations help characterise seasonal changes, with a notable peak in concentrations seen during February. This is attributed to the Harmattan wind, for which back trajectory analysis highlights the role of the Sahara desert as a notable source region. For this project we used a three channel UV-LIF spectrometer known as a WIBS-4M. An inter-comparison was made with Laser Ablation Aerosol Particle Time of Flight mass spectrometer (LAAP-ToF) measurements and the two instruments show good agreement. With the WIBS-4M continuously sampling over an 11-month period, this is one of the longest term experiments to use UV-LIF spectrometry techniques. The following paper was published in Atmospheric Chemistry & Physics.

Atmos. Chem. Phys., 20, 14473–14490, 2020
https://doi.org/10.5194/acp-20-14473-2020

Atmospheric Chemistry and Physics
Open Access
EGU

Quantifying bioaerosol concentrations in dust clouds through online UV-LIF and mass spectrometry measurements at the Cape Verde Atmospheric Observatory

Douglas Morrison[1], Ian Crawford[1], Nicholas Marsden[1], Michael Flynn[1], Katie Read[2], Luis Neves[2], Virginia Foot[4], Paul Kaye[3], Warren Stanley[3], Hugh Coe[1], David Topping[1], and Martin Gallagher[1]

[1]Department of Earth and Environmental Science, University of Manchester, Brunswick St, Manchester, UK
[2]Wolfson Atmospheric Chemistry Laboratory, University of York, York, UK
[3]Science and Technology Research Institute, University of Hertfordshire, Hatfield, UK
[4]Defence Science and Technology Laboratory, Salisbury, UK

Correspondence: Douglas Morrison (douglas.morrison@manchester.ac.uk)

Received: 18 February 2020 – Discussion started: 25 March 2020
Revised: 30 September 2020 – Accepted: 2 October 2020 – Published: 28 November 2020

Abstract. Observations of the long-range transport of biological particles in the tropics via dust vectors are now seen as fundamental to the understanding of many global atmosphere–ocean biogeochemical cycles, changes in air quality, human health, ecosystem impacts, and climate. However, there is a lack of long-term measurements quantifying their presence in such conditions. Here, we present annual observations of bioaerosol concentrations based on online ultraviolet laser-induced fluorescence (UV-LIF) spectrometry from the World Meteorological Organization – Global Atmospheric Watch (WMO-GAW) Cape Verde Atmospheric Observatory on São Vicente. We observe the expected strong seasonal changes in absolute concentrations of bioaerosols with significant enhancements during winter due to the strong island inflow of air mass, originating from the African continent. Monthly median bioaerosol concentrations as high as $45\,L^{-1}$ were found with 95th percentile values exceeding $130\,L^{-1}$ during strong dust events. However, in contrast, the relative fraction of bioaerosol numbers compared to total dust number concentration shows little seasonal variation. Mean bioaerosol contributions accounted for $0.4 \pm 0.2\,\%$ of total coarse aerosol concentrations, only rarely exceeding 1 % during particularly strong events under appropriate conditions. Although enhancements in the median bioaerosol fraction do occur in winter, they also occur at other times of the year, likely due to the enhanced Aeolian activity driving dust events at this time from different sources. We hypothesise that this indicates the relative contribution of bioaerosol material in dust transported across the tropical Atlantic throughout the year is relatively uniform, comprised mainly of mixtures of dust and bacteria and/or bacterial fragments. We argue that this hypothesis is supported from analysis of measurements also at Cabo Verde just prior to the long-term monitoring experiment where UV-LIF single particle measurements were compared with laser ablation aerosol particle time-of-flight mass spectrometer (LAAP-ToF) measurements. These clearly show a very high correlation between particles with mixed biosilicate mass spectral signatures and UV-LIF biofluorescent signatures suggesting the bioaerosol concentrations are dominated by these mixtures. These observations should assist with constraining bioaerosol concentrations for tropical global climate model (GCM) simulations. Note that here we use the term "bioaerosol" to include mixtures of dust and bacterial material.

1 Introduction

Aerosols play a key role in the global climate. Their suspension in the air can scatter incoming solar radiation, reducing the warming effect of the Sun. Rather than scatter light directly, aerosols can also serve as nuclei for cloud droplets, ice crystals and precipitation. This can promote fur-

ther changes in the climate, with cloud cover increasing local albedo effects. Although most cloud condensation nuclei (CCN) are inorganic, there has been increasing evidence to suggest that biological particles play an important role too. This is because despite existing in relatively low concentrations, bioaerosols are more effective CCN than alternative particle types. Bacteria such as *Pseudomonas syringae* are thought to promote rainfall (Sands et al., 1982), while strains such as *Erwinia carotovora carotovora* and *Erwinia carotovora atroseptica* have been shown to be CCN active, with 25 %–30 % activable at supersaturations larger than 1 % (Franc and DeMott, 1998). Bauer et al. (2003) collected cultivable bacteria from cloud water samples in Austria and found all samples to be activable at supersaturations where insoluble wettable particles of comparable size would not have been. Other biogenic aerosols such as pollen have also been shown to have CCN properties (Pope, 2010). This is also true for fragmented pollen grains, significantly raising the number of potential activation sites (Steiner et al., 2015).

Homogeneous ice nucleation occurs in liquid particles at temperatures of −36 °C and below. However, heterogeneous ice nucleation can occur at significantly warmer temperatures, with ice nuclei (IN) reducing the energy required for crystallisation to begin. The effectiveness of IN in this regard depends on their composition, size, surface area and more (Hoose and Möhler, 2012). They also encompass a broad range of particles, including mineral dust, metals, soot, and biological particles. Of these particle types, mineral dust has been one of the most closely investigated, with multiple studies observing a range of conditions at which it can act as effective nuclei. Over the dust belt as outlined by Liu et al. (2008), Zhang et al. (2012) found dust to initiate freezing in midlevel supercooled stratiform clouds (MSSCs) at temperatures of −10 °C and below. This is warmer than findings from Ansmann et al. (2008), who did not find evidence of ice formation in supercooled stratiform clouds with cloud-top temperatures warmer than −18 °C, but colder than findings by Sassen et al. (2003), who attributed African dust to the glaciation of altocumulus clouds at −5 °C.

More recent focus has been placed on biological particles, with many identified as more efficient IN. For example, strains of *Pseudomonas syringae* have been found to initiate freezing at temperatures as high as −2 °C (Yankofsky et al., 1981). They are also capable of influencing clouds across a range of altitudes, with fungal spores as large as 15 µm reaching altitudes of 30 km in a matter of days (Haga et al., 2013). Dispute over bioaerosol's contributions to these meteorological processes focus on their low concentrations, with bioaerosols often accounting for less than 1 % of total particle concentrations. Some estimates are even lower, with Bauer et al. (2002) finding bacterial average mass concentrations accounted for just 0.01 % of organic carbon (OC) in cloud water and precipitation samples. However, in pristine environments, bioaerosol concentrations can be significantly amplified. For example, bioaerosols have been shown to account for 46 % of total coarse aerosol mass concentration in the central Amazon rainforest (Huffman et al., 2012). In these instances, it is thought that bioaerosols are part of a self-sustaining cycle, promoting rainfall that in turn drives vegetative growth (Fröhlich-Nowoisky et al., 2016). Furthermore, Pratt et al. (2009) identified 33 % of the ice crystal residual particles sampled in a wave cloud over Wyoming as biogenic.

Bioaerosols are also capable of global dispersion (McTainsh, 1996). This is because although some are freely suspended in the air, others can utilise mineral dust to act as a vector for their transport. It is perhaps because of this that dust clouds often contain significant concentrations of micro-organisms (Griffin et al., 2001). Furthermore, Yamaguchi et al. (2012) investigated the bacteria's ability to grow and reproduce when attached to dust and found many to remain physiologically active. This can have important implications for cloud formation but also ecological and health impacts too. Asian dust particles and their corresponding microbial concentrations have been found to positively correlate with levels of ice nucleation in snow samples atop Tateyama (Maki et al., 2018). Meanwhile, there is a known association between dust storms and meningitis. Outbreaks often occur in the Sahelian region of northern Africa between February and May, affecting as many as 200 000 individuals annually (Sultan et al., 2005). During this period, conditions are usually dry and dust storms are frequent. Meningitis outbreaks persist up until the wet season begins, when dust events cease (Molesworth et al., 2003).

Trade winds are an important aspect of Aeolian events in Africa, with the point of their convergence known as the Intertropical Convergence Zone (ITCZ). Within this zone, air is made to rise, forming the ascending part of the Hadley cell. The ITCZ is also subject to latitudinal movement, following the progression of the annual solar maximum (Folland et al., 1991). This results in a cycle of atmospheric loading, with dust readily taken to high altitudes during summer. This material is consequently often transported significant distances across the Atlantic, where it is deposited in the ocean along the way. As such, trade winds and dust events can act as major contributors for nutrient deposition. Although the chemical content of what is deposited depends on the source of the dust, most dust particles originate from arid or semi-arid regions and contain large amounts of biogeochemically significant elements. The role of organic components in affecting ocean life is coming under increased scrutiny.

For example, the decline in Caribbean coral reefs has been partially attributed to transatlantic dust events (Rypien, 2008). *Aspergillus sydowii* is a fungal spore implicated in a Caribbean-wide sea-fan disease that has been cultured from Caribbean air samples. It is believed that dust is acting as a substrate for said spores. With Yamaguchi et al. (2012) having analysed the bacterial community structure for Asian dust particles, it was found that more than 20 bacterial classes were present, with *Actinobacteria*, *Bacilli* and *Sphingobacte-*

ria dominating. These findings are similar to previous studies on African dust (Griffin et al., 2001), suggesting that the diversity of such communities is largely similar across arid regions.

Research has shown how bioaerosols can influence the world around them and has also observed their presence during dust events. However, their concentrations have not been readily quantified in such conditions. This study aimed to capture long-term trends in bioaerosol concentrations within a region of the world where dust events are both common and pronounced.

To do this, online measurements using a wideband integrated bioaerosol sensor (WIBS-4M) were taken for 11 months off the west coast of continental Africa. This was preceded by an intensive campaign that paired another ultraviolet laser-induced fluorescence (UV-LIF) spectrometer known as a WIBS-4A (e.g. Gabey et al., 2010; Savage et al., 2017), with a laser ablation aerosol particle time-of-flight mass spectrometer (LAAP-ToF-MS) (Marsden et al., 2018). The latter was used to provide detailed contemporary particle composition analysis and to identify biosilicate particle classes. This biosilicate classification was then used to validate the WIBS-4A biofluorescent classification schemes, e.g. Ruske et al. (2017), to subsequently interpret the long-term ambient datasets collected by a WIBS-4M at the CVAO site. With an estimated 50 % of global annual dust originating from northern Africa (Engelstaedter et al., 2006), the African continent is a high-priority region that is often overlooked for such studies.

2 Methodology

2.1 Site and long-term sampling details

From September 2015 to August 2016, a WIBS-4M was continuously sampling at the Cape Verde Atmospheric Observatory (CVAO), off the west coast of continental Africa (16°51′49″ N, 24°52′02″ W). The observatory is located 50 m from the coastline and is subject to persistent north-easterly trade winds. During this period, the observatory recorded a mean temperature of 23.3 °C and median wind speeds of 6.2 ms^{-1}, which are similar to the long-term trends reported by Carpenter et al. (2010). Given the placement of the observatory on the island, as well as the lack of major coastal features, this site is well suited for observations of unpolluted marine air. Air was drawn vertically down a 10 m stainless steel pipe with an inner diameter of 1 in at a rate of 16.7 L min^{-1}, from which an isokinetic inlet was used to draw a subsample of air at a rate of 0.3 L min^{-1}. The sample line was heated to minimise condensation build up, and a Thermo PM_{10} inlet was used at the top of the pipe. Meteorological data were recorded atop a 30 m tower located at the observatory, with dominant wind direction recorded as one of 16 compass points. This was funded as part of the Ice in Cloud Experiment – Dust (ICE-D) campaign, which had the aim of taking measurements of Saharan dust concentrations to better understand aerosol–cloud interactions and reduce uncertainty in numerical models. Details of the ICE-D surface experiments and accompanying aircraft sampling campaigns are described by Liu et al. (2018). The WIBS-4M was used to observe long-term trends in bioaerosol concentrations and was regularly calibrated using National Institute of Standards and Technology (NIST) calibration polystyrene latex (PSL) spheres.

2.1.1 Intensive campaign and dust samples

The monitoring component of the project was prefaced by a shorter-term but highly intensive campaign, the results from which are used to inform the interpretation of the long-term data. During the shorter campaign, a WIBS-4A was used alongside a LAAP-ToF (Marsden et al., 2018). Ground-based measurements using the LAAP-ToF and WIBS-4A were conducted over a 20 d period in August 2015 located near Praia International Airport, Cabo Verde (14°570′ N, 23°290′ W; 100 m a.s.l.). A full description of the site and experimental setup is provided by Liu et al. (2018) and Marsden et al. (2019), but a brief summary is now given. Ground-based ambient aerosol measurements were made by the LAAP-ToF and WIBS-4A which were installed in the mobile Manchester Aerosol Laboratory, located 1500 m from the airport. Aerosols were sampled via a pumped inlet mounted on a 10 m tower. The total flow down the inlet was 1000 L min^{-1} and a series of aerosol instruments subsampled isokinetically downstream of a common manifold, which subsampled at 186 L min^{-1} from the main inlet. The inlet characterisation and losses are described in Liu et al. (2018) and in the associated references. The LAAP-ToF measured aerosol in the size range of 0.5–2.5 µm, whilst the WIBS-4A measured particles in the size range of 0.5–20 µm; however, the nominal cut-off of the inlet system was approximately 10 µm. When considering size measurements, it should be noted that the LAAP-ToF measures a particle's vacuum aerodynamic diameter (D_{va}), while the WIBS-4A measures a particle's optical diameter (D_o). A more detailed description of the WIBS and LAAP-ToF instruments is provided in Sect. 2.2. The sampling tower was located upwind of the main airport terminal and the city of Praia (400 m and 2.5 km, respectively) in the prevailing northeasterly winds so potential contamination sources were minimal. A full analysis and classification of the back-trajectory wind fields during this intensive experiment period was performed by Liu et al. (2018). They reported that dust plumes from the Sahara and Sub-Saharan Africa were more frequently observed after a synoptic shift on 15 August, when winds became more easterly. They also noted that more efficient transport of dust via stronger easterly winds led to larger advected dust loadings with shorter dust transport times. These different dust advection pathways were reflected in different size and compositions of mineral

dust recorded by the LAAP-ToF during the intensive experiment (Marsden et al., 2016).

Calibration of the LAAP-ToF was performed with pure hematite samples (Liu et al., 2018), whilst both the WIBS-4A and WIBS-4M were calibrated using NIST latex calibration beads and fluorescent glass beads, e.g. Crawford et al. (2015). It should be emphasised here that the WIBS-4A and 4M are almost identical instruments, with the only differences being the trigger levels and flow rates used. A detailed description of the WIBS-4A can be found in Savage et al. (2017) and of the WIBS-4M in Forde et al. (2019). As such, the fluorescence data for each instrument are comparable, although we acknowledge there can be issues even when comparing measurements from two identical models. An intercomparison of the fluorescent responses between instruments when using the NIST calibration particles help affirm the instrument's similarities. This is the same methodology as has been described by Forde et al. (2019), Savage et al. (2017) and Crawford et al. (2014).

In addition, subsequent to the ambient experiments, Moroccan dust samples, hereby referred to as Moroccan dust, were provided that were collected in the M'Hamid region (29°51′43″ N, 6°09′24″ W), which is thought to be representative of the dust material often observed in the continental outflow sampled here. These samples were dispersed through the WIBS-4M in a controlled laboratory experiment alongside additional collected samples of illite. Subsets of these samples were gamma irradiated to remove potential storage and transport contaminants. The UV-LIF response of the pure and irradiated samples were intercompared and are described in the results section. Their respective fluorescent properties, as well as size and shape factors were also compared to the intensive and long-term ambient observations. The negative ion spectra of the pure samples were also analysed using the LAAP-ToF in the laboratory for comparison. These sample properties were used to help contextualise the campaign results and the classification scheme used to identify biosilicate particle concentrations.

2.2 Instrumentation

2.2.1 WIBS

Recent developments in UV-LIF technology have allowed real-time detection of bioaerosols, whereby spectral patterns correlate with specific particle characteristics (Huffman et al., 2019). This technology utilises the intrinsic fluorescent properties found within organic molecules, including proteins, co-enzymes, cell wall compounds and certain pigments to differentiate between biological and non-biological particles. Each organic molecule has its own fluorescent emissions that are dependent on the incoming wavelength of the light that excites it. As such, it is possible for UV-LIF technology to discriminate between organic molecules and help to identify the types of aerosols being observed. The WIBS-4M is a three-channel UV-LIF spectrometer that uses Xenon flash lamps to excite particles with either 280 nm (Xe1) or 370 nm (Xe2) light. The resulting emissions from excited fluorophores are then recorded by one of the instrument's two detection channels (De1 and De2), creating a 2×2 matrix. However, with the Xe1 / De1 channel becoming supersaturated from elastically scattered UV light, only the other three resulting channels are considered. These are called Fl 1, 2 and 3, and are the product of Xe1 / De2, Xe2 / De1 and Xe2 / De2, respectively. De1 is sensitive to 310–400 nm UV light, while De2 covers a broader range from 420 to 650 nm.

Common fluorophores considered in particle analysis include the amino acid tryptophan, the co-enzyme NAD(P)H and the vitamin riboflavin. Each fluorophore excites at 280 nm, 270–400 and 450 nm, respectively, and fluoresces at 300–400, 400–600 and 520–565 nm (Hill et al., 2009), (Lakowicz, 2013). The specificity of a biological compound's fluorescent properties enables particles to be classified into one of seven types, depending on whether they exhibit fluorescence in one, two or three channels (Perring et al., 2015). Particle shape and symmetry is also measured through the use of a 635 nm diode laser that is initially involved in triggering the Xenon flash lamps to fire. The forward scattering light from a particle that passes through the laser hits a quadrant scattering detector. By applying a Mie scattering model, the distribution of the light on each quadrant can be used to estimate diameter, as well as an asymmetry factor between 0 and 100 (Gabey et al., 2010). This has been discussed in detail by Kaye et al. (2007), with values of 0 representing perfectly spherical particles and higher asymmetry factors describing more fibrous and linear shapes. When applying this range in the context of our observations, asymmetry factor (AF) values of 10–20 reflect fairly spherical particles, with values of 30 or more beginning to represent ellipsoidal shapes.

2.2.2 LAAP-ToF

In single particle mass spectrometry (SPMS), an online measurement of aerodynamic size and composition is obtained with high temporal resolution. Several instrument designs have been described (Murphy, 2007), but a typical instrument features an aerodynamic lens inlet for particle beam creation and a high-powered UV pulsed laser for laser desorption ionisation (LDI) of single particles arriving in the ion source. Particle composition is analysed by time-of-flight mass spectrometry (ToF-MS).

Optical particle detection is used for the effective temporal alignment of the UV laser pulse with the arrival of a particle in the LDI source region, and the determination of aerodynamic particle diameter by laser velocimetry.

The LAAP-ToF instrument (AeroMegt GmbH) used for this study featured a $PM_{2.5}$ aerodynamic lens and continuous wave (CW) fibre-coupled optical detection lasers at 532 nm, and LDI was performed by an argon fluoride (ArF) excimer

laser (model EX5, GAM Laser Inc.), set to deliver 3–5 mJ per pulse of 193 nm radiation. Bipolar ToF-MS (TofWerks AG) was implemented for compositional analysis of positive and negative ions. As a technique, SPMS is considered qualitative or semi-quantitative. The ablation and ionisation process of particles is incomplete so that competitive ionisation and charge transfer in the vapour plume results in a strong matrix effect (Reinard and Johnston, 2008). In addition, the reported particle number concentration is affected by optical particle detection efficiency and the frequency of particles "missed" by the pulsed UV laser. A full description of how these issues affected the instrument performance in this study can be found in Marsden et al. (2016), which estimates that the instrument was obtaining composition for 1 % of dust particles in the size range of 0.5–2.5 µm.

Despite the limitations in quantitative analysis, the SPMS has proven useful for the online identification of particle composition types, internal mixing state and their temporal trends in terms of particle number concentrations (Pratt and Prather, 2012). This typically proceeds using cluster analysis to differentiate particles classes and peak marker analysis to track changes in internal mixing state. In recent work, Shen et al. (2018) demonstrated the capability of the LAAP-ToF instrument to differentiate particle composition in a continental environment by a combination of cluster analysis and peak marker analysis.

2.3 Data analysis methods

A 9σ threshold was applied when setting fluorescent baselines for each WIBS model to remove weakly fluorescent inorganic particles that could otherwise act as interferents. This is a substantial increase in the threshold used from previously published work but has been shown to significantly reduce the interference from mineral dust while maintaining the concentration of biological content (Savage et al., 2017). As such, all fluorescent particles observed should contain significant amounts of biological material and are subsequently considered to be a bioaerosol. It should be noted that these are not likely to all be single particles but could instead be agglomerates, including biological particles attached to non-biological ones. The minimum cut-off diameter at 50 % detection efficiency (D_{p50}) for this particular WIBS-4M is 0.8 µm. As such, only particles between 0.8 and 10 µm have been included in the analysis.

Agglomerative hierarchical cluster analysis was performed using Ward linkage with Euclidean distance for the fluorescent particles, using the method described in Crawford et al. (2015). This has been successfully tested in the past when applying a controlled set of fluorescent PSL spheres through the same instrument model (Crawford et al., 2015; Robinson et al., 2013) and has also been shown to accurately capture bioaerosol mixtures within a semi-arid forest (Gosselin et al., 2016). This process begins with individual data points being treated as their own cluster, which are sequentially combined into larger clusters based on the "distance" between data point values. Ward linkage identifies which pair of clusters would yield the minimum increase in total within-cluster variance after merging and consequently merges them next. A Calinski–Harabasz score is then calculated, suggesting an optimum number of clusters. This cluster analysis was performed separately for both the WIBS-4A and WIBS-4M datasets. The transmission efficiency of the inlet as a function of size has also been accounted when considering size distributions for particles up to 10 µm. Inlet penetration as a function of size has also been considered based on the Andersen 321A PM_{10} inlet (McFarland, 1984).

Analysis of the LAAP-ToF data acquired during the ICE-D intensive campaign has been presented by Marsden et al. (2019), in which the mineralogy and mixing state of north African dust transported to the Cabo Verde islands is described in detail with reference to dust samples collected on the ground from potential source areas in northern Africa. Using a combination of cluster analysis and subcompositional analysis, that work showed that differences in mineralogical composition of ground samples can be detected on a regional scale, whilst variations in internal mixing state are much more localised. In transported dust, however, the mixing state was much less varied, suggesting that local sources become well mixed during transport.

In the present study, we used the compositional classes already identified in the above work by cluster analysis and compared the temporal trends in particle number concentrations with that of the biological particles detected by the WIBS. In addition, we used mass spectra of the previously identified mineral dust class to examine internal mixing of dust with biological material using peak marker analysis. More specifically, biological markers CN- (m/z 26) and CNO- (m/z 42) were used to identify those mineral dust particles which had a significant marker of internal mixing with biological material and also compared the temporal trends in those particle number concentrations to the biological particles detected by WIBS.

This approach is similar to that used by Zawadowicz et al. (2019), who examined the biological content of dust particles in North America by comparing temporal trends in particle number of a WIBS with SPMS, in that case the PALMS instrument. However, in our study, we have used different criteria for biomarkers in the mass spectra, using chlorine to normalise the biomarker signals rather than phosphorous. Chlorine is a ubiquitous signal in transported mineral dust and is easily ionised because of its high electro affinity. This reduces the temporal incoherence in biomarker ion signals caused by the matrix effect.

3 Results

3.1 Long-term observations

A clear seasonal trend for fluorescent and total particle concentrations can be seen in Fig. 1a, with both being highest during winter and lowest in summer. Monthly median bioaerosol concentrations as high as $45\,L^{-1}$ were found with 95th percentile values exceeding $130\,L^{-1}$ during strong dust events. Such peaks in concentrations are short lived and regular. Figure 1b suggests that bioaerosols are a minority particle type, with non-fluorescent concentrations consistently dominating particle contributions. The fraction of fluorescent particles compared to total particle concentrations was a mean value of 0.4 ± 0.2 %. The 99th percentile value was a fraction of 1.1 %, with some high-fraction events exceeding 1.5 % in October and May. These will be discussed in greater detail further on. Figure 1c highlights how larger particles are observed during winter. Note that there is no relationship between the total particle concentration and fraction of fluorescent particles ($r^2 = 0.02$), but a strong correlation exists between fluorescent and non-fluorescent particle concentrations ($r^2 = 0.79$).

3.2 Cluster products

Agglomerative hierarchical cluster analysis was performed using Ward linkage with Euclidean distance for all fluorescent particles. A four-cluster solution produced the greatest Calinski–Harabasz score, with information regarding their fluorescence in each channel, size and asymmetry shown in Table 1.

All fluorescent particles seen across the long-term campaign were included in Fig. 2. Fluorescence generally increases with size, but this trend is not equal across all channels and clusters. It is strongest for Clusters 1 and 4, which are also more fluorescent across most size ranges. Figure 2e shows the small size of observed particles, with Clusters 3 and 4 being much smaller than Clusters 1 and 2. Figure 2f shows the median fluorescence in each channel across all fluorescent particles combined.

The relative proportion that each cluster contributes to the total fluorescent concentration shows some variability but no clear trend. This would suggest that Cabo Verde is generally exposed to the same particles year round. Clusters 2 and 3 are clearly the two dominant clusters, accounting for a combined total of approximately 90 % of fluorescent particles. When compared to the average fluorescence values in Fig. 2, these two clusters notably have the weakest fluorescence.

3.3 Back-trajectory analysis

The 120 h back trajectories using National Oceanic and Atmospheric Administration (NOAA)'s Hybrid Single-Particle Lagrangian Integrated Trajectory (HYSPLIT) merged with the Openair package (Carslaw, 2012) were calculated from the observatory, with a starting height set at 10 m. These trajectories were run every 3 h for all 11 months of the campaign, using monthly meteorological data files downloaded from NOAA. Figure 4 captures the enhanced fluorescent particle concentrations seen during periods of continental outflow as compared to Atlantic or coastal back trajectories. Furthermore, it appears that continental trajectories predominantly occur during the same months that the increase in fluorescent and total particles is seen (October–February). Back trajectories were also calculated for periods where the fluorescent fraction was greatest. Particularly high ratio events can be identified during October, May and August in Fig. 1b. These events all show coastal back trajectories, suggesting coastal sites have higher relative biological content.

Fluorescent particle properties were investigated as a function of trajectory direction. Three week-long periods were chosen, where the trajectories were consistently coming from a specific region. These regions were oceanic, coastal and continental. Oceanic regions were defined by trajectories that spent the previous 120 h passing across the Atlantic Ocean, never passing landmass. Coastal regions were defined by northeasterly trajectories passing along the edge of the African continent, and continental regions were described by more easterly trajectories passing through the Sahara. As it was important to have an entire week of trajectories coming from one source, each of these regions was picked out at different times of the year. The continental period took place from 25/01/2016 to 31/01/2016, the coastal from 20/06/2016 to 27/06/2016 and the marine from 20/04/2016 to 26/04/2016. Average fluorescence across the four clusters and three channels has been compared for particles from each region, as shown in Fig. 5. It does not appear that there are significant differences in the fluorescent properties of particles depending on their source region.

3.4 Comparison to laboratory samples

It can be seen in Fig. 6 that all of the dust samples dispersed through the WIBS-4M show relatively weak fluorescence across all three channels but are on average more fluorescent than Clusters 2 and 3. This is particularly true for Moroccan dust in Fl 1. Exposing these samples to gamma irradiation produced little effect, marginally reducing the fluorescent properties of Moroccan dust while increasing the fluorescence of the illite sample. The size and asymmetry values are quite similar across all samples and compare most closely with those of Cluster 2.

3.5 Comparison to ICE-D LAAP-ToF measurements

Analysis of the negative ion spectra revealed that sea-spray aerosol was the dominant aerosol detected at the site by the LAAP-ToF, accounting for approximately 87 % by number. The remainder was comprised of silicate mineral dust (~ 5 %), calcium chloride (~ 3 %) and secondary material

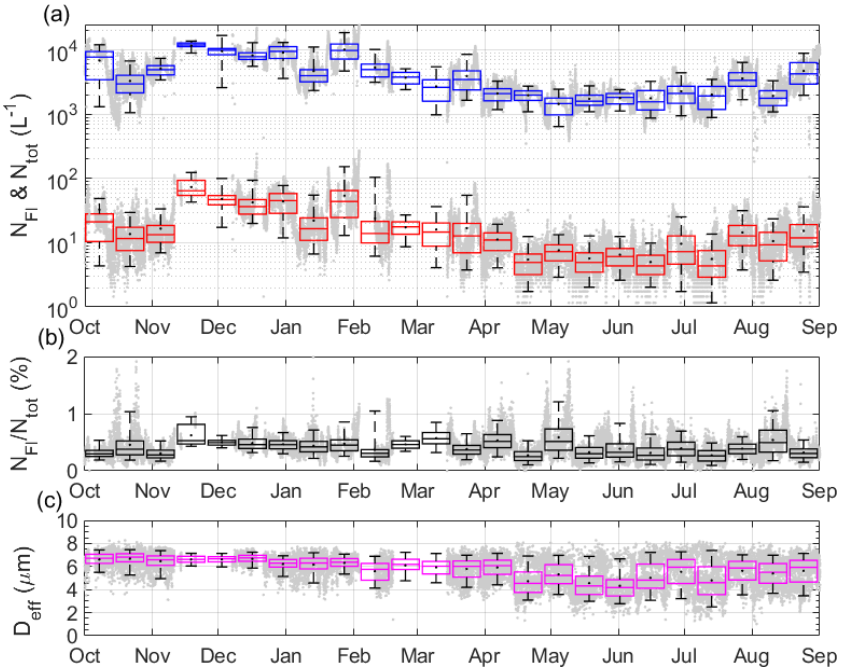

Figure 1. Panel **(a)** represents a box-and-whisker plot of both average fluorescent (red) and total (blue) particle concentrations from 0.8 to 10 µm. Whiskers represent the 5th and 95th percentile values. Boxes represent 14 d average values, with the mean shown as a black dot. Grey dots indicate 15 min data. Panel **(b)** shows the ratio of fluorescent particle concentrations relative to total particle observations, while panel **(c)** shows the trend for the effective diameter (Deff) of fluorescent particles.

(∼ 4 %). Cluster analysis of the WIBS-4A data produced a four-cluster solution which was similar to the long-term CVAO cluster solution, featuring two weakly fluorescent dominant clusters and two highly fluorescent, likely primary biological aerosol particle (PBAP) clusters. A number concentration time series of select LAAP-ToF and WIBS-4A data products are shown in Fig. 7, where similarities in the trends of silicate dust and WIBS-4A Cluster 3 can be observed during a dust event (10/08 onwards), suggesting that this cluster may represent a biodust mixture which will now be examined further.

Deeper analysis of the LAAP-ToF silicate dust class was performed to screen for potential biomarkers. Figure 8 shows example negative ion spectra from laboratory samples of bacteria (top panel) and c-means fuzzy cluster products from ICE-D representative of pure dust and dust containing biomarkers (middle and bottom panels, respectively). It can be seen that the biosilicate spectrogram contains silicate m/z peaks (e.g. SiO_2–SiO_3) and also bacterial biomarkers (e.g. CN^-CNO^-) which are not present in the pure dust spectra, suggesting that a subset of the observed dust is mixed with biological material.

The LAAP-ToF silicate dust is then filtered for biomarkers using the ratio of biomarkers to chlorine (CN + CNO / Cl).

A time series of the LAAP-ToF biosilicate and WIBS-4A Cluster 3 products are shown in Fig. 9. Here, it can be seen that the general trends are in good agreement ($r^2 = 0.63$). This suggests that the WIBS is sensitive to dust particles which are mixed with bacteria, and that these particles can be segregated from the general fluorescent aerosol population and classified using the cluster analysis method described in Sect. 2.3. There is also a moderate correlation between the WIBS-4A Cluster 3 and pure silicate ($r^2 = 0.49$) as expected, since the biosilicate will be a subset of the pure silicate. The correlation between Cluster 3 and sea spray is poor ($r^2 = 0.20$), affirming that our observations of fluorescent particles are genuine and are not being skewed by known interferents.

4 Discussion

4.1 Long-range transport and trade winds

The identified peaks in particle concentration are consistent with back-trajectory analysis showing the sources to be Saharan. Strong Aeolian generating mechanisms mean that potentially significant concentrations of soil bacteria could have attached themselves to dust particles, which are acting as an agent for their distribution and transport. More specifically, it is likely to be the Harmattan wind that is driving these events. This is a north-easterly trade wind that blows across Africa from approximately November to March, although high concentrations of dust are already present almost all year round (Prospero, 1999). Source regions in Tunisia and northern Al-

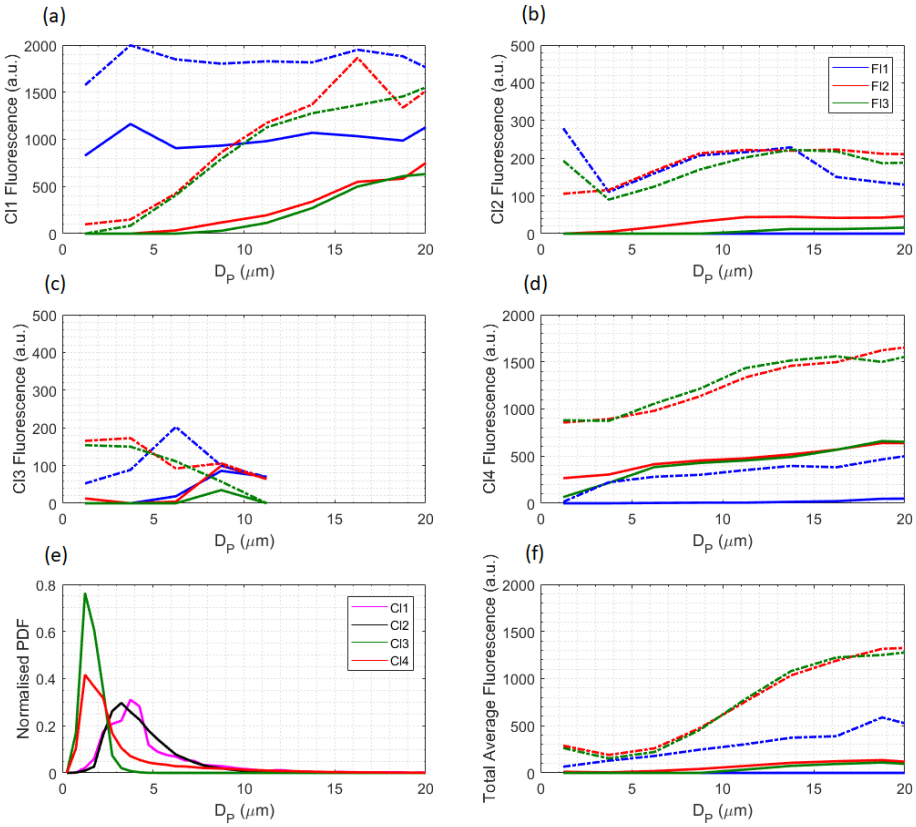

Figure 2. Solid lines represent the median fluorescence of particles as a function of size, instrument channel and cluster. Dotted lines represent 95th percentile values. The 2.5 µm bins have been used for all fluorescence traces. Panels **(a–d)** represent Clusters 1–4, respectively, while panel **(e)** represents the normalised size distribution of fluorescent particles across all clusters, using 0.5 µm bins. Panel **(f)** represents the average across all fluorescent particles.

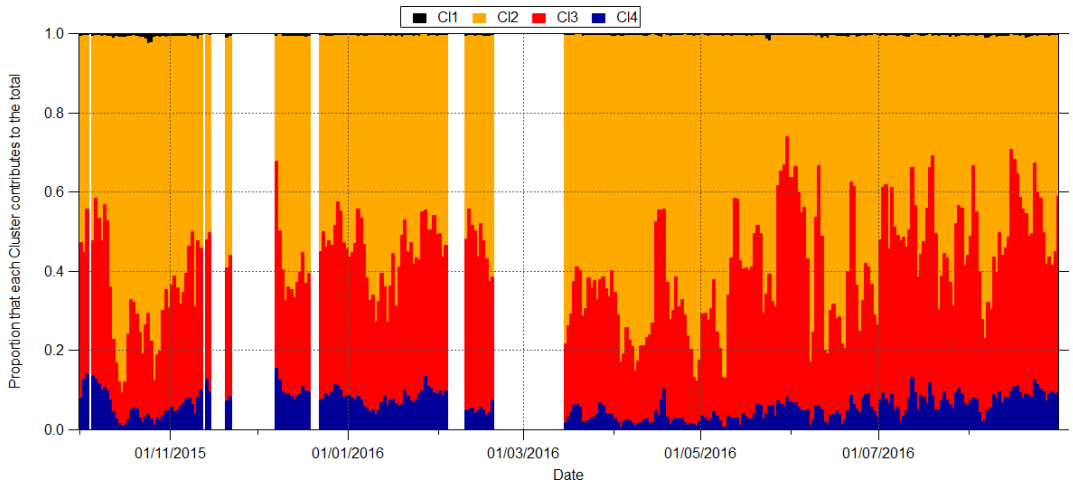

Figure 3. The proportion of the total fluorescent material that each cluster contributes over the 11-month monitoring campaign. Values are taken using 1 d integrations of cluster concentrations between 0.8 and 10 µm. Any gaps reflect missing data.

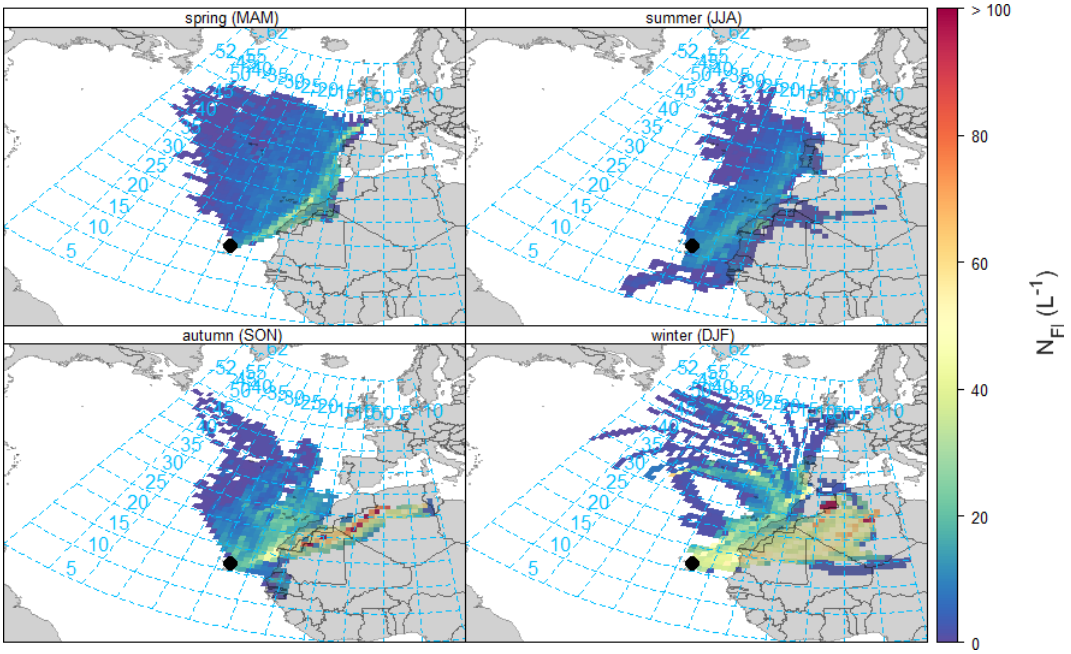

Figure 4. The 120 h back-trajectory analysis for fluorescent particle concentrations using HYSPLIT integrated with the Openair package. Note that autumn is using 2015 data, as is the month of December during winter. Spring and summer are using 2016 data. The colour scale has been capped at 100 L^{-1} for visual purposes and only particles between 0.8 and 10 µm have been included.

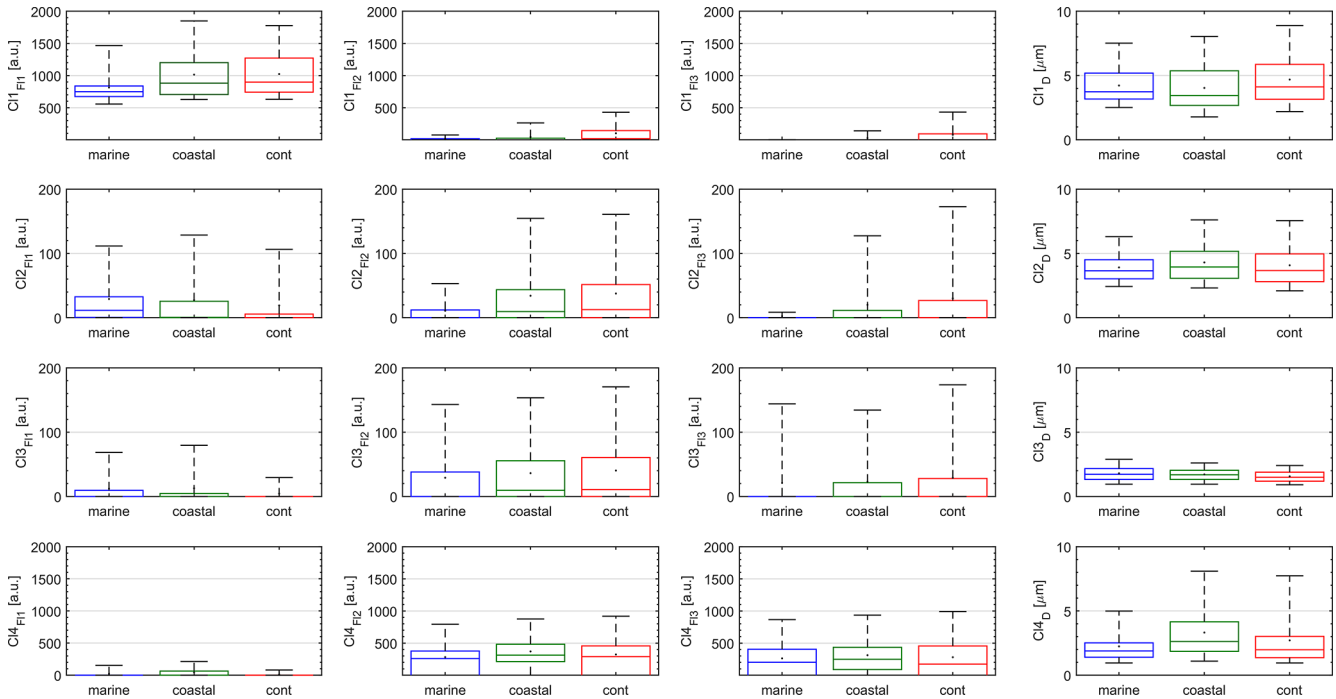

Figure 5. Mean fluorescence and size properties for each cluster, depending on the pathway of the previous 120 h trajectory. Each region (marine, coastal and continental) have taken 1 week's worth of data, from 20/04/2016 to 26/04/2016, 20/06/2016 to 27/06/2016 and 25/01/2016 to 31/01/2016, respectively. Columns represent Fl channels 1–3, with the final column representing size in µm.

Table 1. Characteristics of individual clusters when using a four-cluster solution for exclusively fluorescent particles ± represents 1 standard deviation, calculated using raw, non-zero particle data. AF represents asymmetry factor as given by the WIBS-4M and % reflects the contribution each cluster makes to the total fluorescent particle observations. The "no." column represents the number of particles classified within a given cluster.

	Fl 1 (a.u.)			
	0–5 µm	5–10 µm	10–20 µm	All
Cluster 1	1219.7 ± 497.0	1033.1 ± 372.8	1114.4 ± 361.6	1169.3 ± 469.3
Cluster 2	25. 2 ± 64.1	34.5 ± 70.7	34.9 ± 85.7	27.9 ± 66.5
Cluster 3	8.0 ± 26.1	49.9 ± 63.7	69.8 ± 0	8.0 ± 26.1
Cluster 4	15.7 ± 52.4	64.7 ± 110.9	79.2 ± 133.5	25.4 ± 72.2
	Fl 2 (a.u.)			
	0–5 µm	5–10 µm	10–20 µm	All
Cluster 1	22.9 ± 82.7	132.9 ± 221.9	453.8 ± 453.3	80.1 ± 215.5
Cluster 2	24.0 ± 44.1	43.9 ± 61.1	68.7 ± 72.9	30.3 ± 51.0
Cluster 3	39.7 ± 57.0	27.0 ± 36.0	64.3 ± 0	39.7 ± 57.0
Cluster 4	309.0 ± 299.0	495.1 ± 276.1	618.2 ± 373.1	348.5 ± 313.9
	Fl 3 (a.u.)			
	0–5 µm	5–10 µm	10–20 µm	All
Cluster 1	10.5 ± 56.0	99.5 ± 231.2	366.8 ± 413.8	57.8 ± 195.1
Cluster 2	16.1 ± 48.9	22.6 ± 51.0	47.2 ± 70.9	18.5 ± 50.3
Cluster 3	25.3 ± 54.4	23.5 ± 64.7	–	25.3 ± 54.4
Cluster 4	247.5 ± 319.7	478.4 ± 314.7	611.5 ± 407.3	296.0 ± 342.2
	Size (µm)	AF	%	No.
Cluster 1	4.9 ± 3.2	19.7 ± 16.3	0.4 ± 1.3	7297
Cluster 2	4.4 ± 2.1	23.4 ± 14.8	58.8 ± 17.7	893 241
Cluster 3	1.6 ± 0.5	7.0 ± 4.9	34.7 ± 15.9	547 711
Cluster 4	3.4 ± 3.4	16.5 ± 16.2	6.2 ± 5.5	121 455

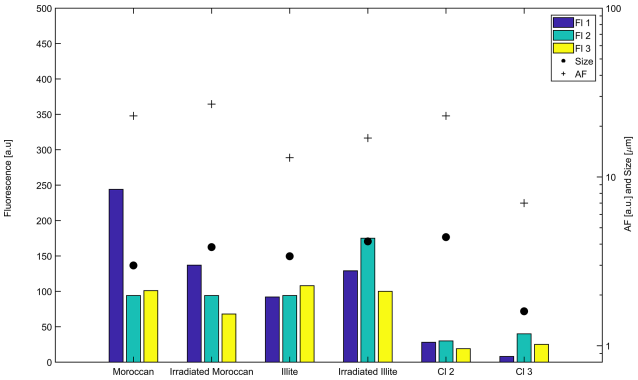

Figure 6. Mean fluorescence, size and shape properties of the four dust samples put through the WIBS-4M in a laboratory environment and their comparison to the two dominant long-term campaign clusters – Clusters 2 and 3.

geria have been identified before, as well as dust that has been transported from the Chad Basin in the Bodélé Depression (Herrmann et al., 1999). Such Harmattan dust clouds have often been found to affect the coastal regions of the Gulf of Guinea. These clouds are a major annual event, noted for exacerbating cardiovascular health issues and increasing daily mortality by 8.4 % (Perez et al., 2008). Previous studies by Enete et al. (2012) found this dust to contain high quantities of silicon, which is consistent with the LAAP-ToF results presented here.

It is interesting that continental back trajectories during summer do not contain similar concentrations of fluorescent material, despite a similar fluorescent ratio and wind speeds to those seen in winter. This is likely due to the seasonal shift in the ITCZ, as outlined by Chiapello et al. (1995). During summer, the ITCZ is located between 6 and 10° N, and dust gets transported into the Saharan Air Layer (SAL) at a maximum altitude of 7000 m. At this height, there is little opportunity for the dust to mix with trade winds, and it is instead transported significant distances across the Atlantic. However, during winter, the ITCZ shifts south and the dust

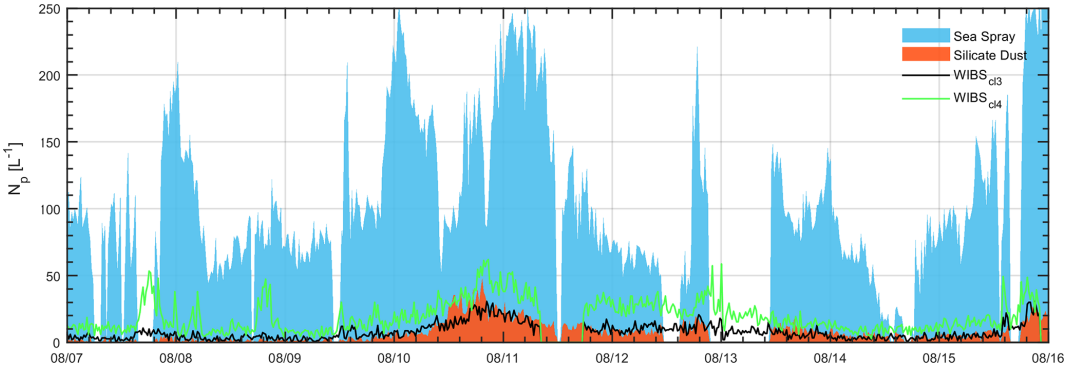

Figure 7. Time series of sea spray aerosol and silicate dust particle numbers concentrations determined by LAAP-ToF and WIBS-4A Clusters 3 and 4; 20 min averages have been used here.

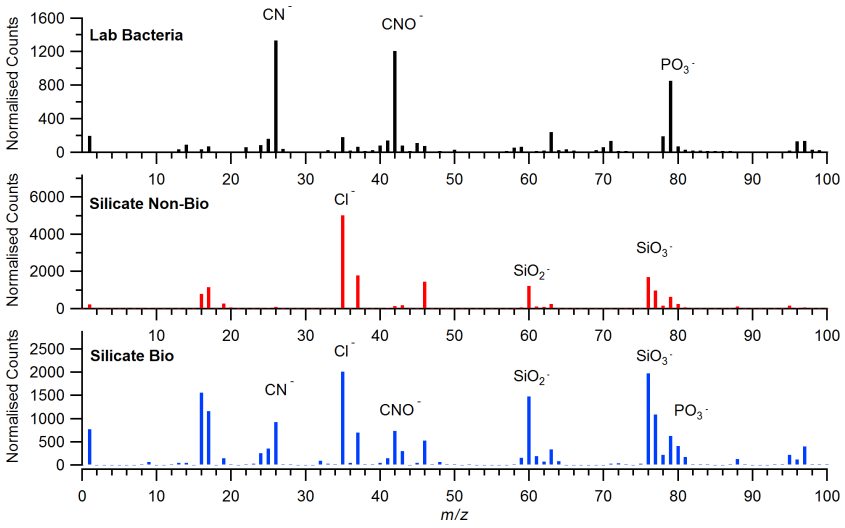

Figure 8. Average negative ion spectra of laboratory-generated bacteria and the ICE-D silicate dust products.

is no longer able to get taken into the SAL. This constrains the dust into lower altitudes, where they are subject to mixing with trade winds, including the Harmattan wind. Dust consequently gets deposited much sooner and often blankets Cabo Verde. The ecological consequences of this have been investigated by Korte et al. (2017), who placed sediment traps across the Atlantic to measure fluxes in biogenic constituents, including biogenic silica. They observed higher biogenic fluxes during winter, due to Saharan dust getting deposited during the previously discussed trade wind events. They also observed a seasonal maxima of biogenic silica towards the west, suggesting that the bioaerosols we observe are not as readily deposited into the ocean as some other particle types.

It is also interesting to consider potential differences in dust from the various source regions. This has been investigated by Patey et al. (2015), who also monitored dust concentrations at the CVAO. By looking at specific elemental ratios within dust samples, they were able to identify where the dust was thought to have come from, as well as what it was comprised of. They found during summer months that 92.5 % of samples contained a contribution from the Sahel, compared to just 52.3 % of samples collected during winter. These observations are supported by previous work from Prospero and Lamb (2003), who found that it was Sahelian dust that was predominantly transported across the Atlantic via the SAL during summer.

4.2 Identification of fluorescent material

The relative contributions of each cluster in Fig. 3 highlight the importance of Clusters 2 and 3. Furthermore, it shows that the mixture of bioaerosols have no clear pattern, with each cluster present all year round. The intensive measurements from the LAAP-ToF and WIBS-4A have provided supporting evidence to suggest that most of the fluorescent particles observed are mixtures of biological and non-biological material, i.e. bacteria attached to dust. It is likely because of this that fluorescence intensity is correlated

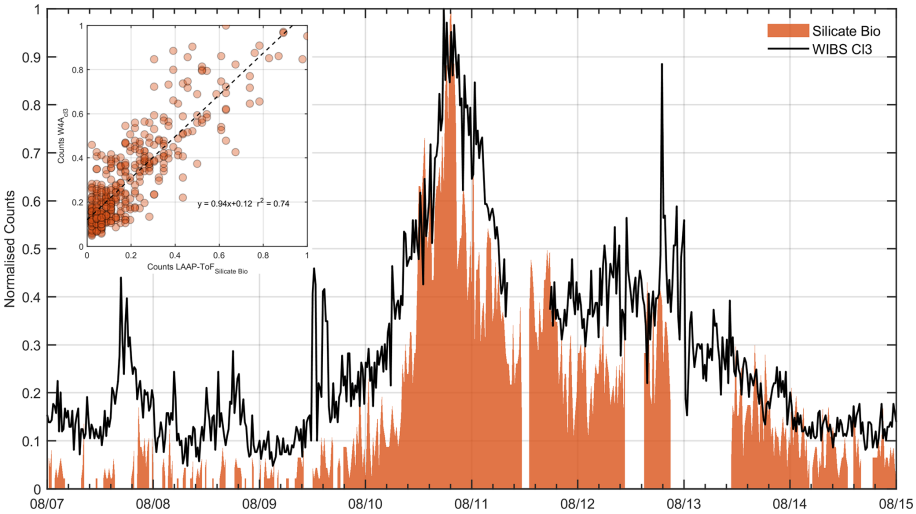

Figure 9. Time series of WIBS Cluster 3 and silicate dust filtered for biomarkers using 20 min averaged number counts normalised by the maximum observed concentration for each instrument. Values for the inset plot are also normalised to the maximum observed concentration.

with particle size. Larger particles may carry greater numbers of bacteria due to increased surface area and as a result should carry more fluorophores for detection by the instrument. The relationship between fluorescence and particle size has been investigated extensively by Hill et al. (2015), who have shown a generally positive correlation.

Concluding that Clusters 2 and 3 are at least partially bacterial in nature is in contrast to findings by Savage et al. (2017), whose laboratory tests on *Bacillus atrophaeus, Escherichia coli* and *Pseudomonas stutzeri* have produced different fluorescent spectra to those observed here. In their tests, bacteria have been shown to fluoresce strongly in Fl 1 and weakly in Fl 2 and 3, while our results show little increase in Fl 1 concentrations during winter but substantial increases in Fl 2 and 3. However, it must be emphasised that they used "pure" bacterial samples, potentially unrepresentative of the mixed aggregates we observed.

Furthermore, they outline previous work by Agranovski et al. (2004), who found that an ultraviolet aerodynamic particle sizer (UV-APS) was effective in identifying fluorophores at similar wavelengths that a WIBS-4A was unsuccessful in doing so. They hypothesise reasons for this, including potential differences in gain voltages applied in the instrument, and weaker excitation intensity in Xe2 with respect to Xe1. With that considered, it must also be noted that there are high levels of agreement between the WIBS-4A used in the intensive measurements and the WIBS-4M for 11 months. As such, the more likely explanation may simply be differences between the samples used in the laboratory and those measured at the observatory. Without proper characterisation of a bacteria–dust aggregate in a controlled setting it is difficult to interpret how this could impact the emissions spectra. Internal reabsorption of fluorescence is known to occur when emitted fluorescent wavelengths overlap with a particle's absorption spectrum. In this instance, it is possible that the dust absorbs certain wavelengths emitted from the bacteria, skewing what is detected by the instrument. It must be emphasised that applying a 9σ threshold to the fluorescent baseline of the WIBS-4M means that our observations are unlikely to be interferents.

Clusters 1 and 4 are interesting because of their high fluorescence intensity. It is possible that these clusters represent "pure" bioaerosols, that have not mixed with non-fluorescent material or are relatively more exposed due to, for example, larger bacterial aggregates present. Cluster 1's spectral profile matches closely with laboratory experiments using bacteria (Savage et al., 2017), with a strong fluorescence in Fl 1 seen across all size ranges. However, Cluster 4 remains difficult to identify. It shows similarly high-intensity fluorescence to Cluster 1 but only in Fl 2 and 3. Its relative contribution to the total bioaerosol count is significant, yet given the location of the observatory seems unlikely to be other common terrestrial bioaerosols such as pollen fragments. Although it may therefore seem likely to have a marine source, its concentrations follow similar seasonal trends to the other clusters which are more easily explained by Aeolian events. With potential differences in their capacity to act as ice nucleators when compared to bacteria and dust aggregates, it is useful to quantify their concentrations.

The dust samples dispersed into the WIBS-4M also support our argument that bacteria–dust aggregates are our dominant bioaerosol type. Many of the sampled particles shared similar spectral profiles to those for Clusters 2 and 3, being weakly fluorescent in all three channels. Each sample also predominantly consisted of non-fluorescent particles, sharing a similarly low fluorescent particle ratio to our campaign observations.

Although the 9σ threshold we have used should eliminate weakly fluorescent non-biological particles, the potential for more highly fluorescent particles to act as interferents should be discussed. Soot is one example, with previous studies having observed higher fluorescence than is typically seen for non-biological particles. Despite this, there are multiple reasons that we do not believe interferents are contributing to particle concentrations. Firstly, studies that found soot to fluoresce above their thresholds had usually only done so when using 3σ thresholding. Toprak and Schnaiter (2013) found propane flame soot to only weakly fluoresce in Fl1 at this threshold, and so we would not expect it to be fluorescent at a more conservative 9σ thresholding. Secondly, the sizes of the observed fluorescent particles are larger than we would expect for soot. Toprak and Schnaiter (2013) found generated soot to only be 0.8 µm after significant coagulation time in the NAUA chamber, while Savage et al. (2017) used a mechanically dispersed dry diesel soot powder to investigate potential interferent aerosol fluorescence. They noted that this powder fluoresced above a conservative 9σ threshold, but this sample aerosol was much larger than soot typically observed in the atmosphere when aerosolised (~ 1.1 µm). Savage et al. (2017) also acknowledged that fluorescence intensity is a strong function of particle size due to surface area/volume effects and that this test soot was likely to be significantly more fluorescent than ambient diesel soot as a result. Furthermore, Savage and Huffman (2018) acknowledge that more highly fluorescent soot is representative of freshly generated soot close to source and is not representative of aged or processed soot. Ambient soot at CVAO should not be fluorescent at 9σ. While it is possible that soot could have internally mixed with dust and therefore become larger, this would still represent aged soot and would be less fluorescent.

We also acknowledge the fraction identified as biological is small ($< 1\,\%$) and that concentrations would consequently be significantly affected by even minor errors in the classification of particle types. However, if a fraction of non-biological particles were "bleeding" through and influencing our concentrations, their mass spectral signatures would differ from our "biosilicate" class. As there is a close correlation between the biosilicate particle counts and our fluorescent fraction, we do not believe that bleeding is significantly changing our observations. More studies comparing such a technique may elucidate the degree to which bleeding occurs, but we believe our study provides a good first estimate of bioaerosol concentrations in this region. As discussed by Savage et al. (2017), UV-LIF results should be considered uniquely in all situations with appreciation of possible influences. We are confident that many common interferent particles such as soot can be further discounted when evaluating properties such as particle size, as well as an appreciation for modelled back trajectories and identified source regions.

4.3 Comparison to previous studies

The results presented here are broadly consistent with previous studies demonstrating that mineral dust is often observed to be mixed with biological material, e.g. Yamaguchi et al. (2012), Griffin et al. (2001) and Maki et al. (2018). Similar to the approach used here, a recent study by Zawadowicz et al. (2019) assessed the prevalence of biological material over the continental United States using single particle mass spectrometry and UV-LIF, finding that 30 % to 80 % of biological particles were mixed with mineral dust. While they provide evidence for biomineral mixtures in their study, the fluorescent number concentration derived from the WIBS is likely an overestimate of the true bioaerosol concentration due to the choice of 3σ thresholding including pure mineral dust interferents in their assumed bioaerosol population, as a small but significant subset of mineral dust naturally exhibits weak fluorescence (Huffman et al., 2019; Savage et al., 2017; Crawford et al., 2016; Pöhlker et al., 2012). The conservative 9σ threshold used in our study excludes these non-biological interferents from the presented PBAP classes (Savage et al., 2017). Furthermore, the use of only negative ion spectra makes resolving biominerals from pure minerals challenging. The use of both positive and negative ion spectra in our study provides greater particle information and consequently improves our ability to classify biological and pure minerals as distinct groups (Shen et al., 2018).

5 Summary and conclusions

This study has utilised UV-LIF technology to provide long-term measurements of bioaerosol concentrations within an important but often overlooked region of the world. Seasonal variations in both fluorescent and total particle concentrations are clearly observed, likely as a result of the annual patterns of the ITCZ and subsequent mixing with trade winds. This can be readily seen from the HYSPLIT back trajectories, with the highest particle concentrations coming from mainland Africa during winter months.

When considering the source regions in the Sahara and significant correlation between fluorescent and non-fluorescent particle concentrations, it is presumed we are observing high mineral dust concentrations with some associated bacteria. This is supported through the LAAP-ToF and WIBS-4A intensive measurements, with a significant correlation between the LAAP-ToF's biosilicate counts and the concentrations of a clustered subset from the WIBS-4A.

Cluster analysis results from the WIBS-4A compare favourably with those from the WIBS-4M, with both suggesting four-cluster solutions that share similar fluorescent profiles. For the long-term campaign, Clusters 2 and 3 dominate fluorescent particle contributions, accounting for approximately 90 % of all bioaerosols. Both are weakly fluorescent, but with a 9σ threshold having been applied they are un-

likely to be interferents. A laboratory experiment using representative dust samples has shown similar fluorescent properties to these clusters, helping to contextualise our observations. These presumed bacteria and dust aggregates are still a minority particle type, accounting for a mean 0.4 ± 0.2 % of total coarse aerosol concentrations. Although this ratio is relatively low, it should be noted that the raw number of bioaerosols present is still quite high, with monthly median concentrations as high as $45\,L^{-1}$ and 95th percentile values exceeding $130\,L^{-1}$. Highly fluorescent and likely primary bioaerosols have also been identified in Clusters 1 and 4, accounting for an average 6.6 % of total fluorescent particles. These have not been conclusively identified, but it should be stated that Cluster 1 most closely resembles the spectral profile of pure bacteria outlined by Savage et al. (2017), while Cluster 4 remains unidentified.

Our long-term measurements are consistent with the observations of Korte et al. (2017), who made an association between the deposition of biogenic silica along the Atlantic and high levels of dust from the African continent. It would be interesting for future work to determine whether there are microbial differences within this dust when compared to other regions, following the approach described by Maki et al. (2018). Either the presence of more efficiently ice-nucleating bacteria strains or simply greater concentrations could potentially explain why Sassen et al. (2003) found dust in African outflow to ice nucleate at significantly warmer temperatures than similar studies by Ansmann et al. (2008) and Zhang et al. (2012). Such work would have the capacity to improve global climate model (GCM) simulations.

Appendix A

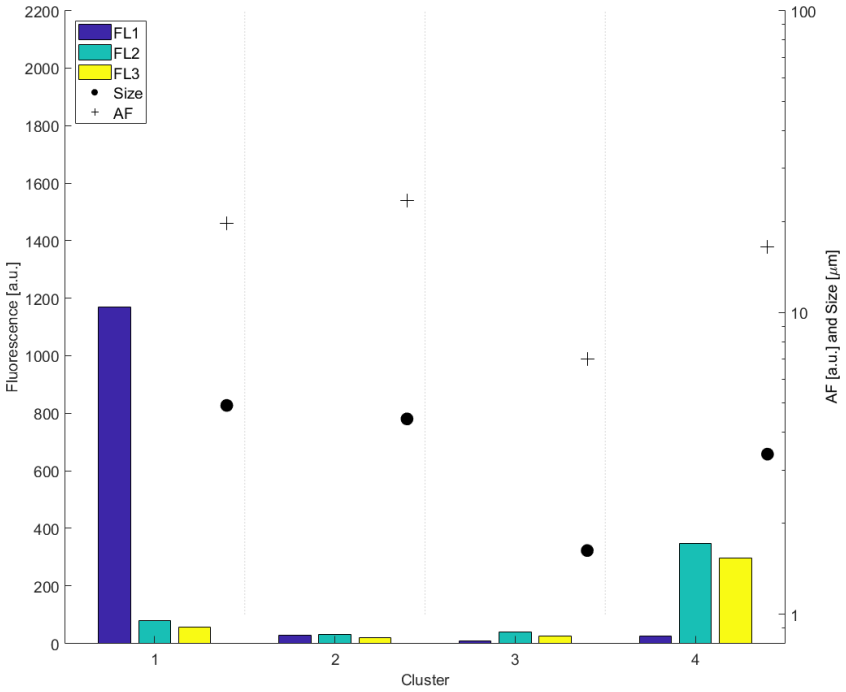

Figure A1. Summary of the average fluorescence, size and AF of each cluster from the long-term campaign.

Data availability. Due to the large file sizes for the dataset, it is available upon request to the lead author.

Supplement. The supplement related to this article is available online at: https://doi.org/10.5194/acp-20-14473-2020-supplement.

Author contributions. DM is a PhD student and primary author for this paper, responsible for most written components. IC processed the data, contributed to the analysis and provided guidance on the paper's contents. NM was involved in operating and analysing the data from the LAAP-ToF and has collaborated with IC to write the sections pertaining to the LAAP-ToF. NM has also sourced the dust samples for the lab experiments. MF was involved in the planning and execution of both the short-term and long-term components of the project, as well as providing an estimate of the transmission efficiency of the sampling line. KR manages the CVAO World Meteorological Organization – Global Atmospheric Watch (WMO-GAW) station and provided support and access to facilities for this experiment as part of ICE-D, including meteorological data which are archived at the WMO-GAW and British Atmospheric Data Centre (BADC). NL was responsible for instrument operation and maintenance during the long-term campaign. VF is part of DSTL and provided technical support and loan of UV-LIF instrumentation. PK and WS helped in maintenance and repair of the instrument. HC was involved in the short-term component of the project, while DT has provided guidance on the direction and written components of the paper. MG has overseen the entire project, acting as the primary lead. MG is the supervisor of DM and has offered guidance at every stage.

Competing interests. The authors declare that they have no conflict of interest.

Acknowledgements. This project was funded by NERC as part of the ICE-D campaign (NE/M001954/1). Douglas Morrison's PhD studentship was funded by the NERC Doctoral Training Program (DTP). Ian Crawford has been funded as part of the BIOARC campaign (NE/S002049/1). We thank DMT for the loan of the WIBS-4A used in the LAAP-ToF comparison.

Financial support. This research has been supported by NERC (grant nos. NE/M001954/1 and NE/S002049/1).

Review statement. This paper was edited by Anne Perring and reviewed by two anonymous referees.

References

Agranovski, V., Ristovski, Z. D., Ayoko, G. A., and Morawska, L.: Performance evaluation of the UVAPS in measuring biological aerosols: fluorescence spectra from NAD (P) H coenzymes and riboflavin, Aerosol Sci. Tech., 38, 354–364, 2004.

Ansmann, A., Tesche, M., Althausen, D., Müller, D., Seifert, P., Freudenthaler, V., Heese, B., Wiegner, M., Pisani, G., Knippertz, P., and Dubovik, O.: Influence of Saharan dust on cloud glaciation in southern Morocco during the Saharan Mineral Dust Experiment, J. Geophys. Res.-Atmos., 113, https://doi.org/10.1029/2007JD008785, 2008.

Bauer, H., Kasper-Giebl, A., Löflund, M., Giebl, H., Hitzenberger, R., Zibuschka, F., and Puxbaum, H.: The contribution of bacteria and fungal spores to the organic carbon content of cloud water, precipitation and aerosols, Atmos. Res., 64, 109–119, 2002.

Bauer, H., Giebl, H., Hitzenberger, R., Kasper-Giebl, A., Reischl, G., Zibuschka, F., and Puxbaum, H.: Airborne bacteria as cloud condensation nuclei, J. Geophys. Res.-Atmos., 108, https://doi.org/10.1029/2003JD003545, 2003.

Carpenter, L., Fleming, Z., Read, K., Lee, J., Moller, S., Hopkins, J., Purvis, R., Lewis, A., Müller, K., Heinold, B., Herrmann, H., Wadinga Fomba, K., van Pinxteren, D., Müller, C., Tegen, I., Wiedensohler, A., Müller, T., Niedermeier, N., Achterberg, E. P., Patey, M. D., Kozlova, E. A., Heimann, M., Heard, D. E., Plane, J. M. C., Mahajan, A., Oetjen, H., Ingham, T., Stone, D., Whalley, L. K., Evans, M. J., Pilling, M. J., Leigh, R. J., Monks, P. S., Karunaharan, A., Vaughan, S., Arnold, S. R., Tschritter, J., Pöhler, D., Frieß, U., Holla, R., Mendes, L. M., Lopez, H., Faria, B., Manning, A. J., and Wallace, D. W. R.: Seasonal characteristics of tropical marine boundary layer air measured at the Cape Verde Atmospheric Observatory, J. Atmos. Chem., 67, 87–140, 2010.

Carslaw, R.: An R package for air quality data analysis, Environmental Modelling and Software, 27, 52–61, 2012.

Chiapello, I., Bergametti, G., Gomes, L., Chatenet, B., Dulac, F., Pimenta, J., and Suares, E. S.: An additional low layer transport of Sahelian and Saharan dust over the north-eastern tropical Atlantic, Geophys. Res. Lett., 22, 3191–3194, 1995.

Crawford, I., Robinson, N. H., Flynn, M. J., Foot, V. E., Gallagher, M. W., Huffman, J. A., Stanley, W. R., and Kaye, P. H.: Characterisation of bioaerosol emissions from a Colorado pine forest: results from the BEACHON-RoMBAS experiment, Atmos. Chem. Phys., 14, 8559–8578, https://doi.org/10.5194/acp-14-8559-2014, 2014.

Crawford, I., Ruske, S., Topping, D. O., and Gallagher, M. W.: Evaluation of hierarchical agglomerative cluster analysis methods for discrimination of primary biological aerosol, Atmos. Meas. Tech., 8, 4979–4991, https://doi.org/10.5194/amt-8-4979-2015, 2015.

Crawford, I., Lloyd, G., Herrmann, E., Hoyle, C. R., Bower, K. N., Connolly, P. J., Flynn, M. J., Kaye, P. H., Choularton, T. W., and Gallagher, M. W.: Observations of fluorescent aerosol-cloud interactions in the free troposphere at the High-Altitude Research Station Jungfraujoch, Atmos. Chem. Phys., 16, 2273–2284, https://doi.org/10.5194/acp-16-2273-2016, 2016.

Enete, I. C., Igu, I., Ayadiulo, R., Ifeanyi, C., Enete, E., Obienusi, A., Igu, I. N. and Ayadiulo, R.: Harmattan dust: composition, characteristics and effects on soil fertility in Enugu, Nigeria, British J. Appl. Sci. Technol., 2, 72–81, 2012.

Engelstaedter, S., Tegen, I., and Washington, R.: North African dust emissions and transport, Earth-Sci. Rev., 79, 73–100, 2006.

Folland, C., Owen, J., Ward, M. N., and Colman, A.: Prediction of seasonal rainfall in the Sahel region using empirical and dynamical methods, J. Forecast., 10, 21–56, 1991.

Forde, E., Gallagher, M., Walker, M., Foot, V., Attwood, A., Granger, G., Sarda-Estève, R., Stanley, W., Kaye, P., and Topping, D.: Intercomparison of Multiple UV-LIF Spectrometers Using the Aerosol Challenge Simulator, Atmosphere, 10, 797, https://doi.org/10.3390/atmos10120797, 2019.

Franc, G. D. and DeMott, P. J.: Cloud activation characteristics of airborne Erwinia carotovora cells, J. Appl. Meteorol., 37, 1293–1300, 1998.

Fröhlich-Nowoisky, J., Kampf, C. J., Weber, B., Huffman, J. A., Pöhlker, C., Andreae, M. O., Lang-Yona, N., Burrows, S. M., Gunthe, S. S., Elbert, W., et al.: Bioaerosols in the Earth system: Climate, health, and ecosystem interactions, Atmos. Res., 182, 346–376, 2016.

Gabey, A. M., Gallagher, M. W., Whitehead, J., Dorsey, J. R., Kaye, P. H., and Stanley, W. R.: Measurements and comparison of primary biological aerosol above and below a tropical forest canopy using a dual channel fluorescence spectrometer, Atmos. Chem. Phys., 10, 4453–4466, https://doi.org/10.5194/acp-10-4453-2010, 2010.

Gosselin, M. I., Rathnayake, C. M., Crawford, I., Pöhlker, C., Fröhlich-Nowoisky, J., Schmer, B., Després, V. R., Engling, G., Gallagher, M., Stone, E., Pöschl, U., and Huffman, J. A.: Fluorescent bioaerosol particle, molecular tracer, and fungal spore concentrations during dry and rainy periods in a semi-arid forest, Atmos. Chem. Phys., 16, 15165–15184, https://doi.org/10.5194/acp-16-15165-2016, 2016.

Griffin, D. W., Garrison, V. H., Herman, J. R., and Shinn, E. A.: African desert dust in the Caribbean atmosphere: microbiology and public health, Aerobiologia, 17, 203–213, 2001.

Haga, D., Iannone, R., Wheeler, M., Mason, R., Polishchuk, E., Fetch Jr, T., Van Der Kamp, B., McKendry, I., and Bertram, A.: Ice nucleation properties of rust and bunt fungal spores and their transport to high altitudes, where they can cause heterogeneous freezing, J. Geophys. Res.-Atmos., 118, 7260–7272, 2013.

Herrmann, L., Stahr, K., and Jahn, R.: The importance of source region identification and their properties for soil-derived dust: the case of Harmattan dust sources for eastern West Africa, Beitrage zur Physik der Atmosphare-Contributions to Atmospheric Physics, 72, 141–150, 1999.

Hill, S. C., Mayo, M. W., and Chang, R. K.: Fluorescence of bacteria, pollens, and naturally occurring airborne particles: excitation/emission spectra, Tech. Rep., Army research lab adelphi md computational and information sciences directorate, 50 pp., 2009.

Hill, S. C., Williamson, C. C., Doughty, D. C., Pan, Y.-L., Santarpia, J. L., and Hill, H. H.: Size-dependent fluorescence of bioaerosols: Mathematical model using fluorescing and absorbing molecules in bacteria, J. Quant. Spectrosc. Ra., 157, 54–70, 2015.

Hoose, C. and Möhler, O.: Heterogeneous ice nucleation on atmospheric aerosols: a review of results from laboratory experiments, Atmos. Chem. Phys., 12, 9817–9854, https://doi.org/10.5194/acp-12-9817-2012, 2012.

Huffman, J. A., Sinha, B., Garland, R. M., Snee-Pollmann, A., Gunthe, S. S., Artaxo, P., Martin, S. T., Andreae, M. O., and Pöschl, U.: Size distributions and temporal variations of biological aerosol particles in the Amazon rainforest characterized by microscopy and real-time UV-APS fluorescence techniques during AMAZE-08, Atmos. Chem. Phys., 12, 11997–12019, https://doi.org/10.5194/acp-12-11997-2012, 2012.

Huffman, J. A., Perring, A. E., Savage, N. J., Clot, B., Crouzy, B., Tummon, F., Shoshanim, O., Damit, B., Schneider, J., Sivaprakasam, V., et al.: Real-time sensing of bioaerosols: Review and current perspectives, Aerosol Sci. Tech., 54, 1–31, https://doi.org/10.1080/02786826.2019.1664724, 2019.

Kaye, P. H., Aptowicz, K., Chang, R. K., Foot, V., and Videen, G.: Angularly resolved elastic scattering from airborne particles, in: Optics of Biological Particles, Springer, 31–61, 2007.

Korte, L. F., Brummer, G.-J. A., van der Does, M., Guerreiro, C. V., Hennekam, R., van Hateren, J. A., Jong, D., Munday, C. I., Schouten, S., and Stuut, J.-B. W.: Downward particle fluxes of biogenic matter and Saharan dust across the equatorial North Atlantic, Atmos. Chem. Phys., 17, 6023–6040, https://doi.org/10.5194/acp-17-6023-2017, 2017.

Lakowicz, J. R.: Principles of fluorescence spectroscopy, Springer Science & Business Media, 2013.

Liu, D., Wang, Z., Liu, Z., Winker, D., and Trepte, C.: A height resolved global view of dust aerosols from the first year CALIPSO lidar measurements, J. Geophys. Res.-Atmos., 113, https://doi.org/10.1029/2007JD009776, 2008.

Liu, D., Taylor, J. W., Crosier, J., Marsden, N., Bower, K. N., Lloyd, G., Ryder, C. L., Brooke, J. K., Cotton, R., Marenco, F., Blyth, A., Cui, Z., Estelles, V., Gallagher, M., Coe, H., and Choularton, T. W.: Aircraft and ground measurements of dust aerosols over the west African coast in summer 2015 during ICE-D and AER-D, Atmos. Chem. Phys., 18, 3817–3838, https://doi.org/10.5194/acp-18-3817-2018, 2018.

Maki, T., Furumoto, S., Asahi, Y., Lee, K. C., Watanabe, K., Aoki, K., Murakami, M., Tajiri, T., Hasegawa, H., Mashio, A., and Iwasaka, Y.: Long-range-transported bioaerosols captured in snow cover on Mount Tateyama, Japan: impacts of Asian-dust events on airborne bacterial dynamics relating to ice-nucleation activities, Atmos. Chem. Phys., 18, 8155–8171, https://doi.org/10.5194/acp-18-8155-2018, 2018.

Marsden, N., Flynn, M. J., Taylor, J. W., Allan, J. D., and Coe, H.: Evaluating the influence of laser wavelength and detection stage geometry on optical detection efficiency in a single-particle mass spectrometer, Atmos. Meas. Tech., 9, 6051–6068, https://doi.org/10.5194/amt-9-6051-2016, 2016.

Marsden, N. A., Flynn, M. J., Allan, J. D., and Coe, H.: Online differentiation of mineral phase in aerosol particles by ion formation mechanism using a LAAP-TOF single-particle mass spectrometer, Atmos. Meas. Tech., 11, 195–213, https://doi.org/10.5194/amt-11-195-2018, 2018.

Marsden, N. A., Ullrich, R., Möhler, O., Eriksen Hammer, S., Kandler, K., Cui, Z., Williams, P. I., Flynn, M. J., Liu, D., Allan, J. D., and Coe, H.: Mineralogy and mixing state of north African mineral dust by online single-particle mass spectrometry, Atmos. Chem. Phys., 19, 2259–2281, https://doi.org/10.5194/acp-19-2259-2019, 2019.

McFarland, A., O. C.: Characterization of Sierra-Anderson Model 321a mm Size Selective Inlet for Hi-Vol Samplers, Air Quality Laboratory, 1984.

McTainsh, G.: Dust concentrations and particle-size characteristics of an intense dust haze event: inland delta region, Mali, West Africa, Atmos. Environ., 30, 1081–1090, 1996.

Murphy, D. M.: The design of single particle laser mass spectrometers, Mass Spec. Rev., 26, 150–165, 2007.

Patey, M. D., Achterberg, E. P., Rijkenberg, M. J., and Pearce, R.: Aerosol time-series measurements over the tropical Northeast Atlantic Ocean: dust sources, elemental composition and mineralogy, Mar. Chem., 174, 103–119, 2015.

Perez, L., Tobias, A., Querol, X., Künzli, N., Pey, J., Alastuey, A., Viana, M., Valero, N., González-Cabré, M., and Sunyer, J.: Coarse particles from Saharan dust and daily mortality, Epidemiology, 19, 800–807, 2008.

Perring, A., Schwarz, J., Baumgardner, D., Hernandez, M., Spracklen, D., Heald, C., Gao, R., Kok, G., McMeeking, G., McQuaid, J., and Fahey, D. W.: Airborne observations of regional variation in fluorescent aerosol across the United States, J. Geophys. Res.-Atmos., 120, 1153–1170, 2015.

Pöhlker, C., Huffman, J. A., and Pöschl, U.: Autofluorescence of atmospheric bioaerosols – fluorescent biomolecules and potential interferences, Atmos. Meas. Tech., 5, 37–71, https://doi.org/10.5194/amt-5-37-2012, 2012.

Pope, F.: Pollen grains are efficient cloud condensation nuclei, Environ. Res. Lett., 5, 044015, https://doi.org/10.1088/1748-9326/5/4/044015, 2010.

Pratt, K. A. and Prather, K. A.: Mass spectrometry of atmospheric aerosols – Recent developments and applications. Part II: Online mass spectrometry techniques, Mass Spec. Rev., 31, 17–48, 2012.

Pratt, K. A., DeMott, P. J., French, J. R., Wang, Z., Westphal, D. L., Heymsfield, A. J., Twohy, C. H., Prenni, A. J., and Prather, K. A.: In situ detection of biological particles in cloud ice-crystals, Nat. Geosci., 2, 398–401, 2009.

Prospero, J. M.: Long-term measurements of the transport of African mineral dust to the southeastern United States: Implications for regional air quality, J. Geophys. Res.-Atmos., 104, 15917–15927, 1999.

Prospero, J. M. and Lamb, P. J.: African droughts and dust transport to the Caribbean: Climate change implications, Science, 302, 1024–1027, 2003.

Reinard, M. S. and Johnston, M. V.: Ion formation mechanism in laser desorption ionization of individual nanoparticles, Journal of the American Society for Mass Spectrometry, 19, 389–399, 2008.

Robinson, N. H., Allan, J. D., Huffman, J. A., Kaye, P. H., Foot, V. E., and Gallagher, M.: Cluster analysis of WIBS single-particle bioaerosol data, Atmos. Meas. Tech., 6, 337–347, https://doi.org/10.5194/amt-6-337-2013, 2013.

Ruske, S., Topping, D. O., Foot, V. E., Kaye, P. H., Stanley, W. R., Crawford, I., Morse, A. P., and Gallagher, M. W.: Evaluation of machine learning algorithms for classification of primary biological aerosol using a new UV-LIF spectrometer, Atmos. Meas. Tech., 10, 695–708, https://doi.org/10.5194/amt-10-695-2017, 2017.

Rypien, K. L.: African dust is an unlikely source of Aspergillus sydowii, the causative agent of sea fan disease, Mar. Ecol. Prog. Ser., 367, 125–131, 2008.

Sands, D. C., Langhans, V. E., Scharen, A. L., and De Smet, G.: The association between bacteria and rain and possible resultant meteorological implications, 148–152, 1982.

Sassen, K., DeMott, P. J., Prospero, J. M., and Poellot, M. R.: Saharan dust storms and indirect aerosol effects on clouds: CRYSTAL-FACE results, Geophys. Res. Lett., 30, https://doi.org/10.1029/2003GL017371, 2003.

Savage, N. J., Krentz, C. E., Könemann, T., Han, T. T., Mainelis, G., Pöhlker, C., and Huffman, J. A.: Systematic characterization and fluorescence threshold strategies for the wideband integrated bioaerosol sensor (WIBS) using size-resolved biological and interfering particles, Atmos. Meas. Tech., 10, 4279–4302, https://doi.org/10.5194/amt-10-4279-2017, 2017.

Shen, X., Ramisetty, R., Mohr, C., Huang, W., Leisner, T., and Saathoff, H.: Laser ablation aerosol particle time-of-flight mass spectrometer (LAAPTOF): performance, reference spectra and classification of atmospheric samples, Atmos. Meas. Tech., 11, 2325–2343, https://doi.org/10.5194/amt-11-2325-2018, 2018.

Steiner, A. L., Brooks, S. D., Deng, C., Thornton, D. C., Pendleton, M. W., and Bryant, V.: Pollen as atmospheric cloud condensation nuclei, Geophys. Res. Lett., 42, 3596–3602, 2015.

Sultan, B., Labadi, K., Guégan, J.-F., and Janicot, S.: Climate drives the meningitis epidemics onset in West Africa, PLoS Medicine, 2, https://doi.org/10.1371/journal.pmed.0020006, 2005.

Toprak, E. and Schnaiter, M.: Fluorescent biological aerosol particles measured with the Waveband Integrated Bioaerosol Sensor WIBS-4: laboratory tests combined with a one year field study, Atmos. Chem. Phys., 13, 225–243, https://doi.org/10.5194/acp-13-225-2013, 2013.

Yamaguchi, N., Ichijo, T., Sakotani, A., Baba, T., and Nasu, M.: Global dispersion of bacterial cells on Asian dust, Sci. Rep., 2, 525, https://doi.org/10.1038/srep00525, 2012.

Yankofsky, S., Levin, Z., Bertold, T., and Sandlerman, N.: Some basic characteristics of bacterial freezing nuclei, J. Appl. Meteorol., 20, 1013–1019, 1981.

Zawadowicz, M. A., Froyd, K. D., Perring, A. E., Murphy, D. M., Spracklen, D. V., Heald, C. L., Buseck, P. R., and Cziczo, D. J.: Model-measurement consistency and limits of bioaerosol abundance over the continental United States, Atmos. Chem. Phys., 19, 13859–13870, https://doi.org/10.5194/acp-19-13859-2019, 2019.

Zhang, D., Wang, Z., Heymsfield, A., Fan, J., Liu, D., and Zhao, M.: Quantifying the impact of dust on heterogeneous ice generation in midlevel supercooled stratiform clouds, Geophys. Res. Lett., 39, https://doi.org/10.1029/2012GL052831, 2012.

3.2 The Observation and Characterisation of Fluorescent Bioaerosols using Real-Time UV-LIF Spectrometry in Hong Kong from June to November, 2018

Hong Kong's monsoon-influenced climate has consequences for subsequent aerosol mixtures. Previous literature has shown an enhancement in anthropogenic aerosols during winter, as northerly trajectories carry these pollutants from the mainland. The objective of our campaign was to broaden the discussion by including the consequences this shift in wind patterns has for bioaeorsols. To do this, we deployed a WIBS-NEO, MBS and PLAIR Rapid-E to each provide quantitative estimates of fluorescent particles from June to November, 2018. We observed two significant enhancement events during October, which have been attributed to dry-weather fungal spore release. This conclusion is reinforced with previous laboratory studies that demonstrate fluorescence spectra similar to those we observe. Our conclusions are also supported by previous off-line research suggesting a high abundance of spores in the region, and a close correlation between the enhancements we observe and significant drops in the relative humidity. This suggests changes in meteorological conditions can have strong effects on bioaerosol concentrations, with implications for human exposure. The following paper was published in MDPI Atmosphere.

atmosphere

MDPI

Article

The Observation and Characterisation of Fluorescent Bioaerosols Using Real-Time UV-LIF Spectrometry in Hong Kong from June to November 2018

Douglas Morrison [1,*], Jinjian Li [2], Ian Crawford [1], Wenwei Che [2], Michael Flynn [1], Man Nin Chan [3], Alexis K. H. Lau [2,4,5], Jimmy C. H. Fung [2,6], David Topping [1], Jianzhen Yu [2,7] and Martin Gallagher [1]

1 Department of Earth and Environmental Science, University of Manchester, Brunswick St, Manchester M13 9PS, UK; I.Crawford@manchester.ac.uk (I.C.); Michael.Flynn@manchester.ac.uk (M.F.); david.topping@manchester.ac.uk (D.T.); martin.gallagher@manchester.ac.uk (M.G.)
2 Division of Environment and Sustainability, Hong Kong University of Science and Technology, Clear Water Bay, Kowloon, Hong Kong, China; jlics@connect.ust.hk (J.L.); wenweiche@ust.hk (W.C.); alau@ust.hk (A.K.H.L.); majfung@ust.hk (J.C.H.F.); chjianyu@ust.hk (J.Y.)
3 Earth System Science Program, The Chinese University of Hong Kong, Hong Kong, China; mnchan@cuhk.edu.hk
4 Institute for the Environment, Hong Kong University of Science and Technology, Clear Water Bay, Kowloon, Hong Kong, China
5 Department of Civil and Environmental Engineering, Hong Kong University of Science and Technology, Clear Water Bay, Kowloon, Hong Kong, China
6 Department of Mathematics, Hong Kong University of Science and Technology, Clear Water Bay, Kowloon, Hong Kong, China
7 Department of Chemistry, Hong Kong University of Science and Technology, Clear Water Bay, Kowloon, Hong Kong, China
* Correspondence: douglas.morrison@manchester.ac.uk

Received: 17 July 2020; Accepted: 30 August 2020; Published: 4 September 2020

Abstract: Hong Kong is an area of complex topography, with mixtures of urban and greenbelt spaces. Local bioaerosol concentrations are multifaceted, depending on seasonal variations of meteorological conditions and emission sources. This study is the first known attempt at both quantitatively measuring and identifying airborne bioaerosol contributions, by utilising multiple single particle ultraviolet light-induced fluorescence spectrometers. Based in the Hong Kong University of Science and Technology's super-site, a WIBS-NEO and PLAIR Rapid-E were operated from June to November, 2018. The purpose of this long-term campaign was to observe the shift in wind patterns and meteorological conditions as the seasons changed, and to investigate how, or if, this impacted on the dispersion and concentrations of bioaerosols in the area. Bioaerosol concentrations based on the particle auto-fluorescence spectra remained low through the summer and autumn months, averaging 4.2 L^{-1} between June and October. Concentrations were greatest in October, peaking up to 23 L^{-1}. We argued that these concentrations were dominated by dry-weather fungal spores, as evidenced by their spectral profile and relationship with meteorological variables. We discuss potential bioaerosol source regions based on wind-sector cluster analysis and believe that this study paints a picture of bioaerosol emissions in an important region of the world.

Keywords: bioaerosol; UV-LIF spectrometry; fungal spores

1. Introduction

Hong Kong is a complex mixture of urban and greenbelt spaces. Although approximately 75% of the region is uninhabited rural land, Hong Kong is the 8th most densely packed city in the world, with a population of over 7 million people and an average of 6700 people per square kilometre (https://www.gov.hk/en/about/abouthk/factsheets/docs/population.pdf). Many studies focussed on poor air quality, with asthma rates and respiratory allergies increasing each year [1,2]. Pollutants linked to anthropogenic activities dominated these studies, as the region becomes both increasingly urbanised and subject to pollutants released from the Chinese mainland [3]. However, other particle types such as bioaerosols were disregarded in their relative importance. These are defined as biological particles emitted from a variety of biogenic sources, including soil, oceans, plants and animals [4]. Although they encompass a large number of potential particles, dominant bioaerosols in outdoor environments are often bacteria, pollen and fungal spores [5].

Hong Kong has a monsoon-influenced climate with a clear annual cycle. During winter, there is a prevailing Northeasterly wind that blows from across mainland China [6]. This period is associated with high levels of pollution and aerosol loading [7], significantly raising the rates of daily mortality [8,9]. During summer, the summer monsoon prevails, bringing warmer and more humid winds from across the South China Sea. These winds are cleaner relative to the winds from the north, and so pollution levels lower accordingly. This cycle also has implications for bioaerosol concentrations. Woo et al. [10] used filter collection methods at four meteorological stations across Hong Kong to examine the microbial mixture. They observed seasonal differences in air-mass trajectories as an important factor, with greater quantities of marine-derived phylotypes present during summer and betaproteobacterial phylotypes—typically found in soil—present during winter. Interestingly, they found no significant effect of urbanisation and population growth on airborne microbial communities. This is in contrast to Yan et al. [11], who examined the composition of fungal spores in Beijing during haze and non-haze days. They found positive correlations between certain fungal groups, PM2.5 and PM10, as well as meteorological factors like relative humidity. These findings were previously supported elsewhere, for example by Liu et al. [12].

Bioaerosol exposure is important to understand because of the potential ramifications it has for both human and ecological health. Common fungal genera such as *Aspergillus* act as known carcinogens and allergens, and are implicated in various respiratory illnesses [13]. High concentrations exacerbate asthma attacks, with one study inferring that *Alternaria* spore counts of 1000/m^3 more than doubled asthma deaths in Chicago [14]. Sensitivity to pollen is also a growing problem, with rates of physician-diagnosed hay fever amongst Chinese school children increasing from 2.9% to 4.1% in just seven years [15]. Whole pollen grains ranging in size from approximately 15–90 µm are the main driver of this condition, as they become deposited in the upper airways of the lungs. However, smaller pollen fragments are able to penetrate deeper, where they can act as a trigger for asthma. The fragmentation of pollen grains is driven in part by meteorological factors, with relative humidity being amongst the most influential. One study on Chinese elm by Miguel et al. [16] observed 70% of pollen grains rupturing after just 30 min of immersion in water. Pollen fragments are commonplace in the atmosphere, yet are not readily identifiable as pollen during microscopic analysis. Consequently, estimates of pollen concentrations and any subsequent respiratory issues are likely to be underestimates. Bioaerosols also affect the world's flora. *Hymenoscyphus fraxineus* is a fungus originating from East Asia that is now responsible for Ash dieback disease in Europe and presents a significant threat to forest health [17]. Caribbean coral reefs are thought to be adversely affected by the spores of *Aspergillus sydowii* [18], and many major crop yields are reduced from low level yet persistent crop diseases [19].

Ultraviolet light-induced fluorescence (UV-LIF) spectrometry is an emerging technology that enables real-time online sampling of bioaerosols. It is founded on the principle that biological particles fluoresce when excited with ultraviolet light, resulting from the presence of biofluorophores. UV-LIF spectrometers are designed to detect emitted light at wavelengths associated with specific biofluorophores, thus, enabling particle identification. This technique was used to provide

measurements in a range of environments, including a high altitude Alpine site, rainforests, Antarctica, Beijing, and more [20–23]. These studies were predominantly conducted using various models of the Wideband Integrated Bioaerosol Sensor (WIBS), which has three fluorescent channels to aid in particle identification. However, as the technology develops, advancements were made in the number of channels available, with the PLAIR Rapid-E offering 32 channels. While such an instrument is capable of offering significant amounts of particle information, it is relatively untested in real-world conditions. A detailed review on the status of UV-LIF spectrometry and bioaerosol research was previously written by Huffman et al. [24]. Our study aimed to utilise both the well-characterised WIBS and the highly advanced PLAIR Rapid-E to better understand Hong Kong's aerosol mixture and provide a comparison between their observations.

2. Materials and Methods

2.1. Site Description and Sampling Details

From June to November 2018, two UV-LIF instruments were continuously sampled inside the Hong Kong University of Science and Technology's (HKUST)' supersite, located on the eastern side of their campus (Latitude 22°19'56.8416" N, Longitude 114°16'1.1316" E). This site was built on a cliff facing Port Shelter and Silver Strand Bay, which is a suburban area with little residential or commercial development. The facility is composed of a weather-proof air-conditioned modular house of 80 m^2, which contains 10 sample inlets and an optical window for instrumentation, a 10 m high automatic weather station and an outdoor plinth area for 8 samplers. Sample inlets were approximately 1.5 m above the roof, with the inner diameters of pipes being approximately 2.8 cm. Humidity control systems including insulation tubing and a heating system were installed to the sampling lines, to avoid condensation. The air temperature inside the sampling lines was controlled within 34 to 36 °C through the heating system. The facility is used for a number of air quality monitoring projects, including those in collaboration with other institutions as well as the Hong Kong Environmental Protection Department (HKEPD).

The two bioaerosol instruments used in this study were the PLAIR Rapid-E and the WIBS-NEO, with each instrument connected to its own sample line. The PLAIR Rapid-E used a top hat type inlet with no upper particle size selection limit, while the WIBS-NEO sampled through a PM10 head. Details for each instrument can be found in Section 2.2. Both sample lines ran with additional flow to reduce the inlet transit time and to operate the PM10 head at the correct flow rate. Each instrument was calibrated approximately every two weeks, using NIST traceable glass beads and fluorescent glass particles of varying sizes (1, 2, and 4 μm) with the flow rates also monitored and maintained. The total flow of the sampling lines and flows of the two bioaerosol sensors were monitored and calibrated by the Brooks SHO-RATE Flowmeter and Gilibrator, respectively. Relative humidity and temperature were also recorded every minute at the same sampling site for the length of the campaign.

2.2. Instrumentation

The PLAIR Rapid-E could detect particles in a size range of 0.5–100 μm, allowing it to more effectively detect larger pollen grains and plant fragments than previous UV-LIF instrument designs [25]. Another advantage of the PLAIR Rapid-E was its high sample volume, sampling at ~3 L min^{-1} to improve counting statistics for coarse particle sizes. It utilised a 337 nm gas laser to excite particles and offered 32 resolution channels that were able to detect emitted wavelengths from 350–800 nm. The PLAIR Rapid-E also measured the light scattered by a particle from 24 angles, in real time to approximate its shape. The rate of fluorescence decay was also recorded, further enabling identification of the protein-bearing particles. Particles between 0.5–5 μm were only detected during activation of the instrument's 'high-intensity mode'. Given the long-term nature of our monitoring campaign and a wish to preserve the strength of the laser, this mode was not employed. The results presented below were consequently only used for particles 5 μm and above.

The WIBS-NEO is a three channel UV-LIF spectrometer similar in design to various models of the WIBS-4 [24,26]. Each particle entering the instrument scattered light from a red 635 nm laser diode. The side-scattered light was collected by two high numerical-aperture chamber mirrors, passed through an aperture in one of the mirrors and onto a dichroic beam-splitter, before being detected by the FL2 (second fluorescence) channel photomultiplier tube (PMT). The scattered intensity was used to size the particles (in the range 0.5 to nominally 30 µm optical diameter) and subsequently trigger two filtered UV excitation flash lamps at 280 nm (Xe1) and 370 nm (Xe2), in succession. The scattering intensity was also recorded across a quadrature PMT and the standard deviation of the 4 scattering intensities were used to provide a measure of the particle asphericity (Asphericity Factor, AF). The detector system was timed to detect the 310–400 nm emission response (De1), followed by the 420–650 nm emission response (De2), following each respective excitation. In this study, we only focused on data from the Xe2/De1 bands, due to detector saturation.

2.3. Data Analysis

Some non-biological particles such as sea salt and mineral dust are capable of weakly fluorescing, potentially being recorded by UV-LIF instruments as false positives and skewing our observations. As such, a conservative 9 sigma threshold was used when setting the baseline for each channel of the WIBS-NEO. This was derived by the instrument recording the average background fluorescence in the absence of any particles, during what is known as the 'Forced Trigger' mode. A particle's fluorescence must exceed 9 standard deviations of this value to be classified as fluorescent [27]. This was an effective way of removing interferents from our observations, while preserving the majority of 'true' bioaerosols [28]. The mechanisms of the WIBS-NEO was described in detail by Forde et al. [27]. For the PLAIR Rapid-E, a fluorescence baseline of 1500 arbitrary units (a.u.) was applied to each channel with the negative values capped at zero. This represented an arbitrary but conservative threshold. When applied, concentrations of fluorescent particles showed good agreement with those detected by the WIBS-NEO. As such, all fluorescent particles observed should contain biological material. De1 and De2 detector baseline shifts were carefully monitored and corrected for, but as such shifts might have adversely affected Fl1 and Fl3 data consistency, we focused on the Fl2 channel for this study. Single-channel instruments such as the UV-APS were successfully used in the past to detect fluorophores indicative of bacteria and other bioaerosols [29]. Deeper analysis was performed using data from the PLAIR Rapid-E, the results of which are described further below.

Particle concentrations were also considered as a function of back trajectory. One hundred and twenty hour-long back trajectories with a starting height of 10 m above ground level (approximately 20 m above sea level), using NOAA's Hysplit merged with the Openair package [30] were calculated from the sampling site for the length of the monitoring campaign. These trajectories were run every 3 h across the whole campaign, using monthly meteorological data files downloaded from NOAA. The back trajectories were averaged into a number of distinct pathways known as 'wind clusters'. A 6-cluster solution was used, revealing a range of sources with a mixture of terrestrial and marine influences.

3. Results

3.1. Campaign Observations

Particle concentrations across the length of the campaign are shown in Figure 1. They were lowest in August, began to increase in September and peaked at the start of October. This level was not sustained during the month, however, with concentrations falling before rising sharply again around the start of November. Concentrations were therefore highly variable, but generally highest from October onwards. From 5th July to 1st October, the mean concentration of particles greater than 5 µm recorded by the PLAIR Rapid-E was 4.2 ± 3.4 L^{-1}. The periods of enhancement observed during October peaked as high as 23 L^{-1}.

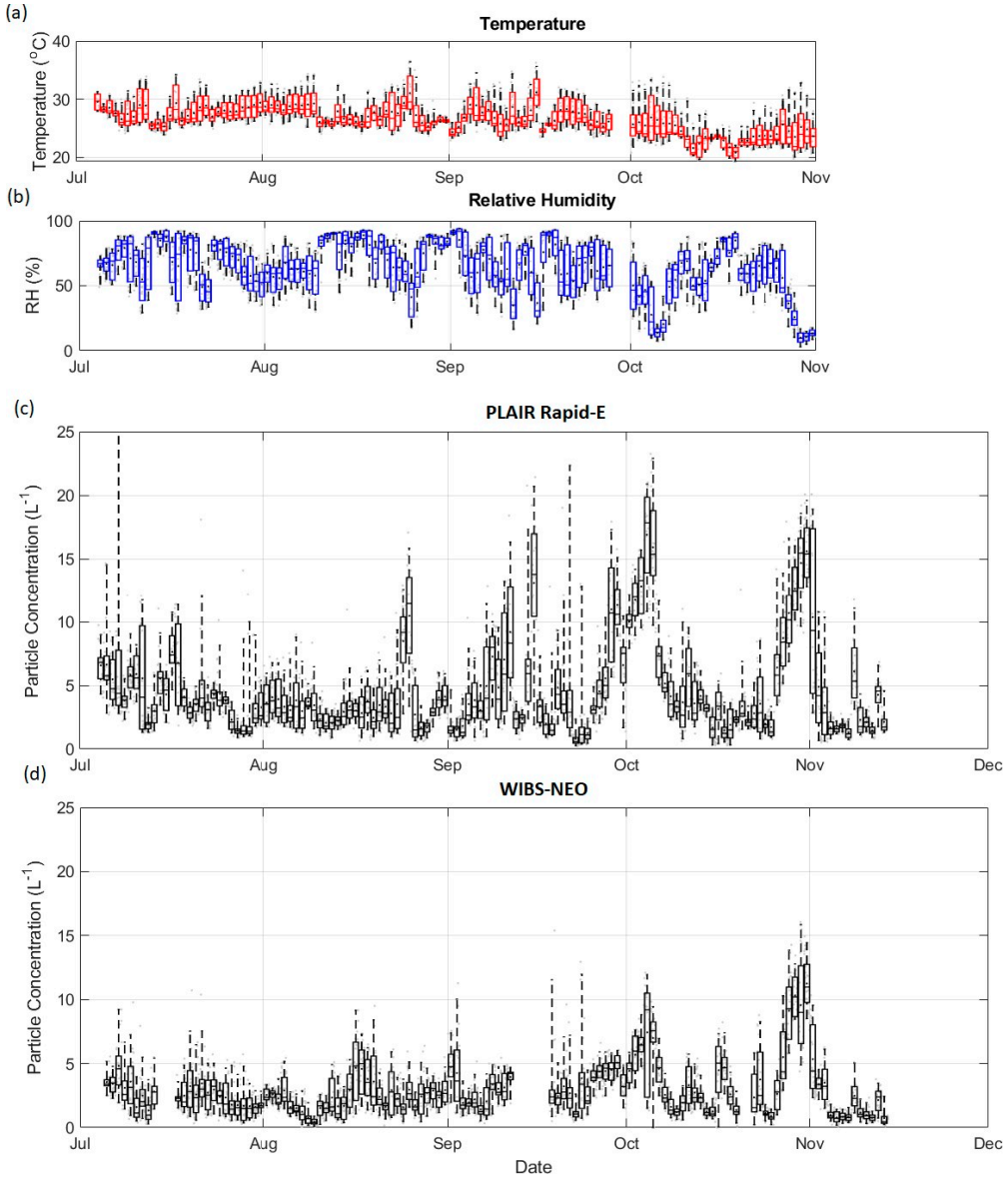

Figure 1. Time-series of the concentration of biofluorescent particles (L^{-1}) from 5th July to 14th November, as measured by the PLAIR Rapid-E and WIBS-NEO, shown in panels (**c**,**d**) respectively. Particles ≥ 5 µm were included for the PLAIR Rapid-E, while the WIBS-NEO recorded particles of 0.5–30 µm. Temperature and relative humidity from 5th July to 1st November are also shown in panels (**a**,**b**) respectively, recorded at the same sampling site. Whiskers represent 5th and 95th percentile values and the width of each box represents one day. Median values are denoted by a horizontal line and mean values by the black dot. Grey dots represent hourly averages.

Similar trends were recorded by the WIBS-NEO. Peaks in biofluorescent concentrations at the beginning and end of October were observed again, although these periods of enhancement were less pronounced when compared to the PLAIR Rapid-E. It was a consequence of the WIBS-NEO recording down to a smaller size range that was responsible for the significantly higher concentrations of biofluorescent particles, when compared to the PLAIR Rapid-E. For the WIBS-NEO, the mean concentration from 5th July to 1st October was 20.6 ± 9.1 L^{-1}. Two peaks were seen at the start of October and November, both exceeding 60 L^{-1}.

The average relative humidity was lower from 1st October onwards than for the previous months, as shown in Figure 2. Two exceptionally low periods at the beginning and end of October were responsible for these averages. Both dry periods were sustained across multiple days with hourly

average values as low as 9%. For both temperature and relative humidity, there was also a greater degree of diurnal variability from October onwards. From 5th July–1st October, diurnal temperatures ranged from 26–29 °C, while for the period from 1st October, values ranged from 22–28 °C. The diurnal pattern for relative humidity was similar across both periods, with the daily minimum occurred at approximately 12:00. However, the minimum diurnal value from 5th July–1st October was higher than the maximum diurnal value seen from 1st October onwards.

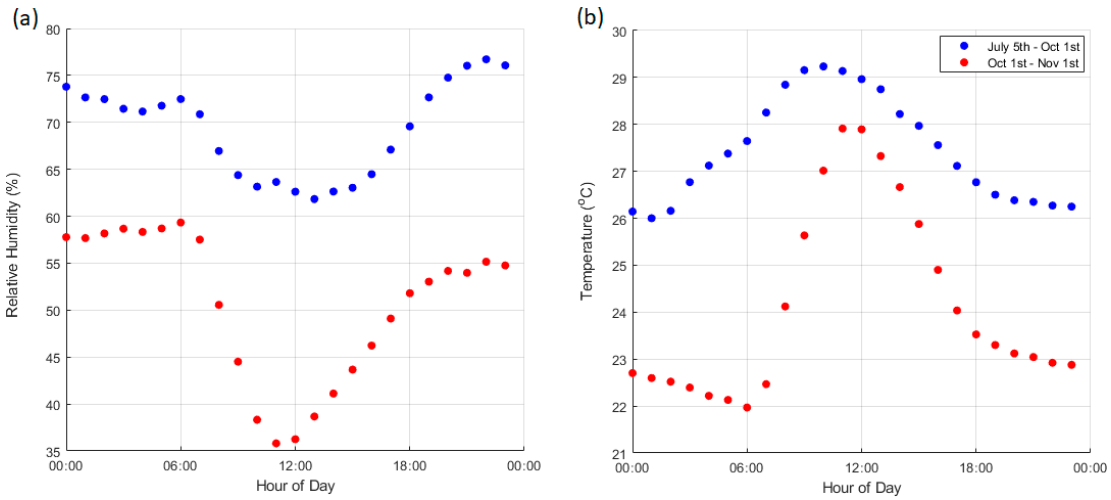

Figure 2. Average diurnal patterns for relative humidity (**a**) and temperature (**b**) recorded at the sampling site. Averages are taken for two periods, with 5th July–1st October shown in blue and 1st October onwards shown in red.

3.2. Biofluorescent Particle Properties

Differences appeared in the sizing of particles between instruments, with the PLAIR Rapid-E skewing towards larger particles. This trend also appeared in the calibration data, suggesting it is a consequence of differences in the method through which the size information was derived by each instrument (see Supplementary Materials). The WIBS-NEO uses standard Mie scattering approximations for sizing, and these were consistent with routine calibrations performed using NIST traceable calibration particles. The PLAIR Rapid-E utilises geometrical optics for particles above 5 µm, while using Mie scattering for particles 0.5–5 µm.

When comparing the size distribution of biofluorescent particles from 1st October (where significant enhancements in concentrations were observed) to the preceding summer months, some differences could be seen. Figure 3 shows that from 1st October onwards, the PLAIR Rapid-E detected a relative increase in particles ~8 µm and up. The WIBS-NEO also captured this trend, but the inclusion of sub-5 µm highlighted an interesting pattern. For the period beginning 1st October, the WIBS-NEO observed a peak in the size distribution at a smaller size than in the previous months (~3 µm from 1st October compared to 4 µm, previously). As such, the period associated with enhanced concentrations displayed a greater range in the size distribution for biofluorescent particles.

The spectral profile of particles excited by the PLAIR Rapid-E was largely consistent across the entire campaign. It can be seen in Figure 4 that fluorescent activity was predominantly recorded in channels five and six, which covered the emission band 406–434 nm and reflected a narrow peak with little to no shoulder. Fluorescence intensity in either channel was not correlated with particle size (R^2 = 0.15 and 0.16).

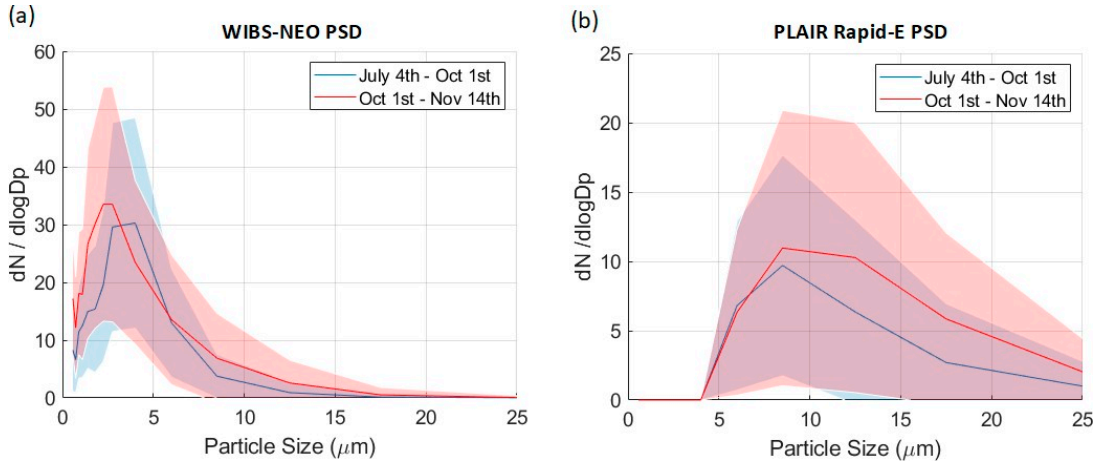

Figure 3. Biofluorescent particle size distribution (dN/dlogDp (L^{-1}) for the WIBS-NEO (**a**) and PLAIR Rapid-E (**b**) for two periods (see text). Blue line—average for the period of 4th July–1st October; red line—average for the period 1st October–14th November. *x*-axis values represent the average size of the bins used. Shaded areas represent ± 1 standard deviation.

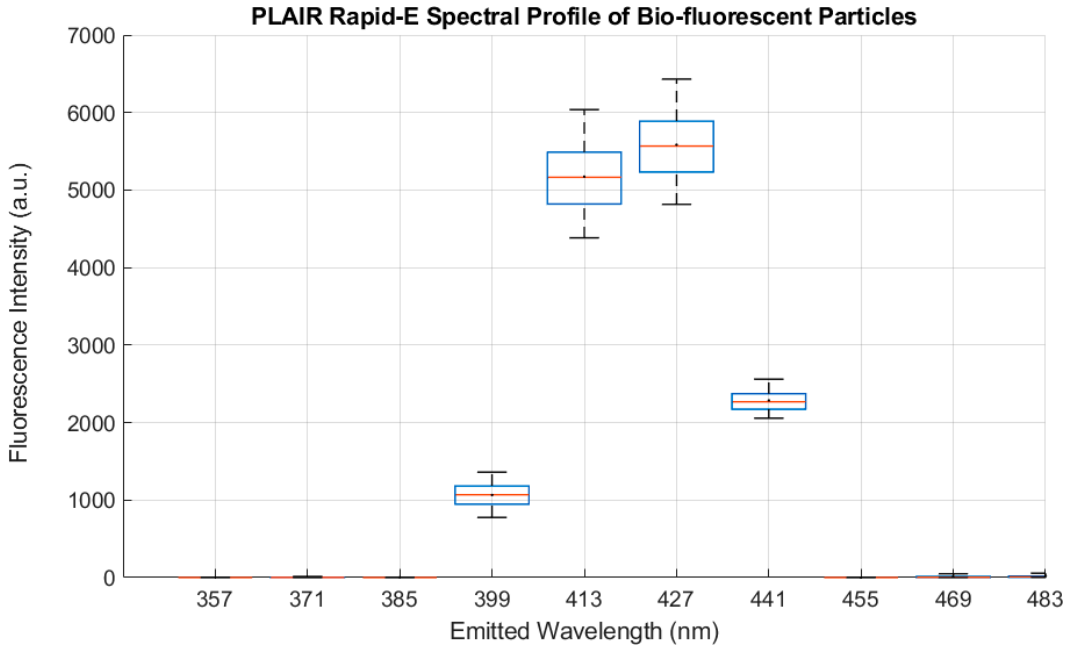

Figure 4. Fluorescence intensity recorded across the PLAIR Rapid-E's first 10 detection channels for all biofluorescent particles. The *x*-axis shows the peak wavelength (nm) associated with each channel, with the width of each box reflecting the 14 nm range of the associated channel. Each red line represents the median value with the mean denoted by a dot. Whiskers represent 5th and 95th percentile values.

3.3. Back Trajectory Analysis

As discussed in Section 2.3, a 6 cluster solution was used to calculate back trajectories that dominated during the length of our campaign. These different clusters can be seen in Figure 5, with a mixture of terrestrial and oceanic influences.

Wind cluster 1 had the most influence from the mainland and was also associated with the highest fluorescent particle concentrations, as shown in Figure 6. Both instruments broadly captured similar diurnal patterns (as shown in Figure 7), although this was more pronounced for the PLAIR Rapid-E, with cluster 1 typically showing higher concentrations during the day. For the WIBS-NEO in October, peak concentrations in cluster 1 appeared from 09:00 and maintained a high level throughout the day,

falling slightly in the evening, before rising again at 21:00. It could be seen that not every wind cluster was present each month, with cluster 1 only appearing from September and cluster 2 also being absent during August. Clusters 3–6 regularly appeared from July-September (with the exception of cluster 5 in July), but all were absent during October and November. The effective diameter (also known as the weighted mean diameter) of biofluorescent particles detected by both UV-LIF instruments also changed as a function of wind cluster. As such, wind cluster 1 was not only associated with higher bioaerosol concentrations, but also with larger particles. This change was particularly pronounced for the WIBS-NEO.

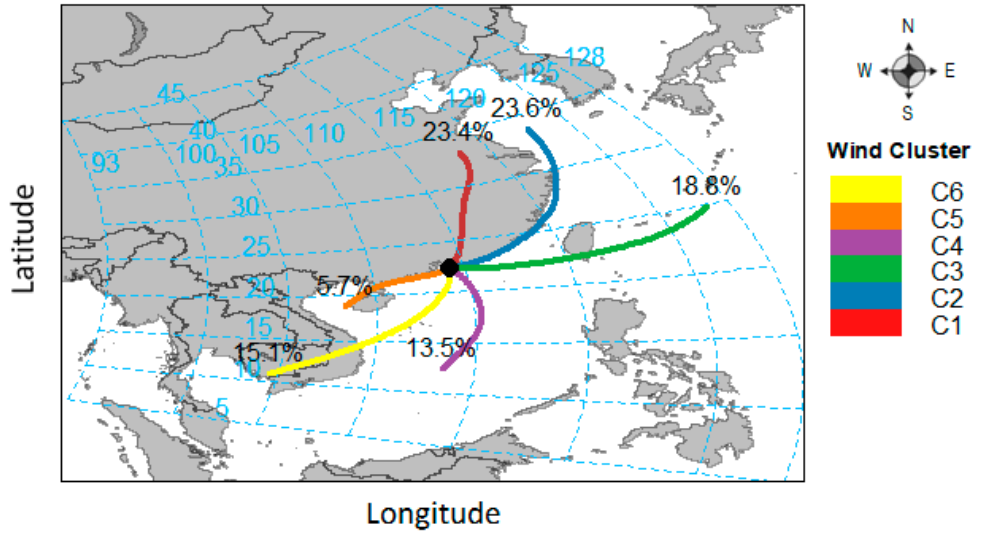

Figure 5. A 6 cluster solution when performing cluster analysis on all back trajectories from 3rd July to 14th November, using NOAA's Hysplit, merged with the Openair package. Each trajectory represents 120 h and start from a height of 10 m above ground level.

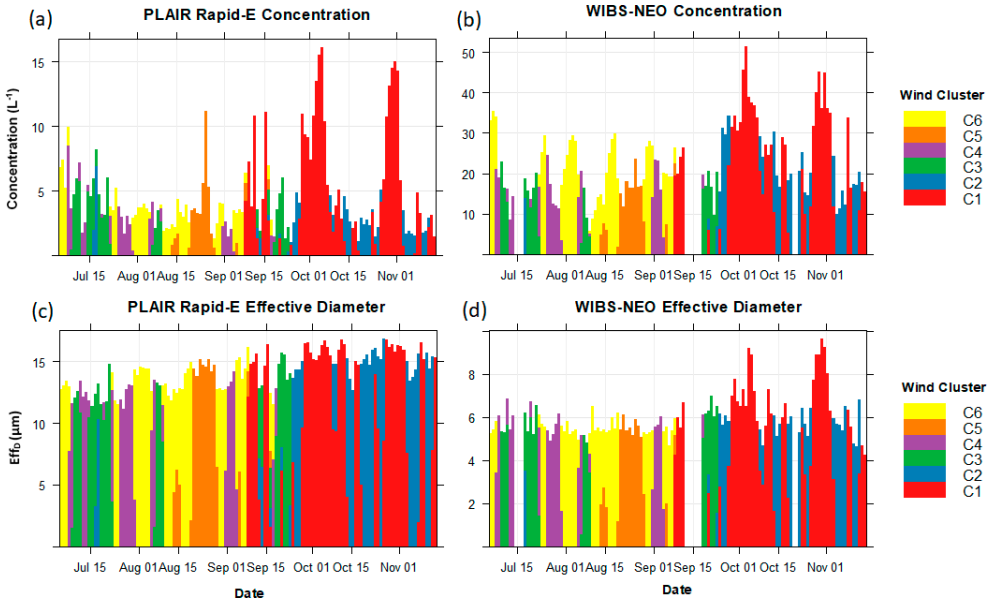

Figure 6. Average daily concentrations (L^{-1}) and effective diameter (µm) of particles detected by both the PLAIR Rapid-E and WIBS-NEO, as a function of wind cluster. Panels (**a**) and (**b**) represent PLAIR Rapid-E and WIBS-NEO concentrations, respectively. Panels (**c**) and (**d**) represent PLAIR Rapid-E and WIBS-NEO Effective Diameter, respectively. Concentrations recorded by the WIBS-NEO are for particles across the instrument's entire size range (0.5–30 µm).

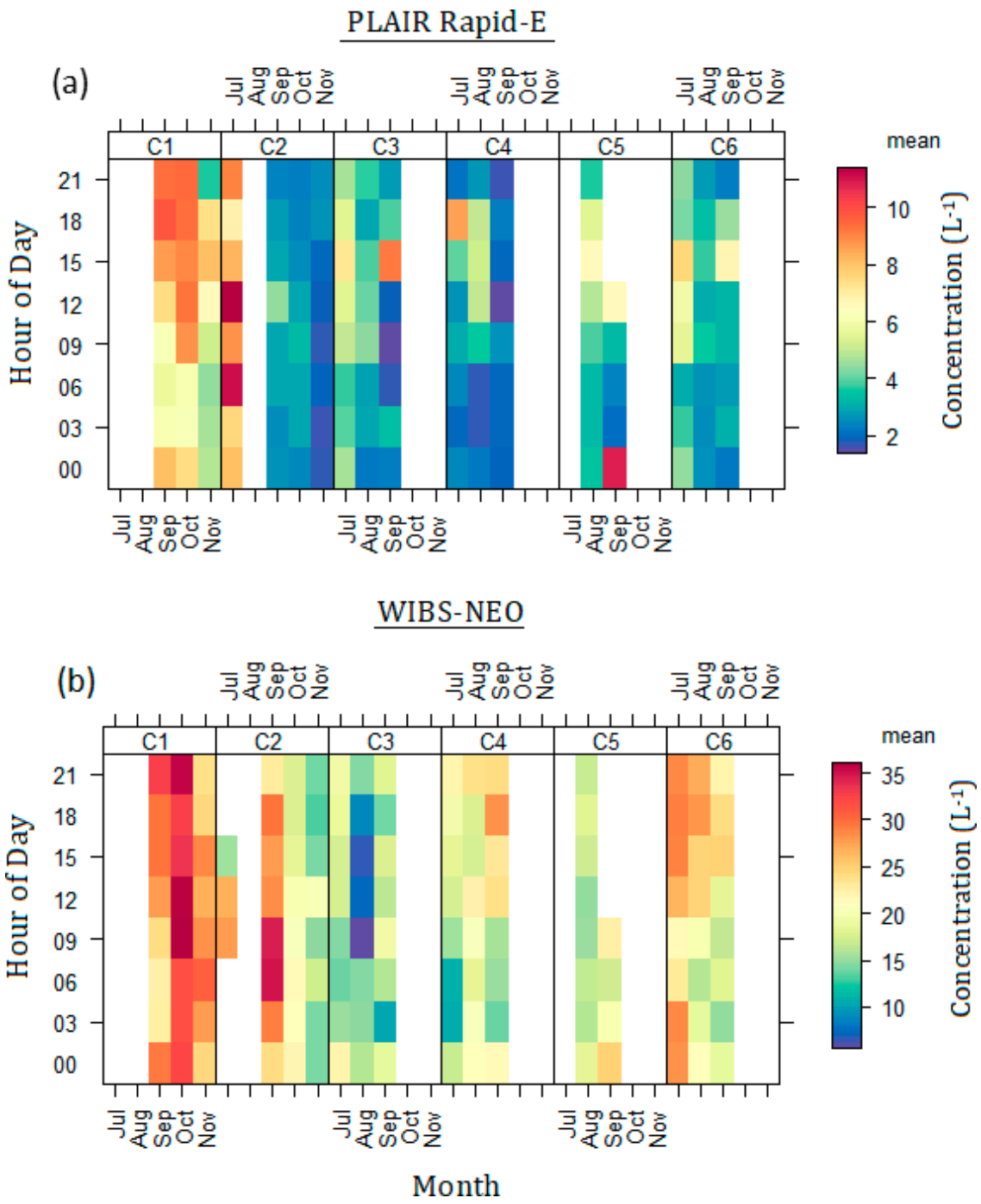

Figure 7. Mean concentrations (L^{-1}) of biofluorescent particles as a function of wind cluster, split by month and hour of day. Concentrations are for particles ≥5 µm for the PLAIR Rapid-E and ≥0.5 µm for the WIBS-NEO. Concentrations as a function of cluster are calculated in three-hour intervals. Panel (**a**) represents the PLAIR Rapid-E and panel (**b**) represents the WIBS-NEO.

It can be seen in Figure 8 that periods of exceptionally low relative humidity were almost exclusively associated with wind cluster 1 and typically contained much higher particle concentrations. For biofluorescent particles recorded by the PLAIR Rapid-E, we noted an R^2 value of 0.40 ($p \leq 0.001$) with relative humidity from July to October. This negative relationship was strengthened to 0.60 from 1st October onwards, with both peaks coinciding with the lowest relative humidity observed (see Supplementary Materials).

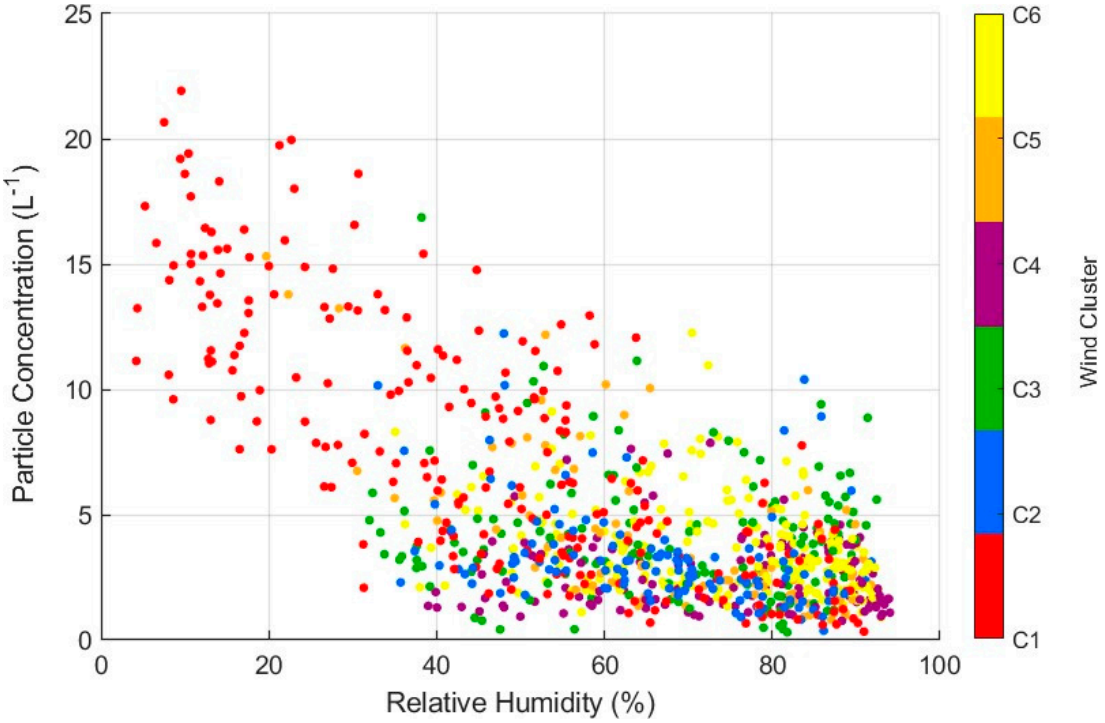

Figure 8. PLAIR Rapid-E particle concentrations (L^{-1}) as a function of relative humidity. The colourbar represents the wind cluster that was dominant at the time of recording. Data points represent three-hour averages across the entire campaign.

4. Discussion

The biofluorescent particle concentrations we observed appeared to be low, when compared to previous studies for other major cities. Yue et al. [23], used a WIBS-4 in Beijing and observed more than an order of magnitude increase in biofluorescent particles greater than 0.8 μm, with an average concentration across their sampling period of 642 ± 297 L^{-1}. The lower level at HKUST could be explained by dominant marine air masses at this coastal suburban site.

The specificity of a fluorophore's excitation and emission bands helped to inform particle identification. Our model of the PLAIR Rapid-E used a gas laser that excited at 337 nm, and we observed the greatest fluorescent response in channels five and six (406–434 nm). Channel 2 of the WIBS-NEO excited particles with 370 nm light and used a detection plate sensitive to 310–400 nm. Although there was no perfect overlap between these instruments, they were both close to the excitation/emission bands commonly associated with NADH [31]. Other possible fluorophores at these wavelengths included sporopollenin (a biopolymer found in the outer coating of pollen grains and plant spores), DNA, phenols, and terpenoids [32,33].

Previous literature attempted to characterise bioaerosols in Hong Kong, but there were some instrumental limitations in our ability to replicate their findings. For example, Woo et al. [10] found many marine-derived phylotypes during summer, with *Chlorophyta* dominating their samples. These are a taxon of green algae, for which previous literature suggests Chlorophyll-∝ as the dominant fluorophore [34]. Neither the PLAIR Rapid-E nor the WIBS-NEO are suited to algal identification because Chlorophyll-∝ has a much higher excitation wavelength of 400–485 nm [35]. Although Xe2 of the WIBS-Neo was close to the lower end of this excitation band, the emitted wavelengths were higher than the instrument's detection range, at 685 nm. As such, our instruments would register any airborne concentrations of *Chlorophyta* as non-fluorescent particles and would overlook them during analysis.

There is strong evidence to suggest that the bioaerosol concentrations we observe are predominantly fungal spores. Turner et al. [36] previously made detailed observations of the fungal genera in Hong Kong and how they vary by season, with manual off-line microscopical analysis. Dominant genera

include *Cladosporium*, *Aspergillus*, *Penicillium*, and *Aureobasidium*, which together accounted for 65.7% of isolates seen across an entire year. Among these, *Cladosporium* was the most prevalent. Although a hugely variable and broad genus, many *Cladosporium* spp. are 'dry-weather spores', noted for their negative correlation with relative humidity [37,38] and therefore demonstrate a good agreement with our observations. The observed diurnal pattern in concentrations also support this conclusion, with previous studies finding peaks in *Cladosporium* counts, at similar times [39], although this appeared to be highly variable, possibly depending on the region [40,41]. *Cladosporium* spores were previously shown to fluoresce at similar wavelengths to the channels in which we observed activity. O'Connor et al. [42] excited two Cladosporium spp. with 370 nm light and observed clear peaks at ~415 nm. Furthermore, exciting the spores with 350 nm light produced almost identical results, suggesting that the 337 nm laser used in the PLAIR Rapid-E might be sufficient. They observed similar spectral profiles in other fungal spores, including *Alternaria*, *Penicillium*, and *Aspergillus*.

Pollen was considered, but did not sufficiently explain our observations. This was despite our instruments detecting fluorescent activity that is potentially indicative of sporopollenin. Hong Kong has two pollen seasons occurring in spring and autumn, neither of which coincide with the enhancements we observed. Furthermore, the spectral signal of pollen is expected to be broader as more channels becoming activated. O'Connor et al. [42] observed three peaks at 420 nm, 465 nm, and 560 nm in *Betulaceae* samples, while grass pollen had an additional peak at 675 nm. It was surprising that we did not see evidence of pollen's presence during our campaign. Concentrations of particles greater than 5 µm remained very low during the summer months, averaging ~3 L^{-1}. It was possible our sampling site was not suitable for capturing pollen, given the close proximity to the sea. As the back trajectories all cross the South China Sea during the months when the pollen levels are expected to be greatest, there is little opportunity for the collection and transport of pollen grains before reaching our sampling site. Fragmentation of pollen grains also remains an issue for detection, with previous studies suggesting an association between biofluorescent fragment concentrations and rain or thunderstorms [16,43].

Bacteria are not thought to be the dominant bioaerosol, despite the fluorophore we likely observed—NADH—being prevalent in bacteria (hence, it is usually used as an indicator of bacterial metabolic activity) [44]. NADH is ubiquitous amongst other bioaerosols, however, its presence alone is not enough for the identification of bacteria. Our conclusions were also in contrast to the observations made by Woo et al. [10], who highlight increased concentrations of soil bacteria during winter, with northerly trajectories carrying soil particles through Aeolian processes. However, the northerly wind clusters associated with higher particle concentrations only show this trend when other conditions are met. When relative humidity is moderate or high, particle concentrations from wind clusters one and two are no different from the concentrations seen in clusters 3–6. As our observations clearly capture the importance of dry periods in driving particle enhancements, and as previous studies found no correlation between bacterial concentrations and relative humidity [45], it is likely that we are observing something else. As previously discussed, past studies confirmed the presence of fungal spores in the region, for which many species are 'dry-weather'. We would expect these fungal spores to also fluoresce in the channels we see activity in. We also argue that because the dry periods are associated with northerly trajectories, this artificially inflates the importance of wind trajectory. We find little evidence that northerly trajectories are carrying particles from new source regions, and it is instead possible that associated meteorological conditions drive bioaerosol release from more local sources. It should be noted here that the two driest periods we observed were exceptional, even for northerly winds. Hong Kong's dry period typically began in November and extended through to February. As such, the first dry period we observed at the beginning of October was unusually early. Furthermore, values for relative humidity did not normally fall as low as we recorded. From 1981–2010, Hong Kong's mean relative humidity during October was 73% (https://www.hko.gov.hk/en/cis/normal/1981_2010/normals.htm), while in 2018 it was 51%. As such, although these conditions clearly enhanced the concentrations of certain bioaerosols, we believe enhancement events such as these would be relatively infrequent.

We acknowledge that the average size of particles detected by the PLAIR Rapid-E was large for fungal spores. Previous studies suggest that *Cladosporium herbarum* spores average around 3 μm [27]. However, these studies were done using different UV-LIF spectrometers to the PLAIR Rapid-E, for which our calibration data suggest that there is a difference in its particle sizing. As such, it is possible many of the fungal spores recorded by the PLAIR Rapid-E would register as smaller if sampled by a different instrument. When looking at particle concentrations across the entire size range of the WIBS-NEO, a peak could be seen for sizes similar to previous studies on fungal spores [27]. Furthermore, *Cladosporium* spp. were highly variable and data on the exact species present in Hong Kong is limited. Consequently, it is also possible that the spores in this region were larger than those used in previous laboratory experiments.

5. Conclusions

This was the first study to quantify bioaerosol concentrations in Hong Kong using the UV-LIF technology. The long-term nature of this campaign enabled us to observe how these concentrations might also change, depending on the season. From 5th July to 1st October, the PLAIR Rapid-E recorded average concentrations of particles greater than 5 μm equal to 4.2 ± 3.4 L^{-1}, while the WIBS-NEO detected 20.6 ± 9.1 L^{-1} for particles greater than 0.5 μm. Two significant peaks were seen during October by both instruments, exceeding 23 L^{-1} in the PLAIR Rapid-E and 60 L^{-1} in the WIBS-NEO. Previous literature suggest that wind trajectories are the dominant influence on bioaerosols in Hong Kong. Southerly winds were attributed with enhanced levels of algae, while northerly trajectories were argued to transport soil bacteria from the mainland. By contrast, we observed relative humidity as the most influential factor, with low levels likely initiating spore release from dry-weather fungi, such as *Cladosporium*.

Such fungi were shown to share similar spectral profiles to the particles we observed and dominated Hong Kong spore counts in previous studies. Spore release for such genera was shown to occur during the day, showing further agreement with our observations. Two prolonged periods of low relative humidity were associated with exceptionally high bioaerosol concentrations, which were possibly indicative of spore showers. Both dry periods were also associated with northerly trajectories, potentially inflating the importance of wind trajectory. We did not find strong evidence that northerly trajectories carry fungal spores from new source regions, but rather the associated meteorological conditions might drive spore release from more local sources. Future work should attempt to use UV-LIF spectrometers of higher excitation wavelengths, with the aim of capturing a different subsection of the bioaerosols present in the region. Since the current measurement site has a close proximity to the South China Sea, the observations in our study during summer months when marine air masses dominate, probably reflect a relatively lower range of bioaerosol concentrations in Hong Kong. It would also be interesting to investigate the long-term variations of bioaerosol concentration and composition in different terrain and land-use situations, to further elucidate the spatio-temporal characteristics of fluorescent bioaerosols in Hong Kong.

Supplementary Materials: The following are available online at http://www.mdpi.com/2073-4433/11/9/944/s1, Figure S1: Time series of the thresholding applied to the three channels of the WIBS-NEO over the course of the campaign. Due to drift in channels 1 and 3, only particles that fluoresced in channel 2 were included in the analysis. Figure S2: Size distribution of NIST traceable calibration particles as recorded by the PLAIR Rapid-E. As 4 μm particles were predominantly used it is clear the instrument is oversizing when compared to the WIBS-NEO. Figure S3: Size distribution of NIST traceable calibration particles as recorded by the WIBS-NEO. As 4 μm particles were predominantly used it is clear the instrument is accurately sizing the calibration particles. Figure S4: WIBS-NEO particle concentrations (L-1) as a function of relative humidity. The colourbar represents which wind cluster was dominant at the time of recording. Data points represent three-hour averages across the entire campaign.

Author Contributions: D.M. is the primary author and responsible for most of the analysis across both instruments. J.L. monitored both instruments for the length of the campaign and was responsible for regularly calibrating them. I.C. pre-processed all data and provided guidance on both analysis and written components. M.F. was responsible for setting up the instruments at the sampling site with the appropriate experimental design. M.N.C. assisted in

organising and cross-project funding. D.T. and M.G. acted as supervisors to D.M., having secured funding for the project and forming the collaboration with HKUST. W.C. is the co-investigator of this research project, responsible for instrument operation and data acquisition. A.K.H.L., J.C.H.F. and J.Y. supervised the research project in design and discussion. All authors have read and agreed to the published version of the manuscript.

Funding: This research was funded by a collaborative project between HKUST and the University of Manchester. The project focussed on building a collaborative framework for improved understanding of airborne biological particles (UOM173). D.M. is a PhD student who has received funding from NERC and is a member of the Doctoral Training Partnership (DTP).

Acknowledgments: We would like to thank K.S. and N.S. at Droplet Measurement Technologies (DMT) for their loan of the WIBS-NEO during this campaign.

Conflicts of Interest: The authors declare no conflict of interest and the funders had no role in the design of the study; in the collection, analyses, or interpretation of data; in the writing of the manuscript, or in the decision to publish the results.

References

1. Leung, R.; Wong, G.; Lau, J.; Ho, A.; Chan, J.; Choy, D.; Douglass, C.; Lai, C. Prevalence of asthma and allergy in Hong Kong schoolchildren: An ISAAC study. *Eur. Respir. J.* **1997**, *10*, 354–360. [CrossRef] [PubMed]
2. Yang, Y.; Tang, R.; Qiu, H.; Lai, P.C.; Wong, P.; Thach, T.Q.; Allen, R.; Brauer, M.; Tian, L.; Barratt, B. Long term exposure to air pollution and mortality in an elderly cohort in Hong Kong. *Environ. Int.* **2018**, *117*, 99–106. [CrossRef] [PubMed]
3. Cao, J.J.; Shen, Z.X.; Chow, J.C.; Watson, J.G.; Lee, S.C.; Tie, X.X.; Ho, K.F.; Wang, G.H.; Han, Y.M. Winter and summer PM2.5 chemical compositions in fourteen Chinese cities. *J. Air Waste Manag. Assoc.* **2012**, *62*, 1214–1226. [CrossRef] [PubMed]
4. Després, V.; Huffman, J.A.; Burrows, S.M.; Hoose, C.; Safatov, A.; Buryak, G.; Fröhlich-Nowoisky, J.; Elbert, W.; Andreae, M.; Pöschl, U.; et al. Primary biological aerosol particles in the atmosphere: A review. *Tellus B Chem. Phys. Meteorol.* **2012**, *64*, 15598. [CrossRef]
5. Jones, A.M.; Harrison, R.M. The effects of meteorological factors on atmospheric bioaerosol concentrations—A review. *Sci. Total Environ.* **2004**, *326*, 151–180. [CrossRef]
6. Yan, Y.Y. Surface wind characteristics and variability in Hong Kong. *Weather* **2007**, *62*, 312–316. [CrossRef]
7. Shi, W.; Wong, M.S.; Wang, J.; Zhao, Y. Analysis of airborne particulate matter (PM2.5) over Hong Kong using remote sensing and GIS. *Sensors* **2012**, *12*, 6825–6836. [CrossRef]
8. Wong, C.M.; Ma, S.; Hedley, A.J.; Lam, T.H. Effect of air pollution on daily mortality in Hong Kong. *Environ. Health Perspect.* **2001**, *109*, 335–340. [CrossRef]
9. Qian, Z.; Lin, H.M.; Stewart, W.F.; Kong, L.; Xu, F.; Zhou, D.; Zhu, Z.; Liang, S.; Chen, W.; Shah, N.; et al. Seasonal pattern of the acute mortality effects of air pollution. *J. Air Waste Manag. Assoc.* **2010**, *60*, 481–488. [CrossRef]
10. Woo, A.C.; Brar, M.S.; Chan, Y.; Lau, M.C.; Leung, F.C.; Scott, J.A.; Vrijmoed, L.L.; Zawar-Reza, P.; Pointing, S.B. Temporal variation in airborne microbial populations and microbially-derived allergens in a tropical urban landscape. *Atmos. Environ.* **2013**, *74*, 291–300. [CrossRef]
11. Yan, D.; Zhang, T.; Su, J.; Zhao, L.L.; Wang, H.; Fang, X.M.; Zhang, Y.Q.; Liu, H.Y.; Yu, L.Y. Diversity and composition of airborne fungal community associated with particulate matters in Beijing during haze and non-haze days. *Front. Microbiol.* **2016**, *7*, 487. [CrossRef] [PubMed]
12. Liu, Z.; Li, A.; Hu, Z.; Sun, H. Study on the potential relationships between indoor culturable fungi, particle load and children respiratory health in Xi'an, China. *Build. Environ.* **2014**, *80*, 105–114. [CrossRef]
13. Richardson, M.; Bowyer, P.; Sabino, R. The human lung and Aspergillus: You are what you breathe in? *Med. Mycol.* **2019**, *57*, S145–S154. [CrossRef] [PubMed]
14. Targonski, P.V.; Persky, V.W.; Ramekrishnan, V. Effect of environmental molds on risk of death from asthma during the pollen season. *J. Allergy Clin. Immunol.* **1995**, *95*, 955–961. [CrossRef]
15. Wang, H.; Zheng, J.; Zhong, N. Time trends in the prevalence of asthma and allergic diseases over 7 years among adolescents in Guangzhou city. *Zhonghua Yi Xue Za Zhi* **2006**, *86*, 1014–1020.
16. Miguel, A.G.; Taylor, P.E.; House, J.; Glovsky, M.M.; Flagan, R.C. Meteorological influences on respirable fragment release from Chinese elm pollen. *Aerosol Sci. Technol.* **2006**, *40*, 690–696. [CrossRef]

17. Stocks, J.J.; Buggs, R.J.; Lee, S.J. A first assessment of Fraxinus excelsior (common ash) susceptibility to *Hymenoscyphus fraxineus* (ash dieback) throughout the British Isles. *Sci. Rep.* **2017**, *7*, 1–7. [CrossRef]
18. Rypien, K.L. African dust is an unlikely source of *Aspergillus sydowii*, the causative agent of sea fan disease. *Mar. Ecol. Prog. Ser.* **2008**, *367*, 125–131. [CrossRef]
19. Fisher, M.C.; Henk, D.A.; Briggs, C.J.; Brownstein, J.S.; Madoff, L.C.; McCraw, S.L.; Gurr, S.J. Emerging fungal threats to animal, plant and ecosystem health. *Nature* **2012**, *484*, 186–194. [CrossRef]
20. Crawford, I.; Lloyd, G.; Herrmann, E.; Hoyle, C.; Bower, K.; Connolly, P.; Flynn, M.; Kaye, P.; Choularton, T.; Gallagher, M. Observations of fluorescent aerosol-cloud interactions in the free troposphere at the High-Altitude Research Station Jungfraujoch. *Atmos. Chem. Phys.* **2016**, *16*, 2273–2284. [CrossRef]
21. Gabey, A.; Stanley, W.; Gallagher, M.; Kaye, P.H. The fluorescence properties of aerosol larger than 0.8 mu m in urban and tropical rainforest locations. *Atmos. Chem. Phys.* **2011**, *11*, 5491–5504. [CrossRef]
22. Crawford, I.; Gallagher, M.W.; Bower, K.N.; Choularton, T.W.; Flynn, M.J.; Ruske, S.; Listowski, C.; Brough, N.; Lachlan-Cope, T.; Fleming, Z.L.; et al. Real time detection of airborne fluorescent bioparticles in Antarctica. *Atmos. Chem. Phys.* **2017**, *17*, 14291–14307. [CrossRef]
23. Yue, S.; Ren, H.; Fan, S.; Wei, L.; Zhao, J.; Bao, M.; Hou, S.; Zhan, J.; Zhao, W.; Ren, L.; et al. High abundance of fluorescent biological aerosol particles in winter in Beijing, China. *ACS Earth Space Chem.* **2017**, *1*, 493–502. [CrossRef]
24. Huffman, J.A.; Perring, A.E.; Savage, N.J.; Clot, B.; Crouzy, B.; Tummon, F.; Shoshanim, O.; Damit, B.; Schneider, J.; Sivaprakasam, V.; et al. Real-time sensing of bioaerosols: Review and current perspectives. *Aerosol Sci. Technol.* **2019**, *54*, 1–31. [CrossRef]
25. Crouzy, B.; Stella, M.; Konzelmann, T.; Calpini, B.; Clot, B. All-optical automatic pollen identification: Towards an operational system. *Atmos. Environ.* **2016**, *140*, 202–212. [CrossRef]
26. Perring, A.; Schwarz, J.; Baumgardner, D.; Hernandez, M.; Spracklen, D.; Heald, C.; Gao, R.; Kok, G.; McMeeking, G.; McQuaid, J.; et al. Airborne observations of regional variation in fluorescent aerosol across the United States. *J. Geophys. Res. Atmos.* **2015**, *120*, 1153–1170. [CrossRef]
27. Forde, E.; Gallagher, M.; Walker, M.; Foot, V.; Attwood, A.; Granger, G.; Sarda-Estève, R.; Stanley, W.; Kaye, P.; Topping, D. Intercomparison of Multiple UV-LIF Spectrometers Using the Aerosol Challenge Simulator. *Atmosphere* **2019**, *10*, 797. [CrossRef]
28. Savage, N.J.; Krentz, C.E.; Könemann, T.; Han, T.T.; Mainelis, G.; Pöhlker, C.; Huffman, J.A. Systematic characterization and fluorescence threshold strategies for the wideband integrated bioaerosol sensor (WIBS) using size-resolved biological and interfering particles. *Atmos. Meas. Tech.* **2017**, *10*, 4279–4302. [CrossRef]
29. Agranovski, V.; Ristovski, Z.D.; Ayoko, G.A.; Morawska, L. Performance evaluation of the UVAPS in measuring biological aerosols: Fluorescence spectra from NAD (P) H coenzymes and riboflavin. *Aerosol Sci. Technol.* **2004**, *38*, 354–364. [CrossRef]
30. Carslaw, D.C.; Ropkins, K. Openair—An R package for air quality data analysis. *Environ. Model. Softw.* **2012**, *27*, 52–61. [CrossRef]
31. Rehman, A.U.; Anwer, A.G.; Gosnell, M.E.; Mahbub, S.B.; Liu, G.; Goldys, E.M. Fluorescence quenching of free and bound NADH in HeLa cells determined by hyperspectral imaging and unmixing of cell autofluorescence. *Biomed. Opt. Express* **2017**, *8*, 1488–1498. [CrossRef] [PubMed]
32. Lakowicz, J.R.; Shen, B.; Gryczynski, Z.; D'Auria, S.; Gryczynski, I. Intrinsic fluorescence from DNA can be enhanced by metallic particles. *Biochem. Biophys. Res. Commun.* **2001**, *286*, 875–879. [CrossRef] [PubMed]
33. Roshchina, V.V. Autofluorescence of plant secreting cells as a biosensor and bioindicator reaction. *J. Fluoresc.* **2003**, *13*, 403–420. [CrossRef]
34. Wang, H.; Zhu, R.; Zhang, J.; Ni, L.; Shen, H.; Xie, P. A novel and convenient method for early warning of algal cell density by chlorophyll fluorescence parameters and its application in a highland lake. *Front. Plant Sci.* **2018**, *9*, 869. [CrossRef] [PubMed]
35. Lamb, J.J.; Røkke, G.; Hohmann-Marriott, M.F. Chlorophyll fluorescence emission spectroscopy of oxygenic organisms at 77 K. *Photosynthetica* **2018**, *56*, 105–124. [CrossRef]
36. Turner, P. The fungal air spora of Hong Kong as determined by the agar plate method. *Trans. Br. Mycol. Soc.* **1966**, *49*, 255–267. [CrossRef]
37. Grinn-Gofron´, A.; Strzelczak, A. Changes in concentration of Alternaria and Cladosporium spores during summer storms. *Int. J. Biometeorol.* **2013**, *57*, 759–768. [CrossRef]

38. Kasprzyk, I.; Kaszewski, B.M.; Weryszko-Chmielewska, E.; Nowak, M.; Sulborska, A.; Kaczmarek, J.; Szymanska, A.; Haratym, W.; Jedryczka, M. Warm and dry weather accelerates and elongates Cladosporium spore seasons in Poland. *Aerobiologia* **2016**, *32*, 109–126. [CrossRef]
39. Hameed, A.A.; Khoder, M.; Yuosra, S.; Osman, A.; Ghanem, S. Diurnal distribution of airborne bacteria and fungi in the atmosphere of Helwan area, Egypt. *Sci. Total Environ.* **2009**, *407*, 6217–6222. [CrossRef]
40. Bardei, F.; Bouziane, H.; del Mar Trigo, M.; Ajouray, N.; El Haskouri, F.; Kadiri, M. Atmospheric concentrations and intradiurnal pattern of Alternaria and Cladosporium conidia in Tétouan (NW of Morocco). *Aerobiologia* **2017**, *33*, 221–228. [CrossRef]
41. Pady, S.; Kramer, C.; Clary, R. Diurnal periodicity in airborne fungi in an orchard. *J. Allergy* **1967**, *39*, 302–310. [CrossRef]
42. O'Connor, D.J.; Iacopino, D.; Healy, D.A.; O'Sullivan, D.; Sodeau, J.R. The intrinsic fluorescence spectra of selected pollen and fungal spores. *Atmos. Environ.* **2011**, *45*, 6451–6458. [CrossRef]
43. Schäppi, G.F.; Suphioglu, C.; Taylor, P.E.; Knox, R.B. Concentrations of the major birch tree allergen Bet v 1 in pollen and respirable fine particles in the atmosphere. *J. Allergy Clin. Immunol.* **1997**, *100*, 656–661. [CrossRef]
44. Wos, M.; Pollard, P. Cellular nicotinamide adenine dinucleotide (NADH) as an indicator of bacterial metabolic activity dynamics in activated sludge. *Water Sci. Technol.* **2009**, *60*, 783–791. [CrossRef]
45. Islam, M.; Ikeguchi, A.; Naide, T. Concentrations of Aerosol Numbers and Airborne Bacteria, and Temperature and Relative Humidity, and Their Interrelationships in a Tie-Stall Dairy Barn. *Animals* **2019**, *9*, 1023. [CrossRef]

3.3 UV-LIF Spectrometry Observations of Transatlantic Bioaerosols on the Coast of Barbados

Acting as a continuation of the CVAO project, this project took place as part of the EU-REC4A-UK on the eastern coast of Barbados at Ragged Point. We repeat the methodology used at Cape Verde to contrast the concentrations of bioaerosols observed on either side of the Atlantic ocean. As bioaerosols are typically some of the largest particles suspended within an aerosol mixture, we would expect them to become deposited sooner and comprise a smaller fraction of the total particle count at Barbados than they do at Cape Verde. Our results confirm this, with bioaerosols peaking at just 0.2% of all particles. The concentrations are once again closely correlated with the arrival of sporadic dust events, suggesting the nature of the bioaerosols we observe is the same as was found at CVAO. The following paper is a draft written in the MPDI Atmosphere template and has not been submitted.

MDPI

Article

UV-LIF Spectrometry Observations of Transatlantic Bioaerosols on the Coast of Barbados

Douglas Morrison [1], Ian Crawford [1], Peter Gallimore [1], Dave Topping [1], Mike Flynn [1], Chris Stopford [2], Keith Bower [1], Hugh Coe[1] and Martin Gallagher[1]

[1] Department of Earth and Environmental Science, University of Manchester, Brunswick St, Manchester, M13 9PS
[2] Science and Technology Research Institute, University of Hertfordshire, Hatfield, U.K.
* Correspondence: douglas.morrison@manchester.ac.uk

Version March 29, 2021

Abstract: The African continent is a significant source of dust events, with continental outflow regularly transporting particles across the Atlantic ocean. A previous study at Cape Verde in 2015-2016 used UV-LIF spectrometry techniques to provide quantitative estimates of the bioaerosol fraction also present within the aerosol mixture. The seasonality of dust events was observed, with a notable peak in particle concentrations from December to February. Here we present results from a follow-on study based at Ragged Point, Barbados. Conducted from January to February 2020 and positioned on the other side of the Atlantic Ocean, this study repeats the UV-LIF spectrometry methods to quantify the bioaerosol concentrations reaching the American continent. Averaging approximately 10 L^{-1}, bioaerosol concentrations at Ragged Point are considerably lower, but correlate closely with sporadic dust events, suggesting the bioaersol mixture is once again predominantly bacterial/dust agglomerates. However, the ratio of fluorescent particle concentrations relative to total particle counts is also much lower, peaking at just 0.2%. This has important implications for climate modellers, who must account for the ice nucleating properties of bioaerosols. Incorporating this change in relative concentrations should improve the accuracy of their models.

Keywords: Bioaerosol, UV-LIF Spectrometry, Transatlantic

1. Introduction

Bioaerosols are increasingly recognised for their influence on atmospheric processes. Once emitted from forests and other natural landscapes, bacteria, fungal spores, pollen fragments and more can all become suspended several kilometers into the atmosphere [1]. Once suspended, bioaerosols act as extremely efficient ice nuclei by lowering the energy required for ice crystallisation to begin [2]. They can have significant consequences for cloud cover, leading to changes in both local albedo effects and precipitation.

Many bioaerosols become inactivated once suspended in the atmosphere, having been exposed to dry conditions, UV rays and nutrient deprivation [3]. However, some species have adapted to remain viable even in such hostile conditions. One such adaptation is the formation of a dormant endospore [4]. Analagous to hibernation, this process shuts down metabolic activity and creates a thicker cell wall to provide protection from the outside. Other species such as some non-spore forming bacteria can utilise other techniques. For example, it is now clear that dust events are significant drivers of the long-range transport of bioaerosols [5], and can have important implications for human health [6]. It is believed dust can act as a substrate for a diverse number of bacterial species [7], enabling them to remain physiologically active. As such, dust events enable bioaerosols to potentially reach novel

environments, where they can can have deleterious effects on species that have not evolved resistances towards them [8].

Considering the number of effects bioaerosols can have, understanding the scale and variability of their concentrations is clearly important. Quantitative estimates of continental outflow were previously recorded at the Cape Verde Atmospheric Observatory (CVAO) using a WIBS-4M [9]. Lasting for 11 months, this represented one of the longest continuous sampling campaigns to use UV-LIF spectrometry methods. This enabled discrete dust events to be observed, as well as seasonal effects on continental outflow. A 9-sigma threshold had been used to remove weakly fluorescent non-biological particles. This led to approximately 0.5% of the total particle count to be considered 'fluorescent' and subsequently be assumed to contain biological material. This assumption was verified by an inter-comparison with the Laser Ablation Aerosol Particle Time of Flight (LAAP-ToF) mass spectrometer. Analysis of this instrument focused on a bio-silicate class, defined as particles containing markers found in bacteria as well as markers found in dust. This class provides good evidence of bacteria attached to dust particles, and the particle counts between this class and those of fluorescent particles in the WIBS-4M showed good agreement ($r^2 = 0.63$).

Continental outflow peaked in February with westerly winds transporting dust from the Sahara and across the Atlantic ocean. However, with the Cape Verde archipelago based 563 km off the western coast of the African continent, fewer suspended dust particles will have been deposited on the ground during transport. Although this study was one of the first to quantify bioaerosol concentrations within this region, it is not clear what the particle concentrations being received on the American continent would be. A follow-up study quantifying this change would be useful for several reasons. For example, dust events can be hazardous for human health, with the Harmattan wind estimated to increase daily mortality rates by more than 8% [10]. Furthermore, bioaerosols have a known impact on climate and environments, with dust clouds containing many efficient ice-nucleating particles. It is also not just consequences for air quality that make this subject worth re-visiting, but for also better understanding the dust event's impact on marine life. This is because dust events can lead to nutrient deposition in the ocean. Korte et al. [11] observed significant quantities of biogenic silica being deposited in the Atlantic ocean with African origin. By observing the decrease in airborne concentrations of both fluorescent and non-fluorescent particles, the feedback loop this creates in the environment can be better understood.

2. Materials and Methods

2.1. Site Description and Sampling Details

The ground-based sampling site utilised the mobile Manchester Aerosol Laboratory to continuously sample from January 17th to February 22nd, 2020. It was located close to the Barbados AGAGE station, on the eastern coast of Ragged Point (13.1638° N, 59.4329° W). This site has direct exposure to the Atlantic Ocean and experiences regular easterly winds. Aerosols were sampled via a pumped inlet mounted on a 10 m tower. The total flow down the inlet was 1000 L min^{-1} and a series of aerosol instruments sub-sampled isokinetically downstream of a common manifold. A suite of instruments were deployed, including a LAAP-ToF, Aerosol Mass Spectrometer, Scanning Mobility Particle Sizer, Condensation Particle Counter and WIBS-4M. Meteorological data was recorded with the use of a Metpack for temperature, relative humidity, pressure and precipitation, as well as a Sonic Anemometer for wind speed and direction. The results presented here are for the WIBS-4M data, which is capable of detecting particles in the size range 0.5-20 μm. Note the nominal cut-off of the inlet system was approximately 10 μm.

2.2. Data Analysis

It is now well established that using a 9-sigma threshold when defining a fluorescent class is an effective way of removing interferents such as sea salt or soot. This is derived by the instrument recording average background fluorescence in the absence of any particles, during what is known as 'Forced Trigger' mode. A particle is defined as fluorescent when their emission intensity exceeds 9 standard deviations of the background value [12]. As interferents typically have a weaker fluorescence than 'true' bioaerosols, this is a reliable method of removing them from the data [13].

Analysis of the resulting fluorescent spectra primarily focus on a few distinct fluorophores. These include the amino acid Tryptophan, the co-enzyme NAD(P)H and the vitamin Riboflavin. Each fluorophore excites at 280 nm, 270-400 nm and 450 nm respectively; and fluoresces from 300-400, 400-600 and 520-565 nm [14], [15]. The specificity of a biological compound's fluorescent properties enables particles to be classified into one of seven types, depending on whether they exhibit fluorescence in one, two, or three channels [16]. Particle shape and symmetry is also measured through the use of a 635 nm diode laser that is initially involved in triggering the Xenon flash lamps to fire. The forward scattering light from a particle that passes through the laser hits a quadrant scattering detector. By applying a Mie scattering model, the distribution of the light on each quadrant can be used to estimate diameter, as well as an Asymmetry Factor between 0 and 100 [17]. This has been discussed in detail by Kaye *et al.* [18], with values of 0 representing perfectly spherical particles and higher asymmetry factors describing more fibrous and linear shapes. When applying this range in the context of our observations, AF values of 10-20 reflect fairly spherical particles, with values of 30 or more beginning to represent ellipsoidal shapes.

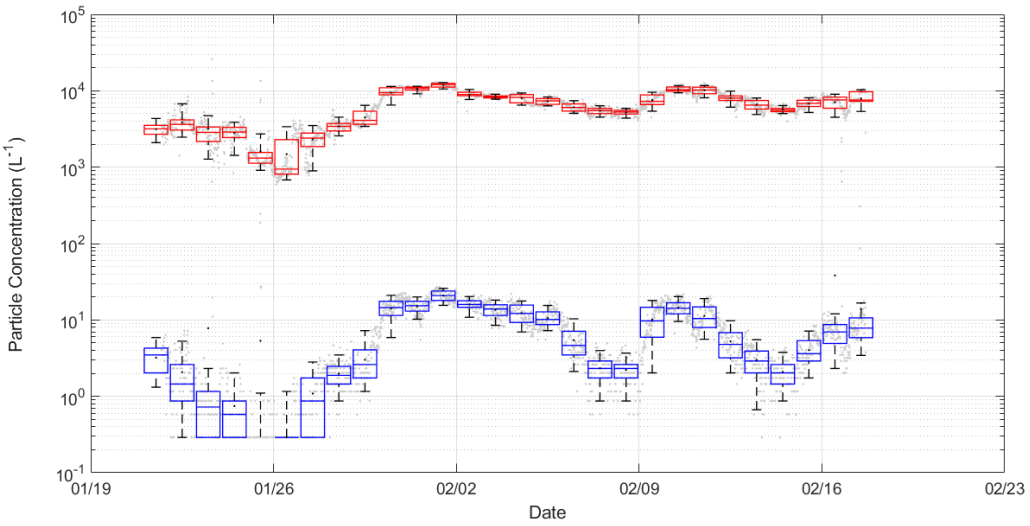

Figure 1. Daily average concentrations per litre of fluorescent (blue) and non-fluorescent particles.

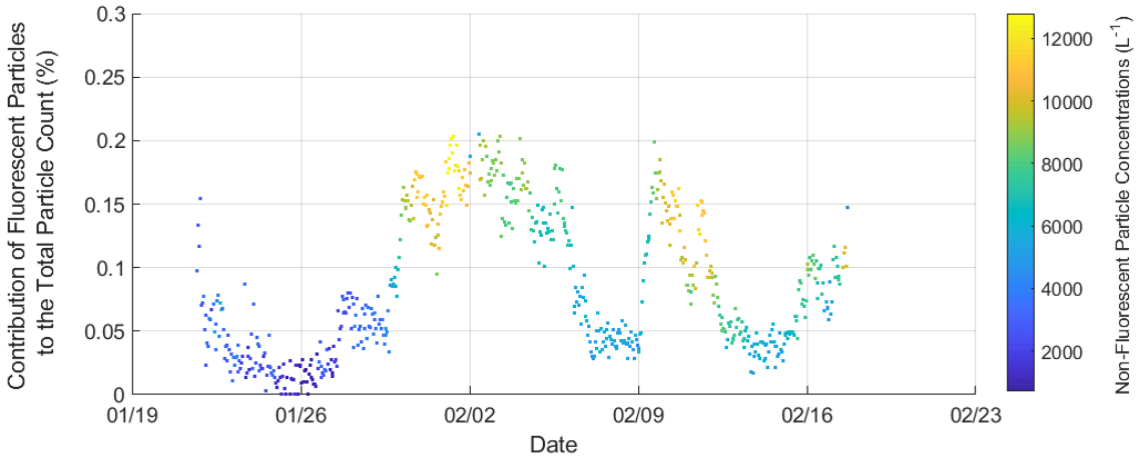

Figure 2. The percentage contribution of fluorescent particles to the total particle count, using a 3-hour average. Each data point is coloured by the average non-fluorescent particle concentration (L^{-1}).

3. Results

Fluorescent particle concentrations averaged $\sim 10L^{-1}$ but showed some fluctuation. It can be seen in Figure 1 that these concentrations were closely correlated with non-fluorescent particle concentrations. Two peaks in particle concentrations were observed during the campaign. The first began on January 31st and plateaued for several days before concentrations fell towards the end of the first week of February. The second event was briefer, lasting from approximately February 10-13th. During these peaks the non-biological particle concentrations exceeded 10,000 L^{-1} and the presumed biological fraction exceeded 20 L^{-1}.

It can also be seen in Figure 2 that a greater relative increase in fluorescent particles is observed during the aforementioned peak events. Prior to these peak events the bioaerosol fraction often accounted for less than 0.05% of the total particles, but rose to as much as 0.2% during peak events. Figures 3 and 4 capture a shift in the asymmetry factor of both fluorescent and non-fluorescent particles during peak events, despite no significant changes in their averages sizes. The observed increases in asymmetry factor are typical for dust events [19].

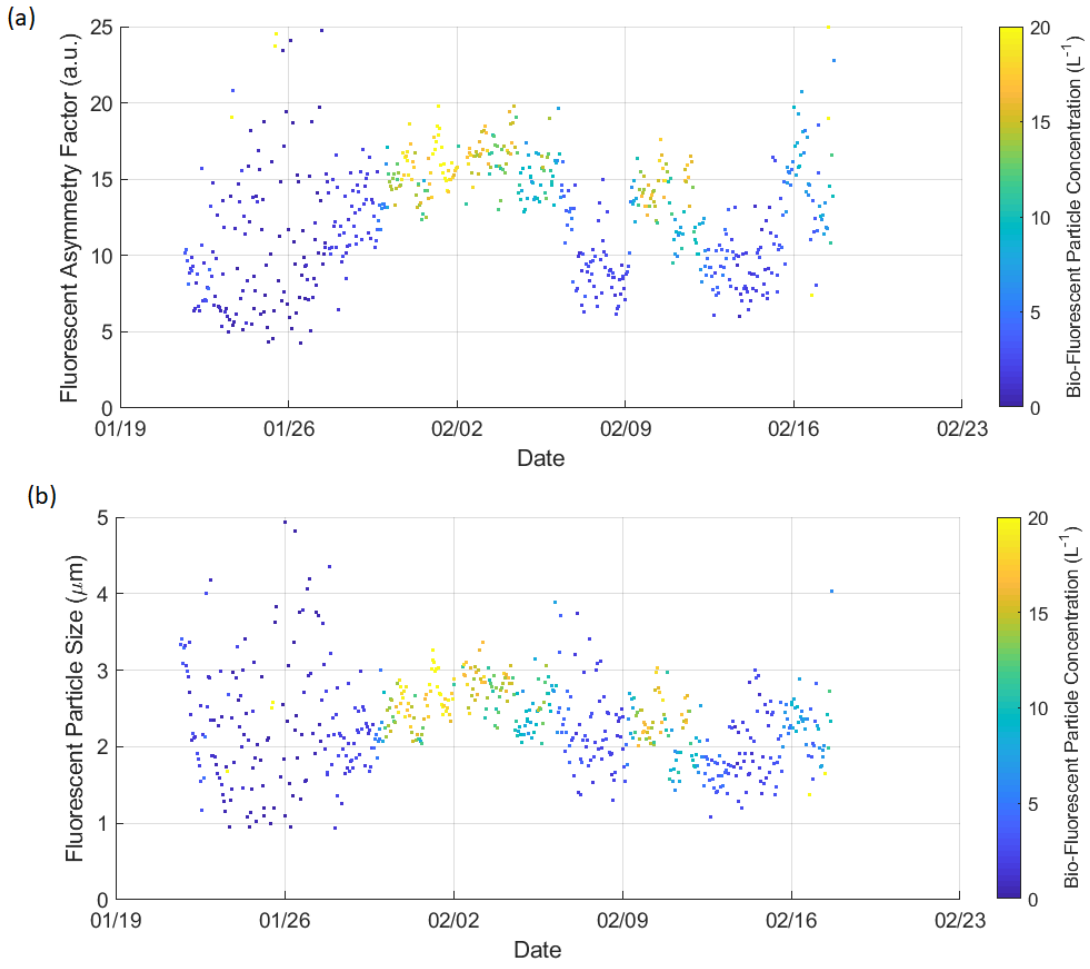

Figure 3. The top panel represents Asymmetry Factor recorded by the WIBS-4M for fluorescent particles using 3-hour averages. The bottom panel represents 3-hour average fluorescent particle size (μm). Each data point is coloured by the average fluorescent particle concentration (L^{-1}).

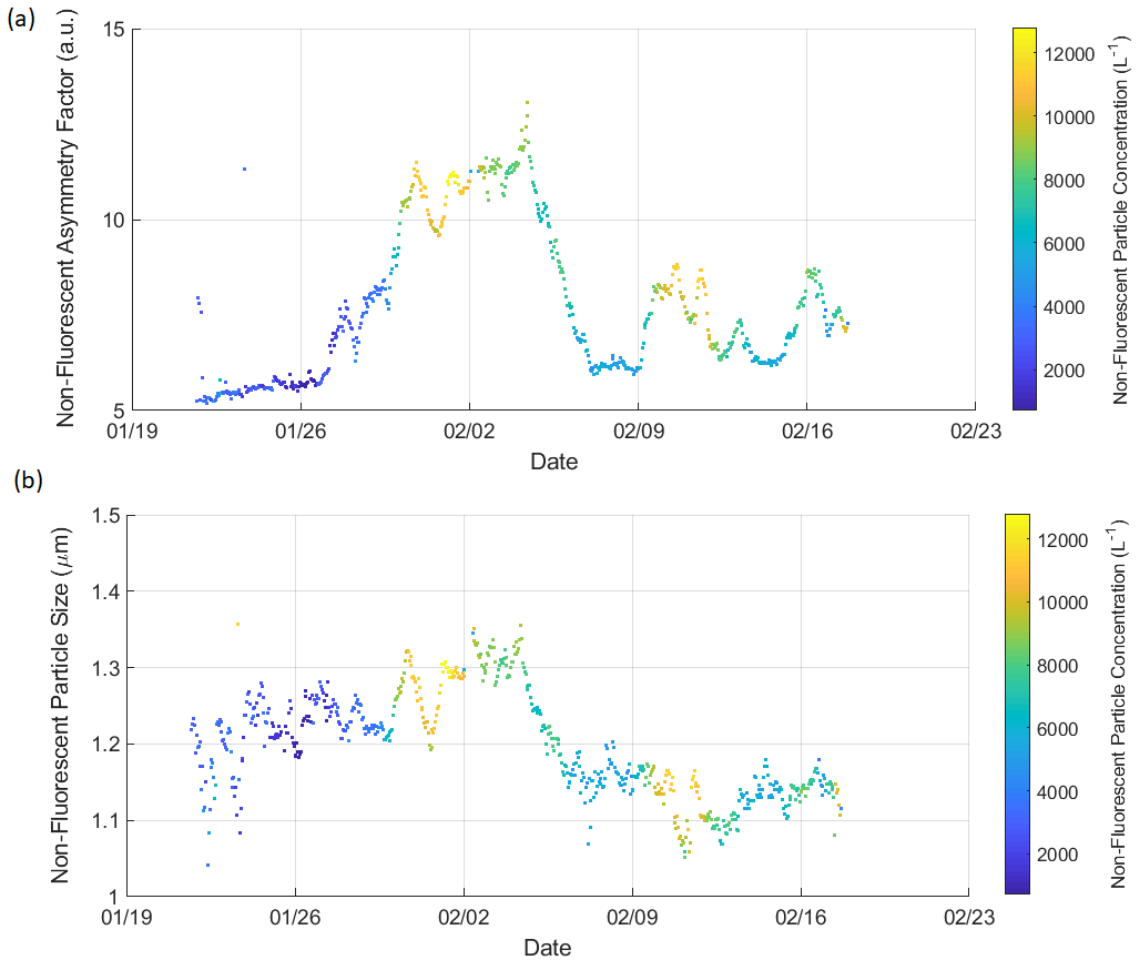

Figure 4. The top panel represents Asymmetry Factor recorded by the WIBS-4M for non-fluorescent particles using 3-hour averages. The bottom panel represents 3-hour average non-fluorescent particle size (μm). Each data point is coloured by the average non-fluorescent particle concentration (L^{-1}).

119 120 hour-long back trajectories were calculated using NOAA's Hysplit merged with the Openair
120 package. These were calculated in 3-hour intervals for the length of the campaign and used a starting
121 height of 10m above ground level. Particle concentrations were subsequently calculated for each
122 trajectory, the results for which are shown in Figure 5. Trajectories consistently crossed the Atlantic,
123 but originate from at least two source regions. The southernmost source region contained higher
124 fluorescent particle concentrations alongside a greater proportion of fluorescent particles within the
125 entire aerosol mixture.
126

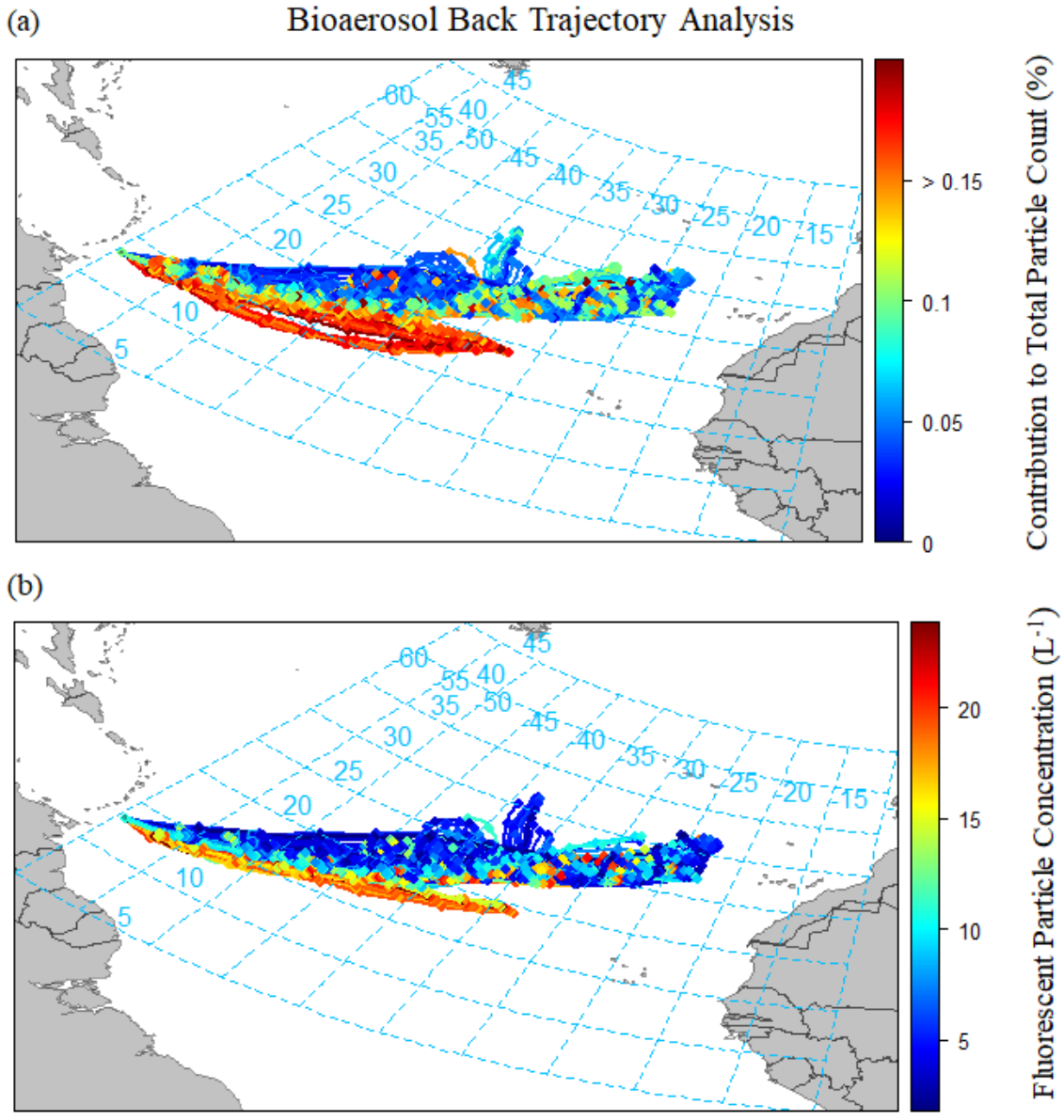

Figure 5. 120 Hour back trajectory analysis for fluorescent particles using Hysplit integrated with the Openair package. Panel (a) represents the contribution of fluorescent particles to the total particle count and panel (b) represents the fluorescent particle concentrations (L^{-1}).

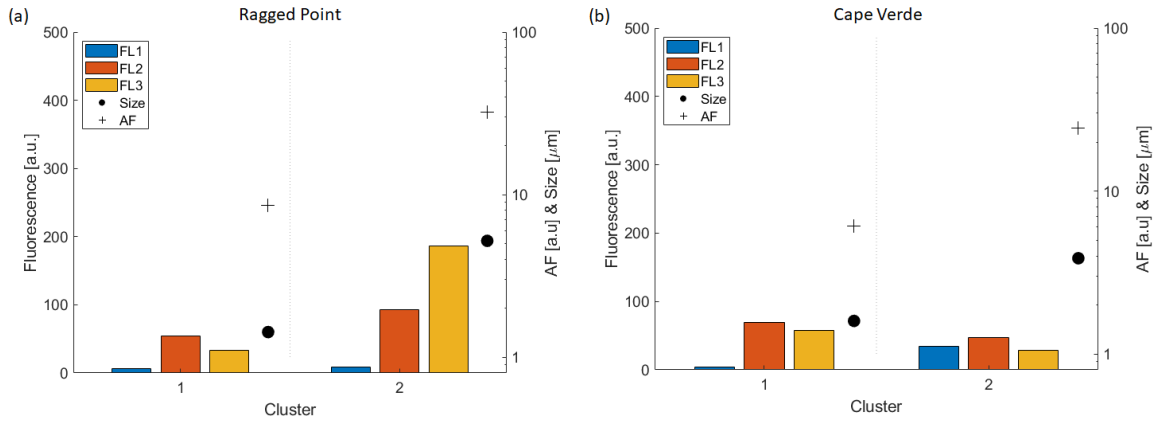

Figure 6. Mean fluorescence, size and shape properties of the two cluster products resulting from hierarchical agglomerative cluster Analysis.

Agglomerative hierarchical cluster analysis was performed using Ward linkage with Euclidean distance for all fluorescent particles. A two cluster solution produced the greatest Calinski-Harabasz score, with information regarding their fluorescence in each channel, size, and asymmetry shown in Figure 5. Although every fluorescent particle has exceeded a conservative 9-sigma threshold and is therefore likely biological in nature, the raw fluorescence values are still relatively low when compared to previous studies. The 2015 study produced a four cluster solution across the campaign, for which two clusters were broadly considered 'pure' biological products on account of high fluorescence in one or more channel. For one of these clusters, average Fl1 fluorescence exceeded 1000 a.u. The other two clusters accounted for the majority of observed fluorescent particles ($\sim$ 90%), and compare most closely with the two cluster products presented here. Interestingly, when cluster analysis is repeated on the 2015 data, but only for the same period in the year that we present results for here, a two-cluster solution is also created. This suggests that the continental outflow follows consistent annual patterns, as would be expected if attributed to known trade winds, but also that the aeorsol mixture arriving at Ragged Point is similar to the original outflow.

EUREC4A

	Fl 1 (a.u.)	Fl 2 (a.u.)	Fl 3 (a.u.)	D μm	AF (a.u.)	%
Cluster 1	6.5 ± 18.2	54.5 ± 125.2	33.2 ± 72.7	1.4 ± 0.9	8.6 ± 6.0	77.1
Cluster 2	8.6 ± 73.4	92.5 ± 156.1	185.8 ± 292.2	5.2 ± 3.4	32.3 ± 15.7	22.9

CVAO

Cluster 1	4.2 ± 12.2	69.0 ± 146.1	58.0 ± 147.2	1.6 ± 0.6	6.1 ± 5.0	33.3
Cluster 2	34.7 ± 106.7	46.7 ± 106.4	28.4 ± 100.6	3.9 ± 2.1	24.3 ± 15.6	66.7

4. Discussion

As would be expected, the concentrations of fluorescent particles recorded at Ragged Point are lower than those observed at CVAO during the same time of year. Many particles will have deposited into the Atlantic ocean during transport, or will have become increasingly dispersed into the atmosphere. The average size of fluorescent particles is smaller at Ragged Point, with a mean of 2.29 $\pm$ 2.41 μm compared to 3.11 $\pm$ 2.07 μm at CVAO. This reduction in particle size is likely due to larger particles being preferentially deposited, and evidence of this is shown in the relative abundances of the cluster products. The smaller sized cluster identified at Cape Verde accounted for 33.3% of fluorescent particles, while the similar cluster observed at Ragged Point accounts for 77.1% of fluorescent particles.

There is a clear divide in the fluorescent to non-fluorescent ratio as a function of back trajectory. Based on our understanding of wind trajectories in this region and by comparing with the back trajectory analysis from the 2015-2016 study, it can be reasonably assumed the southernmost trajectory extends back to the Sahara. The northernmost split appears to run along the northwestern coast of Africa, carrying fewer dust particles as a result. This is reflected in Figure 2, with the northernmost split having significantly lower particle concentrations of all types.

When using a two-cluster solution, the cluster products share a lot of similarities between Ragged Point and CVAO. In each campaign both clusters are weakly fluorescent and are likely separated by differences in their morphology. In both campaigns there is one cluster that is significantly smaller, on average between 1-2 μm. The weak fluorescence in each cluster is interesting because it appears there may be competing explanations as to the nature of the aerosols. Bacteria/dust agglomerates have been convincingly shown to exist in large concentrations, with the 2015-2016 study showing good agreement in an inter-comparison between the LAAP-ToF and WIBS-4M particle concentrations, when looking for both mineral dust and biological markers. As such, we fully expect the presence of bacteria in a significant capacity. However, optical and chemical analysis of the aerosols also indicate mineral dust was mixed to varying degrees with biomass burning smoke. MicroDop lidar observations indicate a layer of dust/biomass burning mixtures not well-mixed into the boundary layer between January 29th to February 3rd, with a similar observation made again on February 9th. These periods correspond closely with our observed peak events.

Unfortunately, the specification of the WIBS-4M and its three detection channels does not provide us the ability to effectively discriminate between dust/bacteria agglomerates and biomass burning particles on their fluorescence spectra alone. However, we do not believe aerosols originating from biomass burning are affecting the presumed bioaerosol concentrations we observe in the WIBS-4M. This is despite some evidence that such particles are capable of acting as interferents [20]. This is because a 9-sigma threshold was applied when classifying particles, removing all weakly fluorescent particles. Toprak and Schnaiter [21] found propane flame soot to only weakly fluoresce in FL1 when using 3-sigma thresholding, suggesting it would not exceed 9 standard deviations of the background fluorescence here. Furthermore, Savage and Huffman et al [22] acknowledge that more highly fluorescent soot is representative of freshly generated soot close to source, and is not representative of aged or processed soot. As all fluorescent particles recorded at Ragged Point will have spent significant time in suspension, any such soot would be significantly aged.

We can confidently rule out bioaerosols associated with oceanic source regions, for example algae that become airborne through sea spray. This is because algae contain fluorophores with a different excitation/emission matrix than the WIBS-4M is sensitive to. Chlorophyll-α is the dominant fluorophore in such particles, and has a much higher emission wavelength of over 700 nm [23].

We acknowledge a shortcoming of ground-based measurements is that only the concentrations at that altitude will be recorded. In 2015 an intensive campaign preceded the long-term sampling, enabling us to observe bioaerosol concentrations along an altitudinal gradient. This is useful as the continental outflow we observed is driven by the Saharan Air Layer, which involves the uplifting of dust particles to 7000 m [24]. It would be useful in climate models to know how these particle concentrations change at different altitudes, as this will have consequences for the height of certain clouds. As such, any future study that is able to identify the altitudinal gradient of bioaerosols at Ragged Point would be providing valuable information.

5. Conclusions

Analysis of the fluorescent fraction at Ragged Point suggests a similar mixture of particle types to those observed at Cape Verde. The key difference between the two regions is the relative abundances of the different particle types, with fluorescent particles often accounting for just 0.05% of all particles and peaking at 0.2% during dust events. Overall concentrations are also much lower than we observed at CVAO, with fluorescent particles averaging just 10 L^{-1}. These lower concentrations are easily explained by the larger size of bioaerosols causing them to deposit more readily into the Atlantic Ocean. When considering the bioaerosols sampled at Ragged Point are smaller than those observed at CVAO, such an explanation appears more likely. Back trajectory analysis once again suggests Saharan and sub-Saharan regions are associated with increased particle concentrations.

Interestingly, although these regions are associated with both fluorescent and non-fluorescent particle types, Saharan back trajectories appear to enhance the fluorescent fraction disproportionately so. This suggests the nature of the aerosols found within these source regions could be distinct from those found in Northern Africa, rather than simply being more numerous. Further study contrasting the mineralogical and biological nature of particles from northern and southern regions could provide interesting information in this regard.

Given the important role bioaerosols play as cloud condensation and ice nuclei, climate modellers should benefit from more accurately factoring in the reduction in bioaerosol concentrations as the African outflow travels to the American continent. We suggest future studies deploy a range of UV-LIF spectrometers so that a wider array of bioaerosols can be detected. Future studies should also attempt to describe the altitudinal profile of the bioaerosols at Ragged Point, as the altitude at which particles are suspended is an important factor when considering their ice nucleation capabilities.

Author Contributions: D.M. is the primary author, responsible for the analysis of the WIBS-4M data. I.C., M.G. and D.T. all assisted in the interpretation and analysis of the WIBS-4M data. P.G. is responsible for the analysis of instruments outside the scope of this paper, while M.F., K.B. and H.C. were all responsible in managing the logistics of this project as co-investigators. C.S. was able to provide additional information regarding the instrumentation.

Funding: This research was funded by NERC (NE/S015752/1).

Conflicts of Interest: The authors declare no conflict of interest and the funders had no role in the design of the study; in the collection, analyses, or interpretation of data; in the writing of the manuscript, or in the decision to publish the results.

1. Els, N.; Baumann-Stanzer, K.; Larose, C.; Vogel, T.M.; Sattler, B. Beyond the planetary boundary layer: Bacterial and fungal vertical biogeography at Mount Sonnblick, Austria. *Geo: Geography and Environment* **2019**, *6*.

2. Huffman, J.A.; Prenni, A.; DeMott, P.; Pöhlker, C.; Mason, R.; Robinson, N.; Fröhlich-Nowoisky, J.; Tobo, Y.; Després, V.; Garcia, E.; others. High concentrations of biological aerosol particles and ice nuclei during and after rain. *Atmospheric Chemistry and Physics* **2013**, *13*, 6151–6164.
3. Després, V.; Huffman, J.A.; Burrows, S.M.; Hoose, C.; Safatov, A.; Buryak, G.; Fröhlich-Nowoisky, J.; Elbert, W.; Andreae, M.; Pöschl, U.; others. Primary biological aerosol particles in the atmosphere: a review. *Tellus B: Chemical and Physical Meteorology* **2012**, *64*, 15598.
4. Löndahl, J. Physical and biological properties of bioaerosols. In *Bioaerosol detection technologies*; Springer, 2014; pp. 33–48.
5. Park, J.; Ichijo, T.; Nasu, M.; Yamaguchi, N. Investigation of bacterial effects of Asian dust events through comparison with seasonal variability in outdoor airborne bacterial community. *Scientific reports* **2016**, *6*, 1–8.
6. Griffin, D.W. Atmospheric movement of microorganisms in clouds of desert dust and implications for human health. *Clinical microbiology reviews* **2007**, *20*, 459–477.
7. Yamaguchi, N.; Ichijo, T.; Sakotani, A.; Baba, T.; Nasu, M. Global dispersion of bacterial cells on Asian dust. *Scientific Reports* **2012**, *2*, 1–6.
8. Fröhlich-Nowoisky, J.; Kampf, C.J.; Weber, B.; Huffman, J.A.; Pöhlker, C.; Andreae, M.O.; Lang-Yona, N.; Burrows, S.M.; Gunthe, S.S.; Elbert, W.; others. Bioaerosols in the Earth system: Climate, health, and ecosystem interactions. *Atmospheric Research* **2016**, *182*, 346–376.
9. Morrison, D.; Crawford, I.; Marsden, N.; Flynn, M.; Read, K.; Neves, L.; Foot, V.; Kaye, P.; Stanley, W.; Coe, H.; others. Quantifying bioaerosol concentrations in dust clouds through online UV-LIF and mass spectrometry measurements at the Cape Verde Atmospheric Observatory. *Atmospheric Chemistry and Physics* **2020**, *20*, 14473–14490.
10. Perez, L.; Tobias, A.; Querol, X.; Künzli, N.; Pey, J.; Alastuey, A.; Viana, M.; Valero, N.; González-Cabré, M.; Sunyer, J. Coarse particles from Saharan dust and daily mortality. *Epidemiology* **2008**, pp. 800–807.
11. Korte, L.F.; Brummer, G.J.A.; Does, M.v.d.; Guerreiro, C.V.; Hennekam, R.; Hateren, J.A.v.; Jong, D.; Munday, C.I.; Schouten, S.; Stuut, J.B.W. Downward particle fluxes of biogenic matter and Saharan dust across the equatorial North Atlantic. *Atmospheric Chemistry and Physics* **2017**, *17*, 6023–6040.
12. Forde, E.; Gallagher, M.; Walker, M.; Foot, V.; Attwood, A.; Granger, G.; Sarda-Estève, R.; Stanley, W.; Kaye, P.; Topping, D. Intercomparison of Multiple UV-LIF Spectrometers Using the Aerosol Challenge Simulator. *Atmosphere* **2019**, *10*, 797.
13. Savage, N.J.; Krentz, C.E.; Könemann, T.; Han, T.T.; Mainelis, G.; Pöhlker, C.; Huffman, J.A. Systematic characterization and fluorescence threshold strategies for the wideband integrated bioaerosol sensor (WIBS) using size-resolved biological and interfering particles. *Atmospheric Measurement Techniques* **2017**, *10*.
14. Hill, S.C.; Mayo, M.W.; Chang, R.K. Fluorescence of Bacteria, Pollens, and Naturally Occurring Airborne Particles?: Excitation/Emission Spectra, Army Research Laboratory. *Applied Physics,(February)* **2009**.
15. Lakowicz, J.R. *Principles of fluorescence spectroscopy*; Springer Science & Business Media, 2013.
16. Perring, A.; Schwarz, J.; Baumgardner, D.; Hernandez, M.; Spracklen, D.; Heald, C.; Gao, R.; Kok, G.; McMeeking, G.; McQuaid, J.; others. Airborne observations of regional variation in fluorescent aerosol across the United States. *Journal of Geophysical Research: Atmospheres* **2015**, *120*, 1153–1170.
17. Gabey, A.; Gallagher, M.; Whitehead, J.; Dorsey, J.; Kaye, P.H.; Stanley, W. Measurements and comparison of primary biological aerosol above and below a tropical forest canopy using a dual channel fluorescence spectrometer. *Atmospheric Chemistry and Physics* **2010**.
18. Kaye, P.H.; Aptowicz, K.; Chang, R.K.; Foot, V.; Videen, G. Angularly resolved elastic scattering from airborne particles. In *Optics of Biological Particles*; Springer, 2007; pp. 31–61.
19. Zhao, G.; Zhao, C.; Kuang, Y.; Bian, Y.; Tao, J.; Shen, C.; Yu, Y. Calculating the aerosol asymmetry factor based on measurements from the humidified nephelometer system. *Atmospheric Chemistry and Physics* **2018**, *18*, 9049–9060.
20. Pan, Y.L. Detection and characterization of biological and other organic-carbon aerosol particles in atmosphere using fluorescence. *Journal of Quantitative Spectroscopy and Radiative Transfer* **2015**, *150*, 12–35.
21. Toprak, E.; Schnaiter, M. Fluorescent biological aerosol particles measured with the Waveband Integrated Bioaerosol Sensor WIBS-4: laboratory tests combined with a one year field study. *Atmospheric Chemistry and Physics* **2013**, *13*, 225–243.

22. Savage, N.J.; Huffman, J.A. Evaluation of a hierarchical agglomerative clustering method applied to WIBS laboratory data for improved discrimination of biological particles by comparing data preparation techniques. *Atmospheric Measurement Techniques* **2018**, *11*, 4929–4942.
23. Wang, H.; Zhu, R.; Zhang, J.; Ni, L.; Shen, H.; Xie, P. A novel and convenient method for early warning of algal cell density by chlorophyll fluorescence parameters and its application in a highland lake. *Frontiers in plant science* **2018**, *9*, 869.
24. Chiapello, I.; Bergametti, G.; Gomes, L.; Chatenet, B.; Dulac, F.; Pimenta, J.; Suares, E.S. An additional low layer transport of Sahelian and Saharan dust over the north-eastern tropical Atlantic. *Geophysical Research Letters* **1995**, *22*, 3191–3194.

3.4 The Application of Gradient Boosting Techniques in the Identification of Pollen Species Present in UK Farmland

During the summer of 2019 a PLAIR Rapid-E and FAB were deployed at the Chilbolton Observatory, located in the south of England. This site is largely rural and is surrounded by agricultural land. The objectives of the project were two-fold. First, we wanted to investigate ambient bioaerosol concentrations during the summer, when pollen levels would be at their maximum. Secondly, we wanted to test each instruments ability to identify specific species of pollen. If successful, a database of each native species' unique signature could be developed and made freely available. This could provide a greater depth of information and expedite bioaerosol analysis in future studies. Particle identification is currently labour intensive and slow, but the application of accurate machine learning techniques could help automate the process. Ultimately, this project encountered a number of issues and it was decided that any potential publications could not be pursued in time. The following section discusses the analysis that led to this decision.

Site Description and Sampling Details

The Chilbolton Observatory (51° 8` 58.6212`` N, 1° 26` 17.6208`` W) is located in the south of England, approximately 300 m from Chilbolton village. As demonstrated in Figure 3.1, this site is surrounded by arable farmland. This site is regularly used for pollutant monitoring, and from May - June 2019 a PLAIR Rapid-E and FAB were used to provide online measurements of bioaerosols. These instruments were placed inside a specialist protective container, sub-sampling from an inlet located at the top of it. At the start of the project each instrument was calibrated using fluorescent polystyrene latex spheres (PSLs) and flowering plants obtained from the neighbouring fields were rubbed around each instrument's own inlet. The flowering plants were sampled with the intention being that each instrument would make a record of their pollen's fluorescence spectra and morphology.

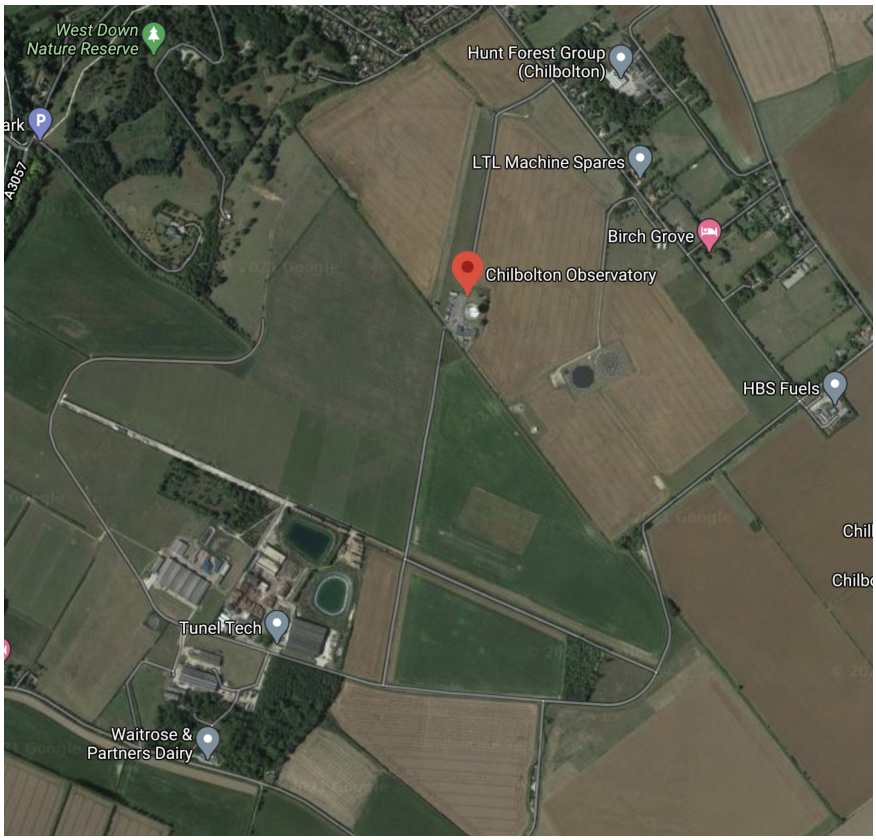

Figure 3.1: Satellite photo of Chilbolton Observatory, taken from Google Maps 2021 .

Sampling Issues

High concentrations of pollen quickly created a blockage in the sampling inlet that both instruments were sub-sampling from. This impacted the quality of the data, with a gradual decline in concentrations shown in Figure 3.2. As such, it was not possible to observe accurate quantitative changes in particle concentrations. Indeed, there are only a few weeks from 14/05/2019 – 07/06/2019 that any particle data exists.

A further problem was that the methodology used to apply the pollen samples may not have been appropriate. As is demonstrated by Figure 3.3, the size of the particles we see for each

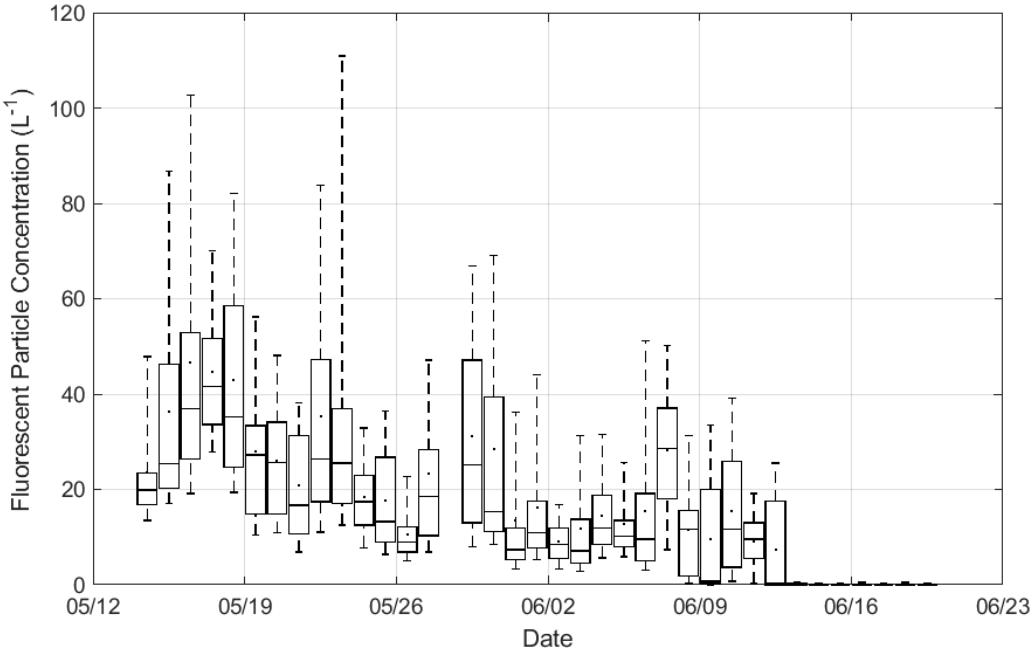

Figure 3.2: Fluorescent particle concentrations (L^{-1}) recorded by the FAB using daily averages. Whiskers represent 5th and 95th percentile values.

species is very small, averaging less than 2 μm. This is too small to be whole pollen grains, which often exceed 100 μm [1]. The particles detected by the instrument will have either been pollen fragments or other plant debris. This problem likely arose for two reasons. Firstly, many plants such as rapeseed - which was a dominant crop in the surrounding areas - are known to have 'sticky' pollen [2]. They depend on insect pollination rather than wind dispersal and as such, may not be easily dislodged by mechanical shaking and rubbing. Secondly, such a mechanical process is imprecise, with the opportunity for other parts of plant debris to be removed instead. Such debris will have been incorrectly classified and will skew the data.

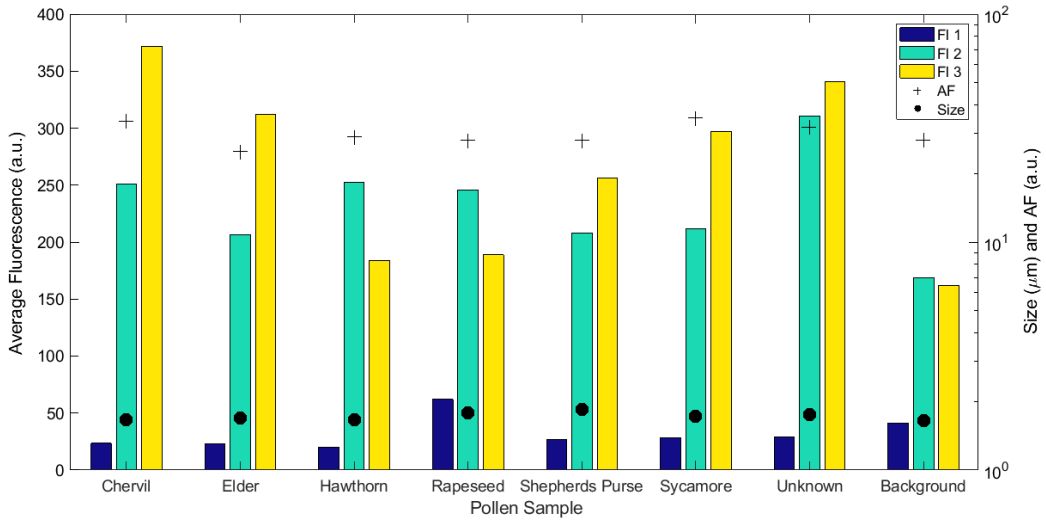

Figure 3.3: The average fluorescence in each of the FAB's three channels, alongside size and asymmetry factor for the seven sampled pollen species.

These factors compounded on one another to create an inaccurate dataset. However, there

were still some interesting details to be discussed. For example, just 2.5 km southwest of the sampling site is a commercial mushroom farm. Large outdoor composting sites are readily seen from satellite data. When fluorescent particle concentrations were integrated with meteorological data using the Openair package in R, potential source regions can be identified. It can be seen in Figure 3.4 that a hotspot is located southwest of our sampling site, and could potentially be attributed to the commercial site. If so, the exact nature of the bioaerosols being released into the atmosphere could have implications for residents in the surrounding area. Fungal spores and thermophilic bacteria are both likely to exist in such a mixture, and in high enough concentrations can create a number of health issues for people [3].

3.4.1 Comparison to a Previous Study

A WIBS-3 has previously been used at the same sampling site from January to March, 2009 [4]. After performing Hierarchical Agglomerative Cluster (HAC) analysis, the authors observed four distinct clusters. They found two clusters shared similar properties and collectively accounted for 81.8% of all fluorescent particles. Their shape, size and fluorescent properties lead to them being identified as fungal spores. The remaining clusters, accounting for 5.6% and 12.6% of fluorescent particles, were identified as bacteria and pollen fragments respectively. Although this study is a helpful measure of the bioaerosol mixture at Chilbolton, it should be noted there are some significant differences in their findings. For example, as shown in Figure 3.5, they observed much higher concentrations to the southwest, while we found an association between high concentrations and the northeast. As their data collection was conducted from January to March 2009, seasonal differences in the crops grown in the surrounding fields could be responsible.

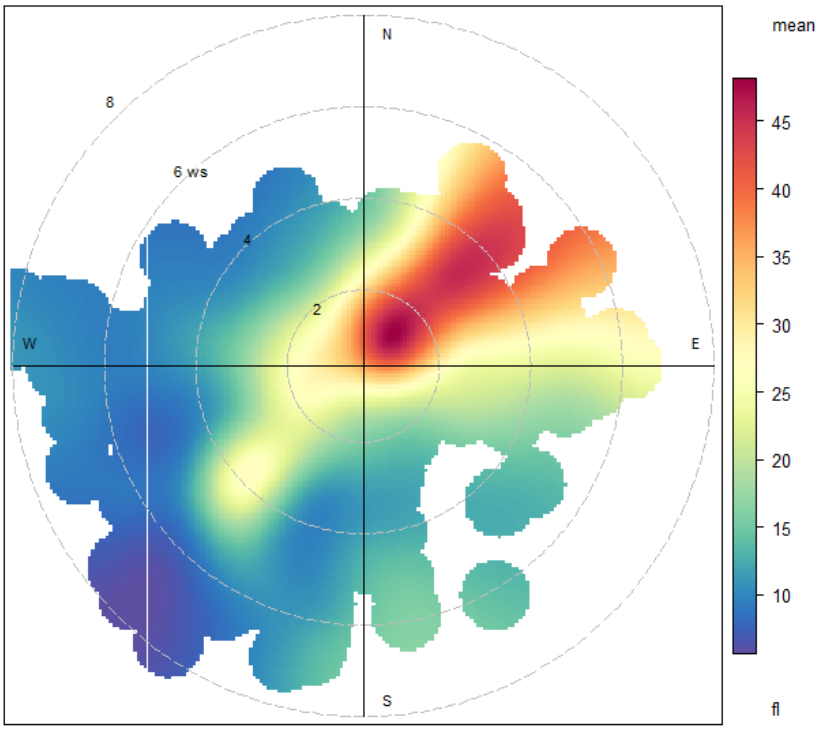

Figure 3.4: Fluorescent particle concentrations as a function of wind speed and direction, using the Openair package in R.

Laboratory-Based Pollen Samples

The project at Chilbolton re-focussed on laboratory-based experiments once it was decided the outdoor environmental data collected by the FAB and PLAIR Rapid-E contained too many inaccuracies to be the focal point. Using pure pollen samples of various species sourced online, they were dispersed into the two instruments using the Swisens Poleno Atomiser. This provided a training dataset for the supervised machine learning method 'Gradient Boosting', to see whether each species had a distinctive enough fluorescence spectra to be accurately classified. Gradient boosting has previously been tested on UV-LIF spectrometers by Ruske et al., [5], who used PSLs to observe classifications with >90% accuracy. The training dataset was created by inputting the average size, asymmetry and fluorescence values of each pollen species into the Python Scikit package. By iteratively weighting these variables to different degrees, a prediction model was created that had the ability to distinguish between each species. Although not demonstrated here, such prediction models can then be applied to other datasets, with the aim of identifying the previously learned species.

Preliminary results were encouraging, as can be seen in Figure 3.4. The training dataset suggests each pollen species was accurately classified, with values ranging from 80 - 93%. However, this training dataset needs to applied to ambient data so that it can tested in its usefulness. It is thought the inclusion of spectral decay rates, as recorded by the PLAIR Rapid-E, would further increase its accuracy. However, including this data requires information from the instrument manufacturers on how to interpret the data output from the instrument, and ultimately was not able to be done in time.

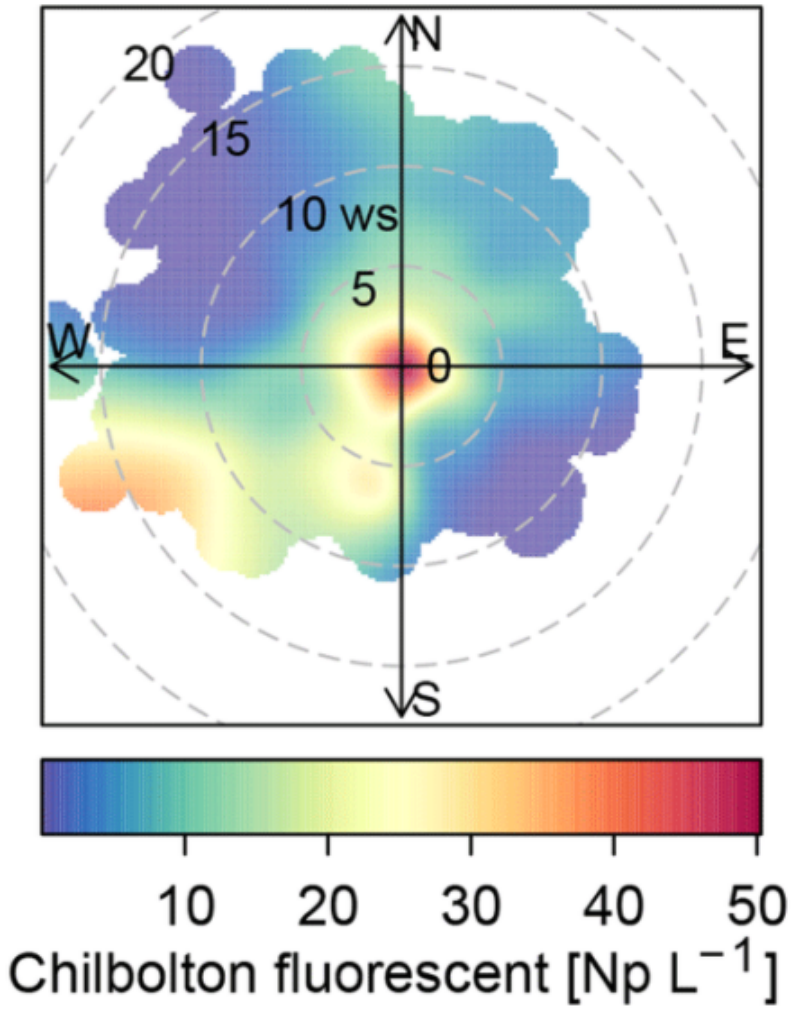

Figure 3.5: Fluorescent particle concentrations as a function of wind speed and direction, taken from Forde at al., [4].

Summary

Machine learning techniques have significant potential to improve bioaerosol identification. However, development of these methods depend on accurate training data that is representative of ambient aerosols. Although modern atomisers offer improved control over pollen dispersal, the samples themselves must also represent the types of pollen that dominate outdoor concentrations. This includes the aged nature of ambient aerosols, as well as using plant species that depend on wind dispersal rather than insect pollination.

Chilbolton offers an interesting location to measure pollen levels in the UK, with the blockage of our sampling inlet clearly demonstrating the high concentrations that can accumulate. Furthermore, the southwestern 'hotspot' that is potentially attributable to the commercial mushroom farm emphasises the wide effects such industries can have for their environment. With composting sites often enabling rare, thermophilic micro-organisms the conditions necessary for them to thrive, active monitoring of bioaerosols released from such sites is important for public health.

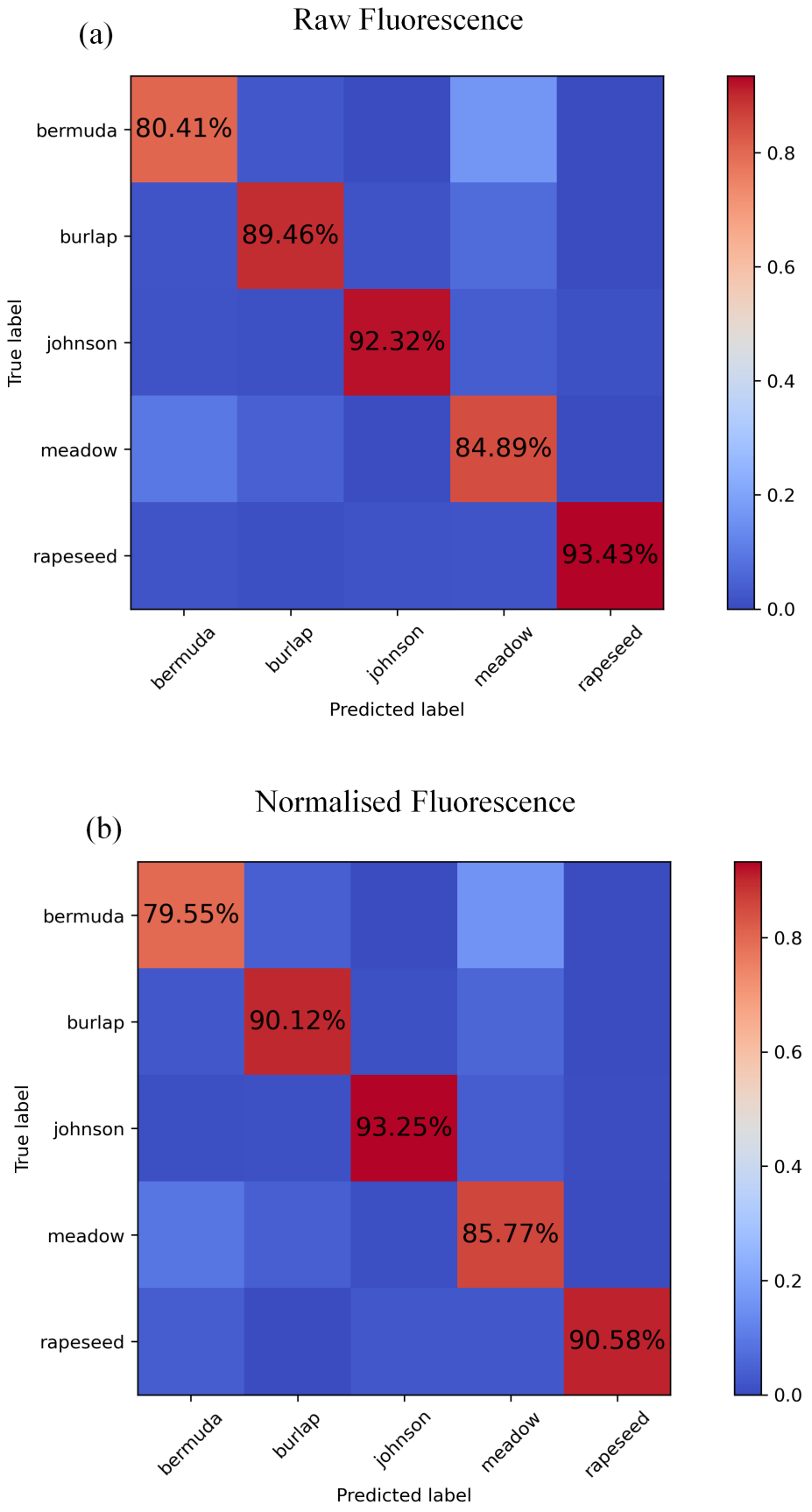

Figure 3.6: Accuracy of pollen species classification using gradient boosting techniques. Panel (a) uses raw fluorescence intensity values recorded by the FAB and panel (b) uses fluorescence intensity values normalised by the sum of values across all 32 channels of the PLAIR Rapid-E.

References

[1] W. C. Hinds, *Aerosol technology: properties, behavior, and measurement of airborne particles*. John Wiley & Sons, 1999.

[2] J. Cresswell, T. Davies, M. Patrick, F. Russell, C. Pennel, M. Vicot, and M. Lahoubi, "Aerodynamics of wind pollination in a zoophilous flower, brassica napus," *Functional Ecology*, vol. 18, no. 6, pp. 861–866, 2004.

[3] C. Rabkin, E. Galaid, D. Hollis, R. Weaver, S. Dees, A. Kai, C. Moss, K. Sandhu, and C. Broome, "Thermophilic bacteria: A new cause of human disease.," *Journal of clinical microbiology*, vol. 21, no. 4, pp. 553–557, 1985.

[4] E. Forde, M. Gallagher, V. Foot, R. Sarda-Esteve, I. Crawford, P. Kaye, W. Stanley, and D. Topping, "Characterisation and source identification of biofluorescent aerosol emissions over winter and summer periods in the united kingdom," *Atmospheric Chemistry and Physics*, vol. 19, no. 3, pp. 1665–1684, 2019.

[5] S. Ruske, D. O. Topping, V. E. Foot, P. Kaye, W. Stanley, I. Crawford, A. Morse, and M. W. Gallagher, "Evaluation of machine learning algorithms for classification of primary biological aerosol using a new uv-lif spectrometer," *Atmospheric Measurement Techniques*, 2017.

Chapter 4

Synthesis and Overall Discussion

UV-LIF Spectrometry continues to be an effective method of bioaerosol detection. The research presented in this document demonstrates the diversity of environments and particle types that such a technique can be used for. We provided good evidence that bacteria dominated in Cape Verde, fungal spores dominated in Hong Kong and that a complex mixture was present in Chilbolton. These studies were also some of the longest sampling campaigns to date that used UV-LIF spectrometry, affirming the reliability of the instruments and their ability to capture seasonal influences. The environments that the aforementioned research projects took place in were also extremely complex. Hong Kong encompassed not a only a mixture of urban and greenbelt spaces; but also significant oceanic influence, changing wind patterns, and varied topography. Chilbolton represented the complexity of rural UK landscapes, with a mixture of pollen species, fungal spores, and anthropogenic influences. The success of each project in light of these factors, as well as the difficulties associated with the operational conditions and long timescales, further emphasises the usefulness of UV-LIF spectrometry.

A number of different instrument models have been used, each with their own advantages and disadvantages. The WIBS continues to provide robust measurements of well characterised fluorophores, enabling clear comparisons to previous literature. However, with UV-LIF spectrometers becoming increasingly advanced, having just three detection channels that each cover a narrow range of emitted wavelengths can be a limiting factor in particle identification. By comparison, the PLAIR Rapid-E uses 32 channels and is sensitive to particles associated with a broader range of wavelengths than any model of WIBS. By observing the distribution of fluorescence intensities across each of these channels, we were able to closely match the spectral profile of the sampled bioaerosols in Hong Kong with the previous work by O'Connor [1]. However, the higher range of the PLAIR Rapid-E is a product of it using a UV-pulsed laser, which in itself comes with a trade-off. This is because each model of the WIBS uses two Xenon flash lamps, enabling a greater range of excitation wavelengths when flashed at sampled particles. As each instrument's spectrometry techniques are situationally advantageous, it is also useful to consider their other functionalities. For example, the PLAIR Rapid-E is able to measure spectral decay rates. Although this data was not used in the research projects presented here, once fluorophore decay rates have been well characterised, this will likely become an important aspect in particle identification. The PLAIR Rapid-E also has a significantly larger size range, measuring up to 100

μm. This makes it much better suited to sampling pollen grains, which typically exceed the upper limits of the WIBS [2]. However, as measuring below 5 μm requires a high-intensity mode to be toggled on the laser, which is known to dramatically shorten the laser's lifespan, it is perhaps less well suited to the long-term detection of smaller sized bioaerosols than the WIBS. Evidence of this is demonstrated in the Hong Kong project, with significantly lower bioaerosol concentrations having been detected by the PLAIR Rapid-E. As such, the research goals of future projects should be well understood before deciding which UV-LIF spectrometer is the appropriate choice.

Despite the many advantages of UV-LIF spectrometry, there are still a number of issues needing to be addressed if future research is to be maximally benefited. First, despite the rapidity of bioaerosol collection afforded by on-line methods, identifying the nature of the fluorescent particles still demands significant time and expertise. The excitation/emission bands associated with specific fluorophores are good indicators of what the presumed bioaerosols are likely to be, but are not definitive. This is because some fluorpohores such as NAD(P)H are ubiquitous in many bioaeorosls. Furthermore, studies often provide seemingly contradictory results when evaluating the fluorescent response of particles. For example, Savage et al., [3] reported strong Fl 1 fluorescence from bacteria, while we report a relatively low Fl 1 response in our observations of bacteria/dust aggregates at CVAO. Although this contrast can potentially be explained by differences between instruments, as well as laboratory samples compared to atmospheric aerosols, such contrasting results highlight some of the difficulties associated with particle identification. As such, it is not sufficient to rely on the fluorescence spectra alone. Instead, it must be compared alongside other data to more accurately classify particles. Useful data includes the size and shape of the particles, meteorological data for the sampling site and a common sense understanding of the region. A good example of this is the campaign in Hong Kong, with the correlation between low relative humidity and particle concentrations leading us to identify the bioaerosols as fungal spores.

4.1 Technological Limitations

A current limitation of UV-LIF spectrometry is that the wavelength specificity of detection plates and excitation lasers/flash lamps mean not every bioaeorsol is likely to be detected by the instrument. For example, the primary fluorophore in algae is Chlorophyll-α, which has an excitation/emission band higher than is found for Tryptophan, NAD(P)H and Riboflavin [4]. As such, studies with marine influences, as was the case at Cape Verde, Ragged Point and Hong Kong, would benefit greatly from having instruments sensitive to a larger range of fluorophores. Projects quantifying bioaerosol concentrations with instruments currently available are likely to provide underestimates of the true bioaerosol concentrations. Although the technology continues to develop and such an issue is likely to be minimised in the future, it is advised that any projects in the immediate future aim to deploy a number of instruments simultaneously, so that a broader range of wavelengths are captured. This is labour intensive and expensive, but an effective way of overcoming such a limitation. It

is also true that UV-LIF spectrometry should not entirely replace offline techniques, but is better suited to complement them. The instrument manufacturers recognise the value of utilising multiple methods, and newer instruments offer some capacity for filter samples to be taken simultaneously.

It is not easy to capture the full size-range of naturally occurring bioaerosols. UV-LIF spectrometers depend on appropriate sampling configurations and flow rates, where accurate inlet characterisation is essential when accounting for sampling losses. This is because bioaerosols are often some of the largest coarse aerosols present within a mixture, resulting in higher losses for any configuration that involves bends in the sampling line. High altitude filter sampling, for example when using FAAM's BAe-146 research aircraft, is particularly susceptible to line losses because of the high sample flows and greater inertia associated with larger particles. Sampling angles are estimated to as much as halve the inlet efficiency for 20 μm particles, while gravitational settling can further halve particle counts for particles greater than 35 μm. Inlet inertial deposition and turbulent inertial deposition also reduce the efficiency of particle collection. Exact reductions depend on the size of the particle and sample flow being used, with estimates presented by Sanchez et al., (2019) [5].

Other issues can occur when measuring sub-micron bioearosols. Although the WIBS-4M is capable of recording down to 0.5 μm, it is estimated half of particles are missed at such a size. Furthermore, as viruses are significantly smaller than bacteria, pollen or fungal spores, often occurring at just 200 nm [2], it is not yet possible for UV-LIF spectrometers to detect their presence. This is because as discussed previously, the intensity of fluorescence depends strongly on a particle's physical cross-section, with larger particles fluorescing more strongly. If a particle is too small, it is unlikely to contain enough bio-fluorescent material to initiate detection by the instrument.

4.2 Future Research Needs

As 9-sigma thresholds become standard procedure in bioaerosol research, it is how to identify and remove highly fluorescent non-biological particles that poses a greater challenge. Soot particles are often identified as a potential issue during analysis, as they are capable of fluorescing strongly and are commonplace in the atmosphere. It is further complicated with different studies observing different fluorescent spectra for soot particles, possibly as a product of atmospheric aging. Current analysis requires an appreciation for the changes such particles undergo, and knowledge of their size, subsequent deposition rates and probable source regions. The difficulties in eliminating soot as a dominant fluorescent particle are well represented by the Cape Verde study. As African biomass burning regularly occurs on a large scale, it seems very likely that significant quantities of soot will be released into the atmosphere. We concluded they could not be responsible for elevated bioaerosol concentrations through an inter-comparison with the LAAP-ToF, sensitive to bacterial markers. If UV-LIF spectrometers were the sole instruments to be deployed, it would have been significantly harder to discount the impact of soot. That being said, it should be emphasised

that laboratory studies aimed at demonstrating the interfering role that soot particles may play, have so far allowed for significant coagulation time. This creates larger soot aggregates that more closely reach the size range seen in bioaerosols. However, this is not representative of real-world conditions, and soot particles are often much smaller, existing at less than a micron in size.

Future particle classification is likely to benefit from the development of open-source datasets that collate the various properties of reliably classified particles. Machine learning techniques are one of the most promising developments in bioaerosol research, with a number of techniques including cluster analysis, gradient boosting, neural networks and more all suggesting accurate results in preliminary studies [6]. The usefulness of these techniques depend on training data that is representative of the bioaerosols observed in real world conditions. This includes accurate representation of aged particles, appropriate morphologies where coagulation and deposition rates are relevant factors, as well as choosing sample species known to be present in ambient aerosol mixtures.

References

[1] D. J. O'Connor, D. Iacopino, D. A. Healy, D. O'Sullivan, and J. R. Sodeau, "The intrinsic fluorescence spectra of selected pollen and fungal spores," *Atmospheric Environment*, vol. 45, no. 35, pp. 6451–6458, 2011.

[2] W. C. Hinds, *Aerosol technology: properties, behavior, and measurement of airborne particles*. John Wiley & Sons, 1999.

[3] N. J. Savage, C. E. Krentz, T. Könemann, T. T. Han, G. Mainelis, C. Pöhlker, and J. A. Huffman, "Systematic characterization and fluorescence threshold strategies for the wideband integrated bioaerosol sensor (wibs) using size-resolved biological and interfering particles.," *Atmospheric Measurement Techniques*, vol. 10, no. 11, 2017.

[4] J. J. Lamb, G. Røkke, and M. F. Hohmann-Marriott, "Chlorophyll fluorescence emission spectroscopy of oxygenic organisms at 77 k," *Photosynthetica*, vol. 56, no. 1, pp. 105–124, 2018.

[5] A. Sanchez-Marroquin, D. H. Hedges, M. Hiscock, S. T. Parker, P. D. Rosenberg, J. Trembath, R. Walshaw, I. T. Burke, J. B. McQuaid, and B. J. Murray, "Characterisation of the filter inlet system on the faam bae-146 research aircraft and its use for size-resolved aerosol composition measurements," *Atmospheric Measurement Techniques*, vol. 12, no. 11, pp. 5741–5763, 2019.

[6] S. Ruske, D. O. Topping, V. E. Foot, A. P. Morse, and M. W. Gallagher, "Machine learning for improved data analysis of biological aerosol using the wibs," *Atmospheric Measurement Techniques*, vol. 11, no. 11, pp. 6203–6230, 2018.

Chapter 5

Conclusions

The key findings of each research project are presented below, with implications for air quality, ocean-atmosphere biogeochemical cycles, human health and machine learning techniques. As such, these projects may provide useful information for climate modellers, public health officials, environmental scientists, data scientists, and more. Each project offers unique insight into bioaerosol emission and dispersion patterns, with a range of particle types, concentrations, source regions and external factors identified. The enhancement in bacterial concentrations at Cape Verde, driven by annual trade winds, is in sharp contrast to the sporadic and irregular spore showers seen at Hong Kong. Furthermore, the capacity for bacterial aggregates to travel such significant distances as to cross the Atlantic ocean, while the fungal spores in Hong Kong are presumed to have been locally ejected, highlights the complexity of bioaerosol exposure. Fluctuating alongside meteorological, seasonal, environmental and ecological factors, they can be locally released, or subject to long-range transport. Models of exposure depend upon studies such as those presented here, so that the various competing factors can accurately accounted for. There is still work to be done, for example better understanding bioaerosol's altitudinal profiles, but these research projects help close the knowledge gap.

5.1 CVAO and Ragged Point

Seasonal bioaerosol concentrations have been quantified at Cape Verde for the first time, with monthly median values as high as 45 L^{-1}. HAC analysis was performed on the fluorescent fraction of coarse aerosols, defined as such when their fluorescence intensity exceeded nine standard deviations of the background value. This is a marked increase from previous studies, that typically used just three standard deviations. The HAC analysis produced a four cluster solution, for which two weakly fluorescent clusters dominated particle concentrations after collectively accounting for over 90% of total fluorescent particles. An inter-comparison made with the LAAP-ToF provided good evidence that the nature of these clusters were bacteria/dust agglomerates, with back trajectory analysis suggesting a Saharan origin. Accounting for a mean 0.4% of total coarse aerosols, the ice-nucleating capabilities of such particles carry important implications for cloud formation and albedo.

The follow-up study at Ragged Point acts as both a useful confirmation of the CVAO observations, but also enables a contrast to be made regarding particle concentrations on ei-

ther side of the Atlantic. Averaging just 10 L^{-1}, it is clear many bioaerosols deposit into the ocean during transport, or increasingly disperse into the atmosphere. Either way, climate modellers should once again benefit by accounting for this reduction in concentrations. HAC analysis of the Ragged Point dataset suggests just a two cluster solution is optimal, both of which share similar spectral and morphological properties of the bacteria/dust agglomerate clusters identified at CVAO. When the CVAO dataset was retrospectively analysed for the same calendar months as the Ragged Point study, a two cluster solution was once again optimal. This is interesting because if the two clusters in each study are presumed to be the same in nature, there is once again a clear contrast between findings. The larger average sized cluster at CVAO accounted for 67% of all fluorescent particles, but only accounted for 23% at Ragged Point. This suggests many of the larger particles will have deposited into the Atlantic ocean during transport, with implications for subsequent nutrient deposition. The morphologies of the clusters between each study are not identical however, obfuscating any direct comparisons.

5.2 Hong Kong

The project in Hong Kong was intended to observe how a monsoon-influenced climate might affect bioaerosol concentrations. This is because anthropogenic pollutants are known to increase during winter, when southerly winds transport them from the Chinese mainland. Observed bioaerosol concentrations were generally low during the summer months, averaging just 20.6 ± 9.1 L^{-1} in the WIBS-NEO. However, two periods of significant enhancement were observed at the beginning and end of October that exceeded 60 L^{-1}. Interestingly, due to these events coinciding with exceptionally low levels of relative humidity, it is thought climatic factors were responsible for driving these enhancements rather than specific wind trajectories. This is despite these concentrations also coinciding with southerly trajectories, as was rightly expected to be prevalent at that time of year. We conclude it is the climatic factors that are primarily responsible, as when relative humidity levels are average or high, we see no significant increase in bioaerosol concentrations compared to previous months. We conclude the bioaerosols are predominantly dry-weather fungal spores due to the association with low relative humidity, their fluorescent emission spectra, and previous literature that recorded significant quantities of fungal spores through offline microscopical techniques. As many fungal spores are easily inhaled into human lungs, and can often act as opportunistic infectious agents, public health officials should benefit from our quantification of peak concentrations during enhancement periods.

5.3 Chilbolton

Finally, it is regrettable the project in Chilbolton could not overcome the challenges that occurred. It remains an interesting sampling location that can potentially identify bioaerosols associated with commercial food production. Machine learning techniques remain a promis-

ing avenue for improving bioaerosol identification. The Gradient Boosting training dataset, developed with the application of pollen samples through the Poleno Swisens Atomiser, suggested pollen species could be identified with 90% accuracy. This can likely be improved even further with the addition of spectral decay rates, as recorded by the PLAIR Rapid-E. However, the training dataset developed in this project still needs to be tested against real-world datasets collected in outdoor environments. It remains to be seen what effect including more sample species has on the accuracy of particle identification, but as outdoor environments will have far more complex aerosol mixtures, it seems likely that more information regarding particle properties must be extracted by the instruments. Once machine learning techniques are more fully developed, particle identification may become an automated process. This will significantly reduce the time and difficulty associated with analysing environmental datasets, and is therefore a worthwhile pursuit.